

Paleoseismic Investigation of the Cheraw Fault at Haswell, Colorado

Dean A. Ostenaa¹ and Mark S. Zellman²

¹ Ostenaa Geologic LLC., 25 Grays Peak Trail, Dillon, CO 80435

² BGC Engineering, Inc., 701 12th St., Suite 211, Golden, CO 80401



Paleoseismic Investigation of the Cheraw Fault at Haswell, Colorado

Principal Investigators:

Dean A. Ostenaa¹ and Mark S. Zellman²

¹ Ostenna Geologic LLC, Dillon, CO 80435 ² BGC Engineering, Inc., Golden, CO 80401



Dr. Ramona M. Graves
VICE PROVOST,
EARTH RESOURCES
AND ENGINEERING



Karen A. Berry
DIRECTOR AND
STATE GEOLOGIST



Cover, inside photos by Mark Zellman and Matt Morgan (inset)
Layout and cover design by Larry Scott (CGS)

DOI: <https://doi.org/10.58783/cgs.mi97.oqqm3054>

TABLE OF CONTENTS

ABSTRACT	1
1.0 INTRODUCTION	3
2.0 BACKGROUND	7
2.1 Prior Investigations at the Haswell Site	10
3.0 METHODOLOGY	13
3.1 LiDAR-based Mapping of the Cheraw Fault Scarp	13
3.2 Trenching Investigations at the Haswell Site	13
4.0 LIDAR-BASED MAPPING RESULTS	15
4.1 Cheraw Fault Main Scarp	15
4.2 Cheraw Fault Secondary Scarp	16
5.0 RESULTS OF THE HASWELL TRENCHING INVESTIGATION	18
5.1 Haswell Site Stratigraphy	18
5.1.1 Soil Profile Descriptions and Age	20
5.1.2 Luminescence Dating Analysis	20
5.1.3 Age of Nussbaum Alluvium at the Haswell Site	20
5.2 Haswell Site Structure and Deformation	21
5.2.1 Trenches T1 and T2	21
5.2.2 Ditch Exposure	22
5.2.3 Relationship of Folding to Basal Nussbaum Alluvium Thickness	24
5.2.4 Deformation and Fracture Analyses	27
5.2.5 Deformation of Nussbaum Alluvium	30
5.2.6 Timing of Deformation	30
5.2.7 Interpretation of the Cheraw Fault Structure at the Haswell Site	31
6.0 IMPLICATIONS FOR SEISMIC HAZARD CHARACTERIZATION	33
7.0 SUMMARY OF RESULTS	35
8.0 ACKNOWLEDGEMENTS	37
9.0 REFERENCES	39

TABLES

TABLE 1	Trench units and soil profile horizon correlations.....	20
TABLE 2	Haswell site luminescence dating results and interpretations.....	21
TABLE 3	Three point combinations from Haswell ditch exposure.....	25
TABLE 4	Cheraw fault stratigraphic datums, estimated vertical offsets, and slip rates (updated from Zellman and Ostenaar, 2016).....	33

FIGURES AND PLATES

Figure 1	General location map of the Cheraw fault in Colorado.....	4
Figure 2	Seismotectonic setting of the Cheraw fault.....	5
Figure 3	Geologic map and field investigation sites near the Cheraw fault.....	6
Figure 4	Geomorphologic map along the Cheraw fault.....	9
Figure 5	Haswell area site investigations.....	11
Figure 6	Detailed map of Haswell site investigation and data locations.....	12
Figure 7	Composite profile with trench and boring data (panel A), and lower Nussbaum Alluvium bed thickness (panel B).....	19
Figure 8	Overview of site 01 and stratigraphic site in ditch along CO Hwy 96.....	23
Figure 9	Stratigraphic section of Nussbaum Alluvium exposed in ditch adjacent to CO Hwy 96.....	24
Figure 10	Closeup view of deformed Nussbaum Alluvium at site 01 in ditch.....	25
Figure 11	Overview of ditch exposure sites 01 to 06.....	26
Figure 12	Photos of deformed Nussbaum Alluvium at site 03 (Photo A) and site 05 (Photo B).....	27
Figure 13	Lower hemisphere, stereonet plots of Niobrara Formation bedding poles and fracture orientations from trench and outcrop exposures.....	28
Figure 14	Lower hemisphere, stereonet plots of Nussbaum Alluvium and Niobrara Formation bedding poles from ditch exposures along CO Hwy 96.....	29
Figure 15	Schematic summary of compiled tectonic and outcrop data from the Haswell site.....	32
PLATE 1	LiDAR-Based Map of the Cheraw Fault Scarp	
PLATE 2	Logs of Trenches T1 and T2	

APPENDICES

APPENDIX A. Soil Profile Field Logs

APPENDIX B. Luminescence Dating - Sample Analysis Report Summary

APPENDIX C. Three-Point Strike and Dip Solutions from Surveyed Points Along Haswell Ditch Exposure

ABSTRACT

This report presents findings of recent paleoseismic investigations of the Cheraw fault in southeastern Colorado. The Cheraw fault is one of the few faults within the Central and Eastern United States (CEUS) known to have experienced a surface rupturing earthquake in the Holocene (Crone et al., 1997; Crone and Wheeler, 2000). Regardless, relatively few studies have been conducted to characterize this fault. This investigation builds on availability of new LiDAR data along the Cheraw fault and on our recent study (Zellman and Ostenaar, 2016) of the fault near Haswell, CO.

Analyses and mapping on the LiDAR data shows new details of the scarps along the previously mapped 45-km-long fault trace of Sharps (1976) and Crone et al. (1997). The LiDAR data shows the full extent of scarps to be a minimum of 80 km and affords new insights into the characteristics of geomorphic surfaces and their relationships to the scarps.

At Haswell, Zellman and Ostenaar (2016) collected surface and geophysical data, drilled a borehole transect, performed geologic and structural mapping, and identified a field location with the potential to define and date the total displacement of the Cheraw fault since cutting of and deposition on an early (?) Quaternary Nussbaum pediment. With additional mapping and trenching, that displacement could be compared to displacement estimates for the fault in Cretaceous bedrock derived from nearby seismic reflection profiles, and to displacement estimates of late Quaternary offset from geomorphic data and prior trench studies.

This investigation consisted of additional mapping of nearby exposures, and excavation and detailed logging of two trenches sited across the scarp, to characterize bedrock structure associated with the Cheraw fault and to define the amount of offset of the basal portion of the early (?) Quaternary Nussbaum Alluvium. This alluvium overlies an erosional unconformity cut on the Cretaceous Niobrara Formation. Five samples from key stratigraphic units in the alluvium were collected and submitted for luminescence dating to provide minimum age estimates for the Nussbaum Alluvium and to estimate a time history of deformation. The new age data from the Haswell investigation provides upper limits for the ages of geomorphic surfaces and scarps mapped here and elsewhere along the fault.

We make the following conclusions:

- 1) The entire Cheraw fault scarp is closely associated with an underlying bedrock fault and fold structure.
- 2) The total length of Quaternary faulting associated with the Cheraw fault is at least 80 km and appears to be relatively uniform in vertical offset.
- 3) The surface expression of the Cheraw fault at the Haswell site is complex, as a local 10° change in fault strike is partly accommodated through a leftstep of the main fault trace. Trenches T1 and T2 expose deformation associated with the fault relay ramp between two left-stepping fault traces.
- 4) Nussbaum Alluvium at the Haswell site is deformed and its basal contact is vertically offset at least 5 to 6 m in the trenches, and total offset is likely about 9 m when combined with boring data.
- 5) Internal stratigraphy within the Nussbaum Alluvium, exposed in the trench walls, is deformed in the same manner as its basal contact with bedrock, suggesting that all deformation postdates the youngest Nussbaum strata at the site.
- 6) Deposition of the Nussbaum Alluvium, and erosion of the basal strath surface which underlies that alluvium, is much younger than previously inferred from regional correlations. New luminescence ages from the Haswell site indicate deposition of units within the Nussbaum Alluvium spanned an age range from <126 ka to >160 ka.
- 7) Deformed stratigraphy and age constraints from luminescence dating suggests that post-Nussbaum Alluvium slip on the Cheraw fault occurred after <126 to 160 ka, yielding a minimum vertical slip rate of ~ 0.06 to 0.07 mm/yr at the Haswell site since that time.
- 8) Inset relations of Rocky Flats Alluvium near the Cheraw fault, indicate that it must be significantly younger than the Nussbaum Alluvium at Haswell. Scarps on the Rocky Flats Alluvium appear to range from 5 to 7 m in height, suggesting a similar or slightly higher late Quaternary slip rate than the rate derived from the Nussbaum Alluvium at Haswell.

1.0 INTRODUCTION

This report presents findings from new mapping of the Cheraw fault and from paleoseismic investigations near Haswell, Colorado (**Figure 1**). In 2016, Colorado Geological Survey (CGS) coordinated the acquisition of 1 m LiDAR data along the mapped and extended trace of the Cheraw fault. Analyses of that data provides a basis for detailed mapping and extension of the fault scarp along the Cheraw fault to a total length of about 80 km. At the Haswell field site, the Cheraw fault scarp intersects the western edge of a pediment surface capped with early (?) Quaternary Nussbaum Alluvium. Previously, Zellman and Ostenaar (2016) investigated the site, delineated a fault zone, and established preliminary vertical offset estimates on the base of the Nussbaum Alluvium. In this investigation we excavate two trenches along the base of the Nussbaum Alluvium, and document Nussbaum Alluvium in nearby ditch exposures, to further characterize the fault zone and to constrain the paleoseismic history of the northeast section of the Cheraw fault.

The Cheraw fault of southeastern Colorado is one of the few faults east of the Rocky Mountains, in the Central and Eastern United States (CEUS), with documented Holocene surface rupture. As seen on **Figures 1 and 2**, the Cheraw fault lies within the western Great Plains of Colorado, 150 km east of the Southern Rocky Mountains. The physiographic boundary of these two provinces generally coincides with the larger scale seismotectonic contrasts between the CEUS and the Western United States (WUS), shown by a higher density of Quaternary faults and more abundant natural seismicity in the WUS than the CEUS. The Cheraw fault has a length of at least 80 km, and is a significant contributor to seismic hazard estimates for the Colorado Front Range communities of Pueblo, Colorado Springs, and Denver. Despite the significance of the Cheraw fault as a

seismic source in Colorado, the characterization of the fault thus far (e.g. fault length, slip rate, earthquake recurrence) is based on information from a single paleoseismic investigation. Crone et al. (1997) excavated a trench across what is now the southern third of the fault (**Figure 3**, site 5) and documented three faulting events (two latest Pleistocene and one early Holocene) with a combined total vertical offset of 3.2 to 4.1 m. They further suggested a long period of tectonic quiescence, perhaps >100 ka, prior to about 25 ka. Subsequent investigations (Zellman and Ostenaar, 2016) extended the fault length from 45 to 59 km, provided new data on total offset, and showed the relationship to older structures, but left open questions about fault segmentation, rupture history, slip rate, and other important seismic hazard parameters.

The initial scope of this project was to conduct a paleoseismic investigation of the northeastern section of the Cheraw fault near Haswell, Colorado to address major uncertainties related to the characterization and understanding of the fault. The two primary objectives were to:

- 1) confirm the presence, or absence, of Quaternary deformation on the northeast extension of the Cheraw fault by excavating a trench that exposes the basal contact of Nussbaum Alluvium, and,
- 2) obtain luminescence geochronology ages that provide constraints on the deformation history of the fault.

When CGS LiDAR data became available shortly after completion of the primary field work for the trenching studies, we undertook additional mapping using that data to better define the full extent and characteristics of the Quaternary faulting on the Cheraw fault.

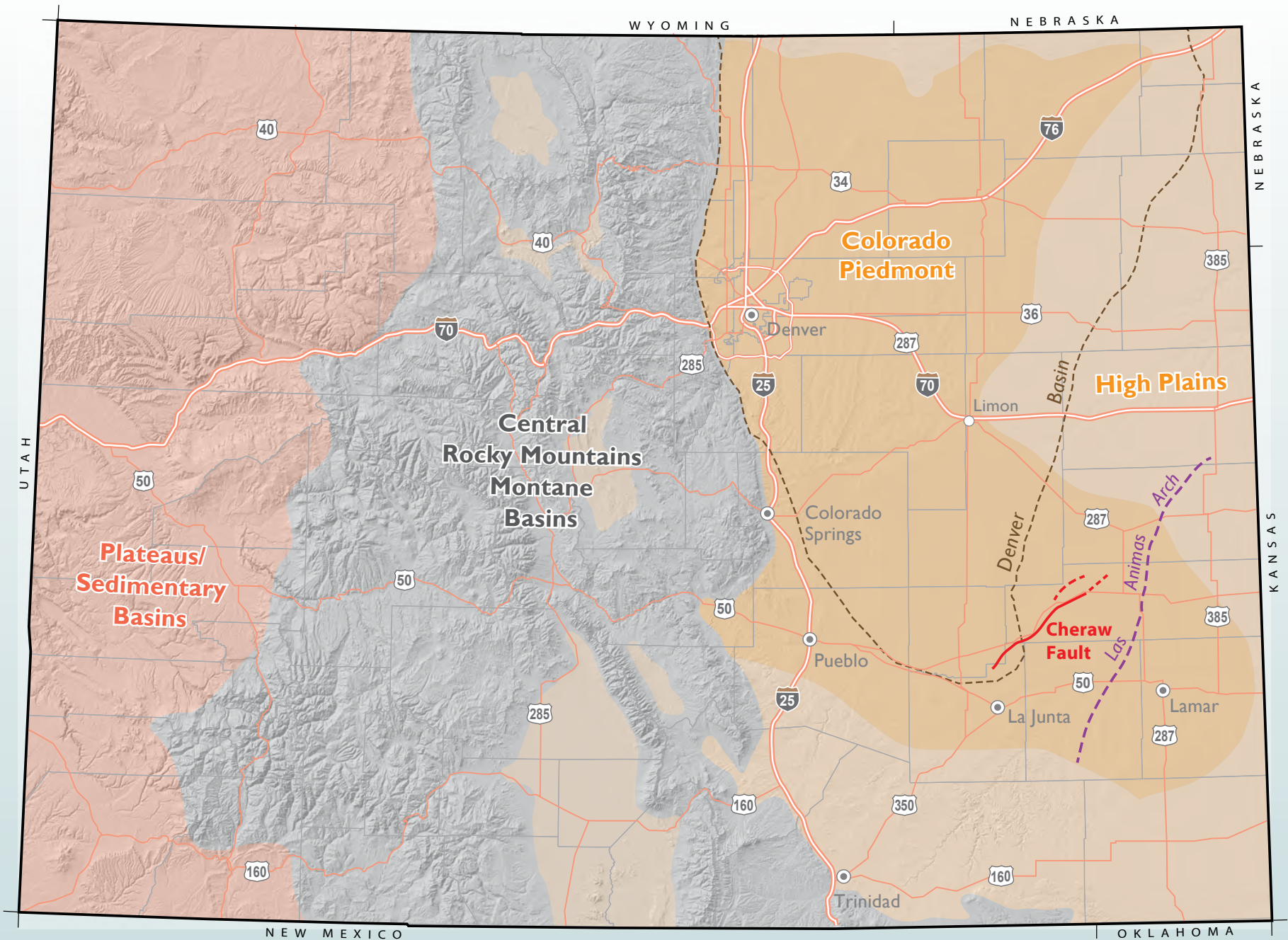


Figure 1. General location map of the Cheraw fault in Colorado. Note the physiographic contrast between the Rocky Mountains and the western Great Plains, where the Cheraw fault is located.

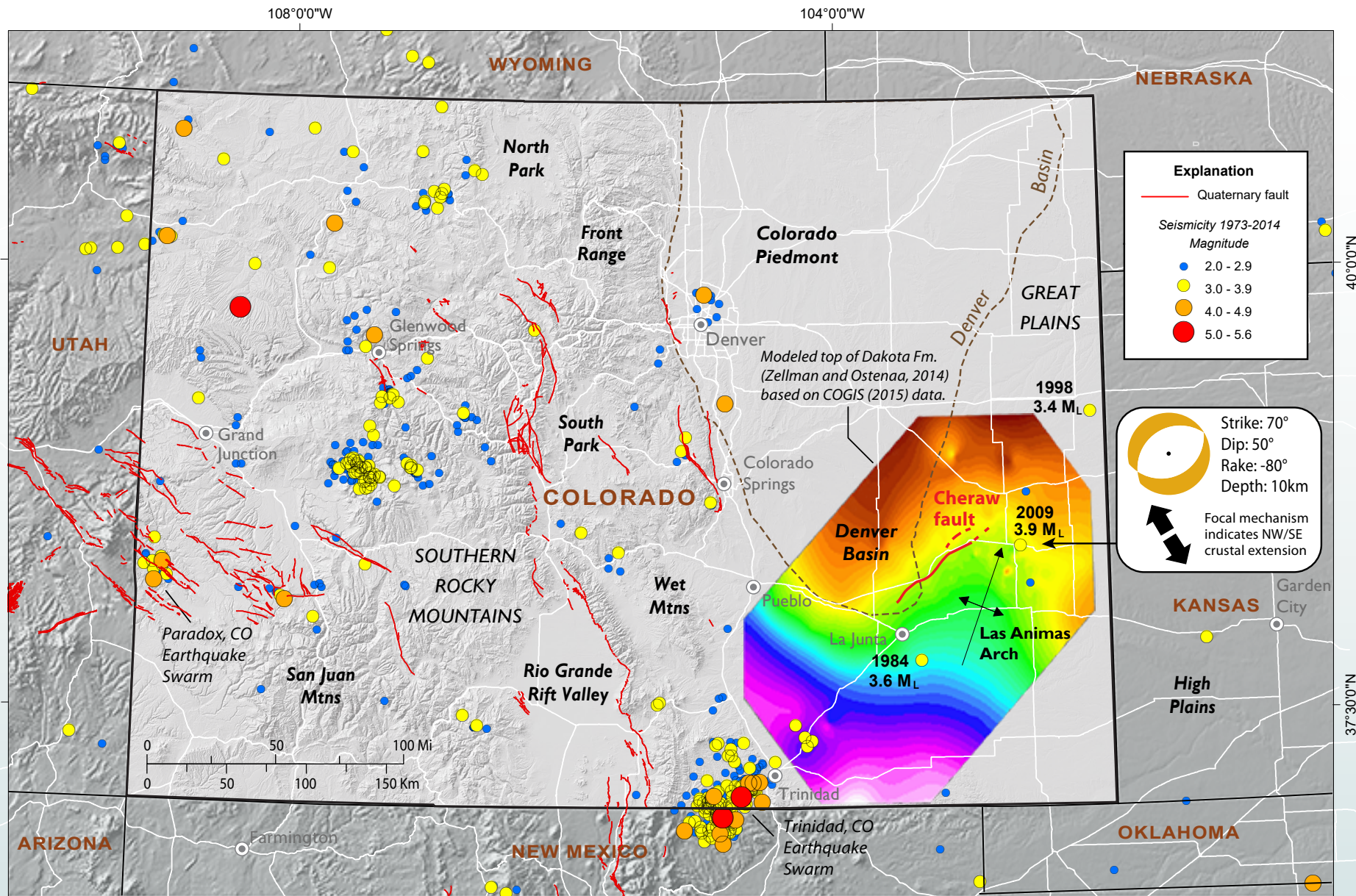


Figure 2. Seismotectonic setting of the Cheraw fault. Colorbanded overlay shows the modeled top of the Dakota Formation from Zellman and Ostenaa (2014) based on COGIS (2015) data. These data illustrate the location of the Cheraw fault along the northwest flank of the Las Animas Arch. Red lines on the figure show Quaternary faults from USGS (2016). Cheraw fault trace is modified based on Zellman and Ostenaa (2016) and is the only long fault on the western Great Plains, east of the Rocky Mountain Front Range. Seismicity is shown for period between 1973 to 2014 (NCEDC, 2014). The focal mechanism of the 2009 M3.9 earthquake on the northeast flank of the Las Animas Arch, and footwall block of the Cheraw fault, is consistent with northwest-southeast directed extension across the Cheraw fault.

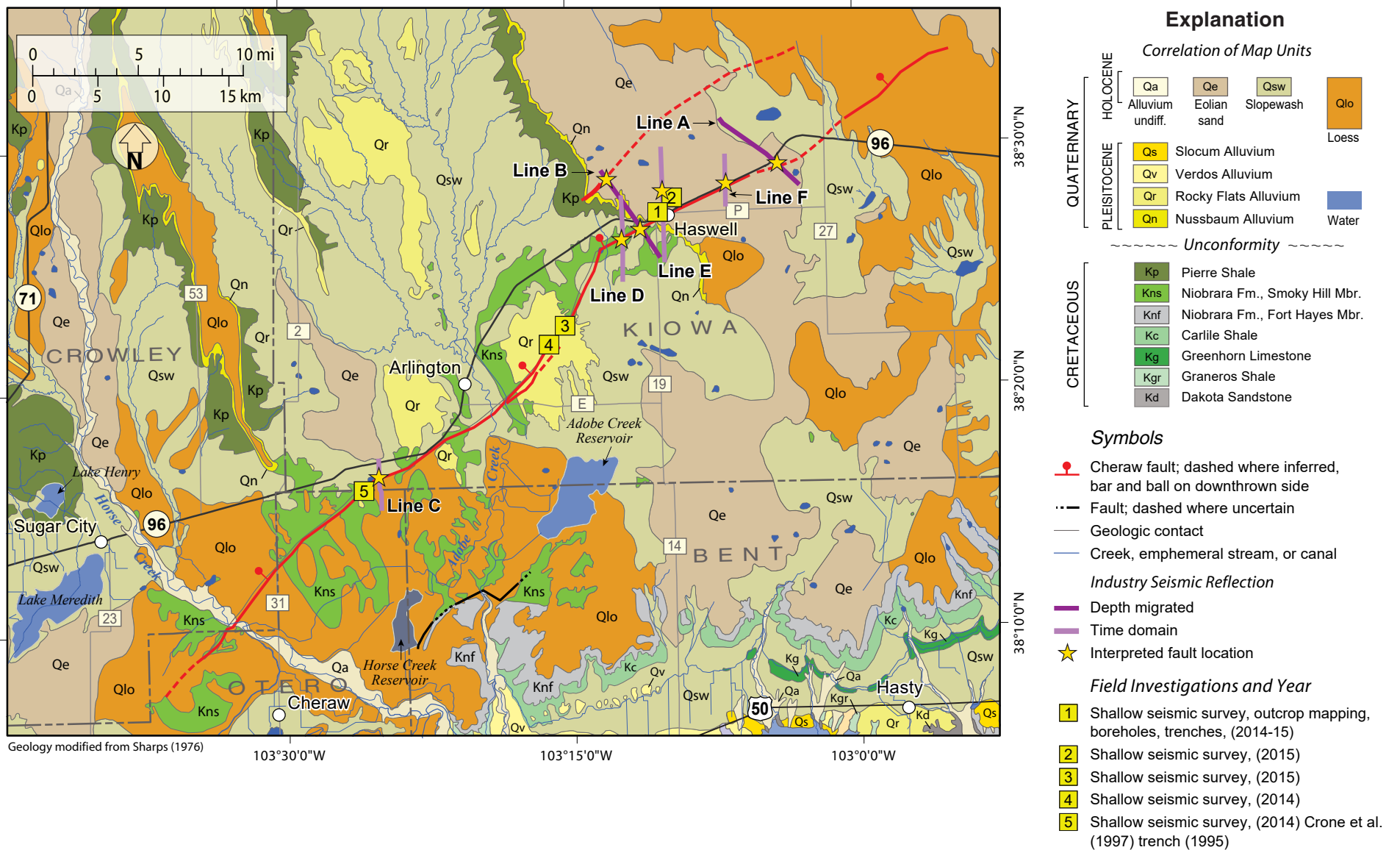



Figure 3. Geologic map and field investigation sites near the Cheraw fault. Geologic map of the area near the Cheraw fault, digitized from Sharps (1976), depicts the gentle northwest dip of Cretaceous bedrock units. Smoky Hill Member of the Niobrara Formation is exposed on both the hanging wall and footwall of the Cheraw fault, indicating that maximum vertical offset of the Cheraw fault is less than the thickness of the Smoky Hill Member (~ 150 to 215 m). Early (?) Quaternary Rocky Flats and Nussbaum Alluvium outcrop appear as narrow bands along the edge of mesa or upland areas and are often covered with younger loess and eolian deposits. The location of field investigation sites are shown (see Explanation).

2.0 BACKGROUND



The Cheraw fault is located on the western limb of the northeast-plunging Las Animas Arch (**Figure 2**), a structure which overlies a basement suture zone and has experienced tectonic reactivation multiple times (Whitmeyer and Karlstrom, 2007; Tickoff and Maxson, 2001; Merewether, 1987; Rascoe, 1978). Beginning in the Proterozoic, Mazatzal terrain accreted against Yavapai terrain (Carlson, 2007). The suture zone between the terrains is recognized as a northeast trending structure within crystalline basement in southeastern Colorado and in the vicinity of the Las Animas Arch (Sims et al., 2001). The Las Animas Arch first became a positive structure in the late Paleozoic as a result of north-northwest directed, regional compression during the Ouachita-Marathon orogeny (Rascoe, 1978; Kluth and Coney, 1981), or alternatively from southwest-northeast directed, regional compression as proposed by Ye et al. (1996). The Las Animas Arch experienced its second period of tectonic uplift as a result of Laramide shortening during the orogeny when Cretaceous rocks were warped over the broad anticline and the Denver Basin subsided to the northwest (Tickoff and Maxson, 2001; Curtis, 1988). The most recent period of activity is represented by down-to-the-northwest normal faulting along the Cheraw fault. The focal mechanism solution (Herrmann, 2009) from a 2009 M 3.9 earthquake about 40 km east-northeast of the fault (**Figure 2**) confirms the existence of contemporary extensional stress regime in the region with minimum horizontal stress axis oriented northwest-southeast, consistent with contemporary reactivation of arch-parallel structure as normal faults.

The Cretaceous Smoky Hill Member of Niobrara Formation (Kns) occurs on both the hanging wall and footwall of the Cheraw fault along most of its length. As mapped by Sharps (1976) (**Figure 3**), this relationship appears to limit the post-Cretaceous vertical offset of the Cheraw fault to less than the thickness of the Smoky Hill Member, about 150 to 215 m. The Smoky Hill Member is a thinly bedded, chalky, fissile shale which weathers to a distinct yellow-gray regolith. It has limited surface exposure because it is mantled by windblown, colluvial, and alluvial Quaternary sediments (e.g. Qlo, Qe, Qsw, Qr, and Qn on **Figure 3**). Underlying the Niobrara Formation is a thick sequence of Cretaceous and Paleozoic siliciclastic and carbonate rocks which unconformably overlies Precambrian

crystalline basement. All of these units are folded across the axis of the Las Animas Arch (**Figure 3**) (Merewether, 1984). Within the Paleozoic strata is an interval of Permian evaporite deposits which includes the Blaine Formation. These evaporite deposits are known to be susceptible to dissolution and the formation of evaporite karst (e.g. sinkholes, and discontinuous unorganized faults) in Kansas, Oklahoma, and eastern Colorado (Meriam, 1963; Walker, 1985; White, 2012; Johnson and Neal, 2003).

Zellman and Ostenaar (2016) interpreted the bedrock structure of the northeast extension and south-central portions of Cheraw fault. Their analysis of industry seismic reflection data collected across the fault included two depth-migrated and four time-domain 2D seismic reflection profiles (**Figure 3**). These data show a steep, planar, fault dipping about 75° to depths of 2 to 3 km into lower Paleozoic and basement units. The up-dip projection of this structure is spatially correlative with the topographic scarp that defines the Cheraw fault at the ground surface (**Figure 3**). The fault is observed in the seismic data to cut cleanly through the full stratigraphic column to depths at least 1 km below the Permian evaporite interval into lower Paleozoic and basement units, and the Permian interval maintains a constant thickness across the fault zone. Based on these observations, Zellman and Ostenaar (2016) interpreted the Cheraw fault to be a seismogenic tectonic structure rather than a feature related to dissolution.

Oil and gas exploration 2D depth-migrated seismic Line B (**Figure 3**) from Zellman and Ostenaar (2016) shows about 30 to 60 m of apparent vertical offset in Upper Cretaceous units across a distance up to 250 m from the discrete fault break, and increases to about 100 m of vertical offset across a distance up to 2 km from the discrete fault break. Slightly less vertical offset was observed in depth-migrated seismic Line A (**Figure 3**): 30 to 61 m of near-fault offset (up to 250 m away) and 46 to 58 m of far-field offset (up to 2 km away). In both seismic lines, the measured vertical offsets for both near-fault and far-field increase in Paleozoic strata. It remains uncertain how much measured Cretaceous offset across the fault is associated with Laramide deformation and how much is associated with late Cenozoic deformation.

The Cheraw fault was originally identified and mapped by J.A. Sharps in 1968 and described by Scott (1970) (Kirkham and Rogers, 1981). Sharps (1976) showed a 45-km-long fault as an inferred structure cutting the Upper Cretaceous Smokey Hill Shale Member of the Niobrara Formation, and concealed beneath undifferentiated Quaternary alluvium, loess, and slopewash deposits, and early (?) Quaternary Rocky Flats Alluvium. The fault as mapped by Sharps (1976) extends from about 3 km southwest of Horse Creek to about 6 km southwest of Haswell along a somewhat sinuous trace with an overall strike of about 225° (**Figures 3 and 4**). A possible northeast extension of the fault has been discussed at least since Kirkham and Rogers (1981) recognized that the characteristic topographic scarp associated with the mapped trace (Sharps, 1976) continues to the northeast. Their map extended the fault to the northeast, striking about 245° from the northern end of the Sharps (1976) fault and included a short, subparallel, queried trace a few kilometers to the northwest. However, the Kirkham and Rogers (1981) extended fault length was never included in subsequent map depictions. More recent evaluations using USGS National Elevation Dataset (NED) 10-m digital elevation model (DEM) data (e.g., see discussion in CEUS-SSCn, 2012) define a total length of at least 59 km (Zellman and Ostenaar, 2014; 2016) and a scarp striking about 245° that extends at least another 14 km from the fault trace originally mapped by Sharps (1976) (**Figures 3 and 4**).

The defining surficial characteristic of the Cheraw fault is the subtle, yet distinct, northwest-facing topographic scarp which forms a gradient barrier for the local drainages flowing across the southeast-sloping regional drainage, and an obstruction to southeast-directed prevailing winds (Kirkham and Rogers, 1981; Crone and Machette, 1995; Crone and Wheeler, 2000) (**Figures 3 and 4**). Erosion of the relatively soft Cretaceous bedrock units, and the partial burial of the scarp by eolian deposits and locally ponded alluvium, contribute to the subtle expression of the scarp and the appearance of being a much older feature than it is known to be (Crone and Wheeler, 2000). Along the base of the scarp, vegetation lineaments and numerous closed depressions that intermittently hold water form a clearly visible alignment on topographic maps, DEM derivative slope, aspect, and hillshade maps, aerial photography, and multispectral imagery. Although the scarp is subtle, it has consistent morphologic expression for its entire 80 km length, with a typical surface offset less than 10 m. It is visible in all surfaces and all ages of material it intersects, with the possible exception of late Holocene alluvium in floodplains and terraces adjacent to streams (**Figure 4**).

At three locations along the scarp, pediments and alluvium of Nussbaum and Rocky Flats ages are transected and offset by the Cheraw fault (**Figures 3 and 4**).

Kirkham and Rogers (1981) reported that the early Quaternary Rocky Flats Alluvium is offset as much as 12 m across the fault. Crone et al. (1997) suggested as much as 7 to 8 m of offset of the Rocky Flats Alluvium, apparently based on topographic profiles, but documented only 3.2 to 4.1 m of bedrock offset from trenching and boring profiles at a site where the surface scarp height is 3.6 m (Crone et al., 1997).

The pediments that underlie the Nussbaum and Rocky Flats Alluvium are mantled with thin alluvium, and covered with variable thickness of younger eolian deposits. The Nussbaum Alluvium was not directly dated in previous investigations, but fossils from the type locality north of Pueblo (~100 to 120 km west of the Cheraw fault) and from gravel pits in Morgan and Logan Counties suggest an early Quaternary, or possible late Pliocene age (Scott, 1963, 1965, 1975, 1982). Schildgen et al. (2002) assigned an age of 1.35 Ma to the Rocky Flats Alluvium near Boulder based on soil profile development described by Birkeland et al. (1999), and thus by inference dated the Nussbaum Alluvium as >1.35 Ma.

Mapping and correlation of the Nussbaum and Rocky Flats pediments and alluvium have relied for the most part on the relative geomorphic position of the pediments, soil development, and thin overlying alluvium units above stream grade, and their inset relations. There are only a few published investigations describing the relationships and ages of the overlying alluvial and eolian cover on these older surfaces in eastern Colorado, although it is long recognized that these units must have a composite history (e.g., Scott, 1975). More than 120 km north of the Cheraw fault, extensive trenching and dating on the Anton escarpment by Noe (2010), shows the complex history of erosion and deposition associated with this large geomorphic feature in this setting, which apparently formed primarily since about 30 ka. Work along the Front Range north and west of Denver (Riihimaki, et al., 2006; Duhnforth et al., 2012; and Foster et al., 2013, 2014) suggests that the Rocky Flats and Nussbaum surfaces may have been established long ago, but abandonment ages are much younger (by an order of magnitude) than previously suspected and that no single age may be appropriate for both the basal alluvium and overlying deposits and geomorphic surfaces. Work on both the Anton escarpment and the northern Front Range surfaces indicates that the erosional and depositional history of the Colorado Piedmont and High Plains has been much more dynamic than implied by early age models linked to simple, long-term, base level fall on the master streams. For the Cheraw fault evaluations, the implication of these studies is much greater uncertainty in the potential range of ages for older alluvium and geomorphic surfaces mapped as Nussbaum and Rocky Flats.

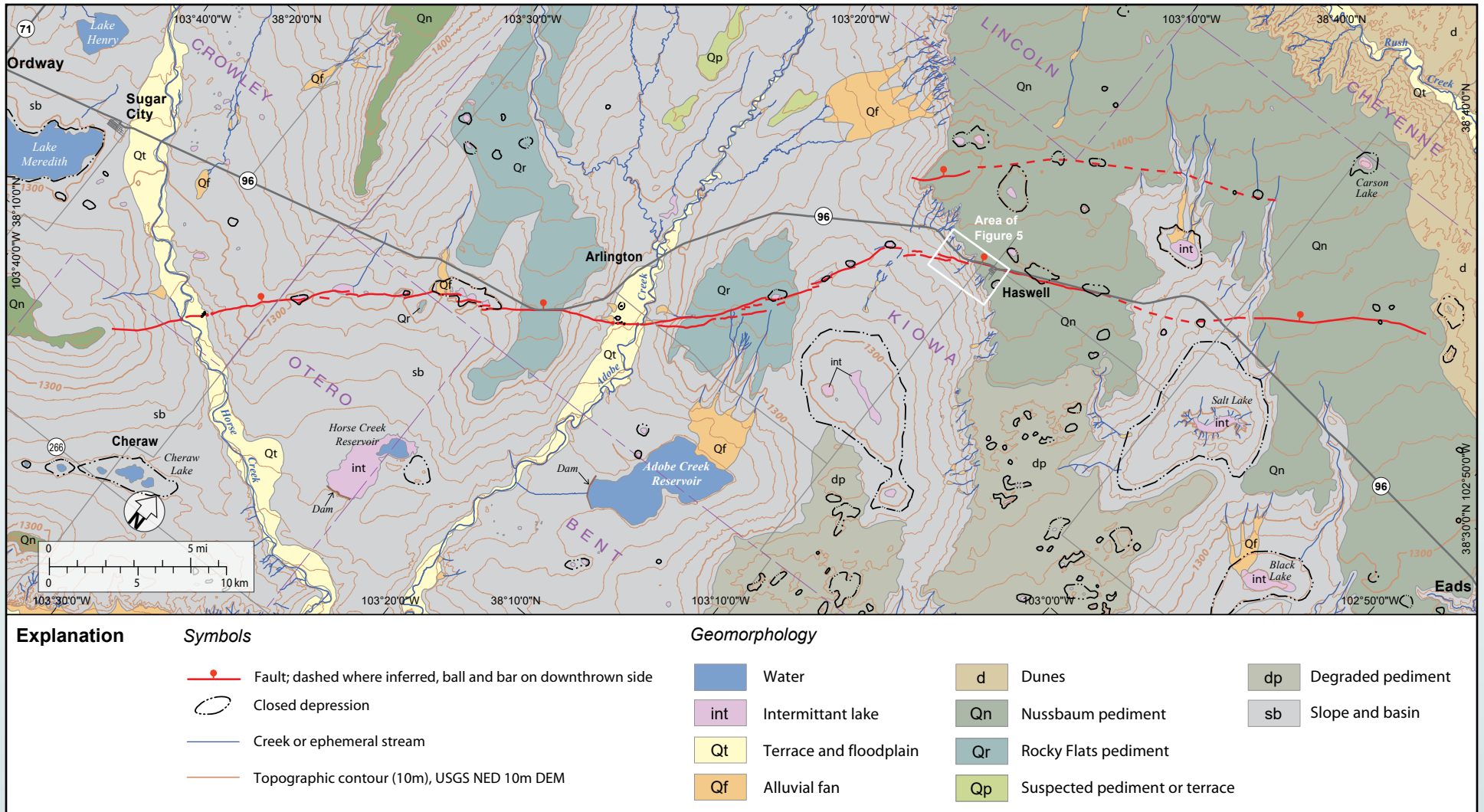


Figure 4. Geomorphic map along the Cheraw fault. Cheraw fault is expressed as a broad, subtle, upslope-facing scarp with relatively continuous expression across the landscape (red line). The fault has three distinct planform sections from southwest to northeast. The southwestern and central sections of the fault are the original extent mapped by Sharps (1976). The southwestern section extends from southwest of Horse Creek to a point 2 km southwest from CO Hwy 96, or about 10 km southwest of Arlington. This section is linear to slightly convex to the northwest, with small right steps. The central section extends from that point, to a point about 6 km southwest of Haswell where the fault makes an abrupt $\sim 30^\circ$ bend to the northeast. The central section of the fault forms a broad arc, concave to the northwest, with a total strike change of $\sim 55^\circ$ through the trace of the arc. The northeastern section, or northeast extension, is again linear. Numerous large closed depressions, most prominent along the eastern side of the Cheraw fault, are thought to be related to dissolution of evaporite bedrock in the subsurface (White, 2012; Walker, 1985). Smaller closed depressions along the Cheraw fault trace may be related to similar processes, or to drainage disruption due to young movement along the fault. Site investigation area near Haswell depicted on **Figure 5** is outlined with white box.

In the area near the Cheraw fault shown on **Figure 4**, surfaces mapped as Nussbaum Alluvium typically project to levels of 80 to 90 m above the modern channel of the Arkansas River, and adjacent first-order tributaries such as Adobe Creek and Horse Creek. Mapped Rocky Flats alluvial surface are inset well below the Nussbaum surfaces and project to levels about 40 to 45 m above these tributaries. Smaller areas of still younger Pleistocene alluvium are locally preserved at several levels below the Rocky Flats surfaces. Latest Pleistocene and Holocene alluvial surfaces are limited to narrow bands adjacent to channels, and are most extensive along the larger tributaries such as Horse Creek and Adobe Creek.

In their detailed paleoseismic study of the Cheraw fault, Crone et al. (1997) excavated soil pits, drilled a shallow borehole transect, and excavated a 110-m-long trench across the fault (**Figure 3**, site 5). The trench was sited within an abandoned channel of inferred late Pleistocene age, inset more than 10 m below nearby remnants of Rocky Flats Alluvium, and earthquake timing was constrained through thermoluminescence (TL) and radiocarbon dating. The trench exposure identified three events within the past 20 to 25 ka, with the best estimate for the age of the most recent event of 8 ka (Crone et al., 1997). Based on their age of the oldest faulted deposits (20 to 25 ka) and the offset of those deposits (~3.2 to 4.1 m), latest Pleistocene-Holocene slip rates may be in the range of 0.13 to 0.21 mm/yr. The oldest faulted deposits on the footwall in the trench are fluvial deposits occupying the Late Pleistocene abandoned channel. These deposits were not dated during the Crone et al. (1997) study because charcoal for radiocarbon dating was not found, and TL was not effective at dating these types of deposits (S. Mahan, personal communication, April 9, 2015). Based on the inferred geomorphic age of the Late Pleistocene channel, Crone et al. (1997) suggest that the Cheraw fault was inactive from 20 to 25 ka to about 100 ka or earlier. However, Crone and Machette (1995) and Crone et al. (1997) note that the offset of nearby Rocky Flats Alluvium may be only 7 to 8 m. Crone et al. (1997) suggest long-term behavior of the Cheraw fault may be characterized by long periods of inactivity punctuated by relatively short episodes of seismic activity, similar to other CEUS faults such as the Meers fault in Oklahoma (Petersen et al., 2014). Thus, the estimated recurrence intervals may only apply to the fault during its active phases (Crone et al., 1997).

2.1 Prior Investigations at the Haswell Site

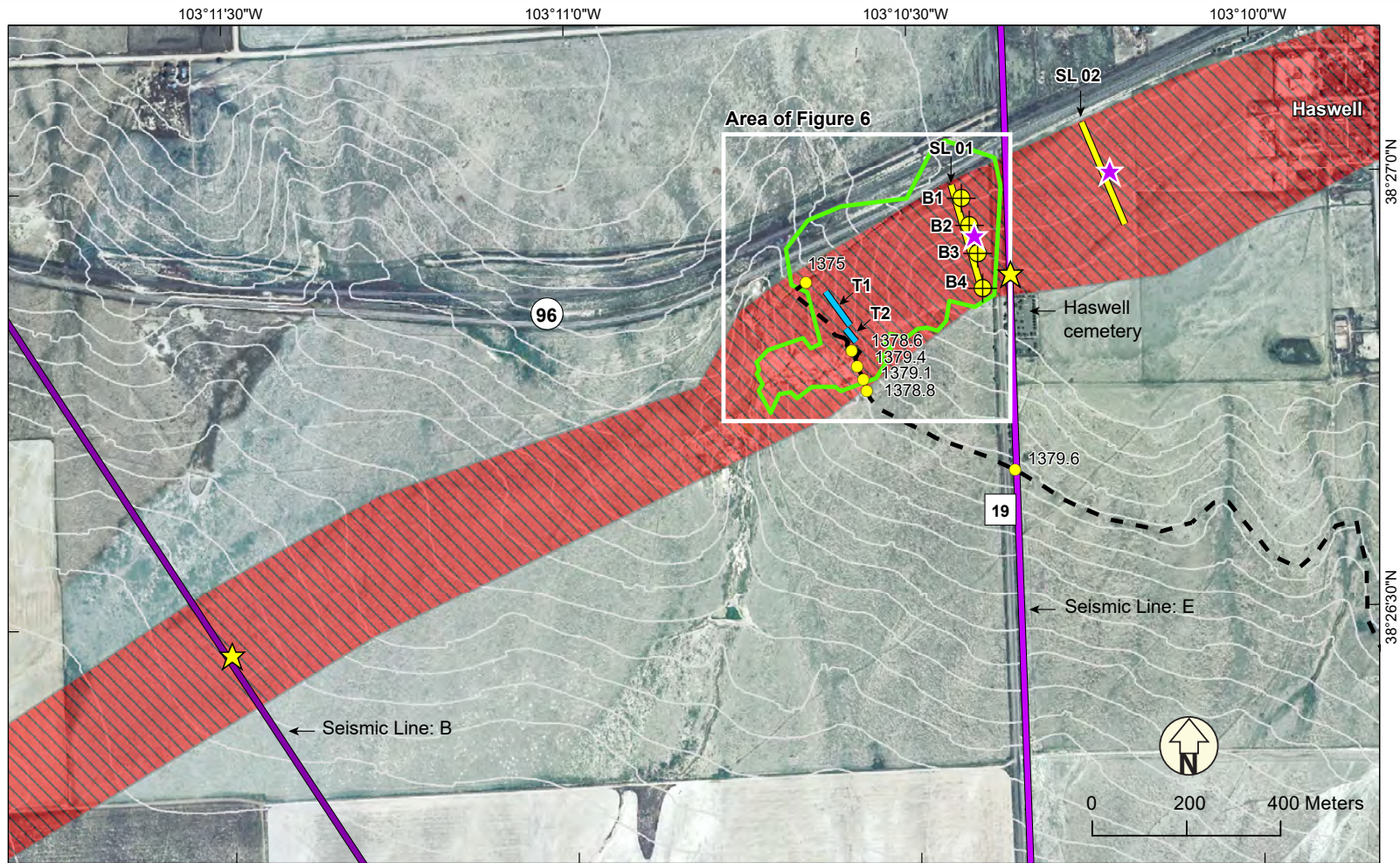
The Haswell site is located approximately 1 km west of Haswell, Colorado (**Figure 5**). The site area is bounded to the north by Colorado State Highway 96 and to the east by Kiowa County Road 19 (**Figure 6**). At this location the Cheraw

fault scarp intersects the western edge of a pediment surface capped with Nussbaum Alluvium, and it is here that the only bedrock exposure along the entire Cheraw fault scarp has been identified. At this site in 2015, the Zellman and Ostenaar (2016) field investigation applied shallow 2D seismic refraction surveys, a shallow borehole transect drilled into the top of bedrock, aerial photo collection, structure-from-motion (SfM) DEM processing, and geologic and structural mapping to constrain the near-surface zone of faulting estimation of the apparent down-to-the-northwest vertical offset on the base of the Nussbaum Alluvium (**Figures 5 and 6**). In addition to the field data, two industry seismic reflection lines (Line B (depth migrated) and Line E (time domain)) (**Figure 5**), licensed for the investigation, provide a basis for interpreting structure and stratigraphy at depth below the site.

Shallow seismic survey SL-01 was collected at the Haswell site, and survey SL-02 was collected approximately 400 m to the northeast on the east side of County Road 19 (**Figures 5 and 6**). These surveys were oriented approximately orthogonal to the scarp. The P-wave tomography profiles produced from the survey data image the subsurface to a depth of 20 to 30 m and provide basis for constraining and interpreting a zone of deformation on the base of Nussbaum Alluvium based on vertically offset velocity structure. A borehole transect consisting of 4 auger borings drilled adjacent, and approximately parallel to, SL-01 confirms the depth to top of Niobrara bedrock, characterizes the alluvium and bedrock substrate, and provides a basis to better interpret the shallow seismic refraction profiles.

High-resolution SfM orthoimagery and DEMs (**Figures 5 and 6**) provide basemaps for geologic mapping and elevation control for geologic profiles and analysis at the Haswell site. The photographs were collected and processed using AgiSoft software following methodology of Johnson et al. (2014) to produce high-resolution SfM orthoimagery and DEMs with <20 cm grid cell resolution.

Geologic structures and bedding contacts exposed in the bedrock outcrops at the Haswell site were mapped in the field to document fault-related deformation and to constrain the location of the Cheraw fault. At this site, the Smoky Hill Member of the Niobrara Formation is exposed in a cut-bank outcrop and on the ground surface within an eroding landscape. Faults, joints, and bedding orientations were measured, and the in situ, basal contact of the Nussbaum Alluvium was mapped where it is naturally exposed (**Figures 5 and 6**). Two industry seismic lines, licensed for the Zellman and Ostenaar (2016) study, cross the Cheraw fault scarp within 1 km of the Haswell site (**Figure 5**). Depth-migrated seismic Line B crosses the fault at a near orthogonal angle ~1 km southwest of the



Imagery from NAIP, 2009, contours from: NED 10 m DEM, contour interval: 2 m

Explanation

Data from this study

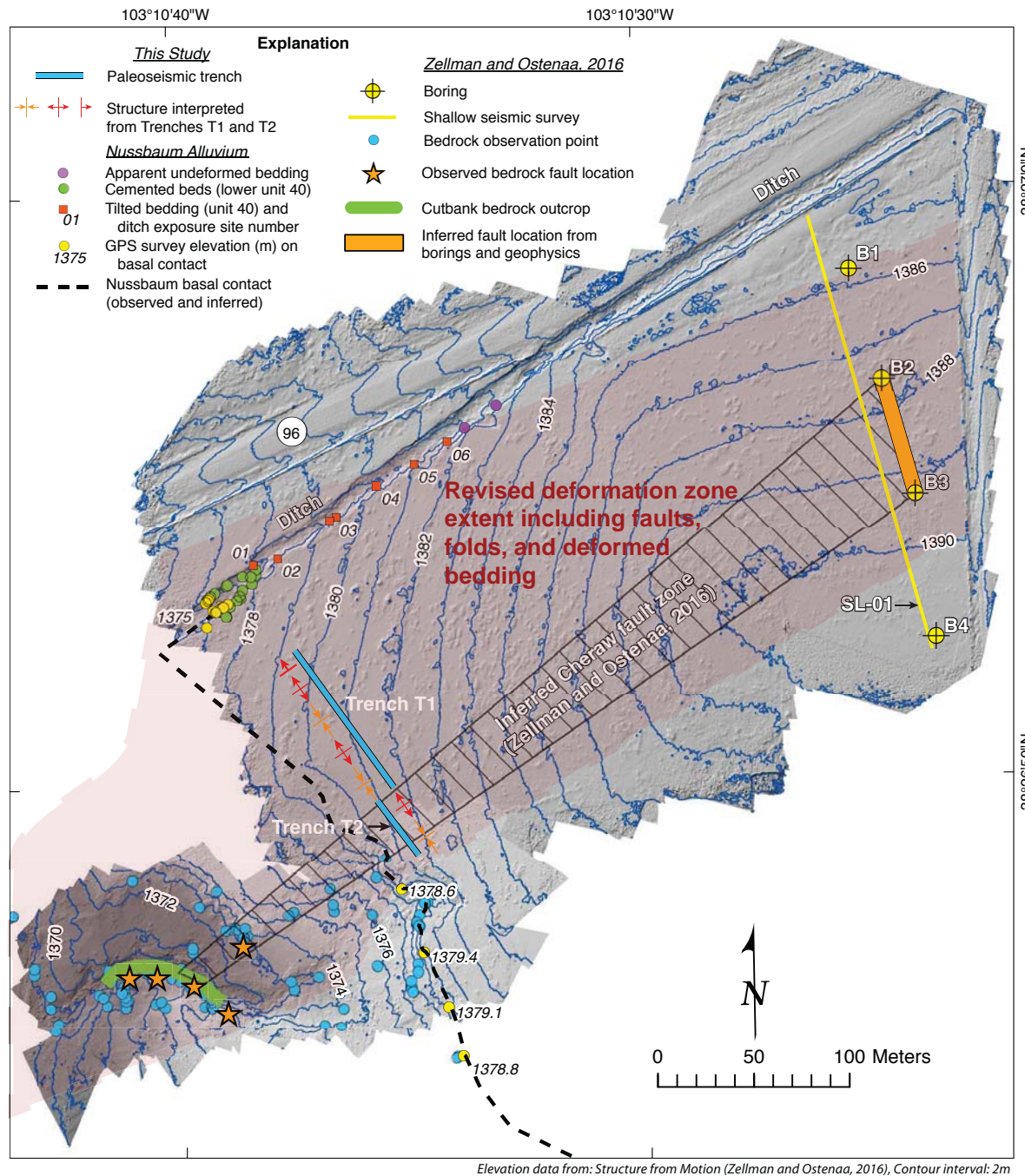
- Paleoseismic trench
- GPS survey elevation (m) on base of Nussbaum Alluvium
1379.1
- - Basal contact of Nussbaum Alluvium (observed and inferred)

- ⊕ Boring
- Seismic Survey
- Seismic refraction (shallow)
- Seismic reflection
- Depth migrated
- Time domain

Data from Zellman and Ostenaar (2016)

- ★ Surface projection of interpreted fault location in 2D seismic profiles
- ★ Estimated deformation zone interpreted from shallow seismic refraction survey and boreholes
- SfM aerial survey boundary
- ▨ Topographic scarp extent

Figure 5. Haswell area site investigations. Extent of the Cheraw fault scarp as mapped on 10 m NED DEM data is shown with red, hashed polygon. Detailed Haswell site investigation locations and types of data are shown with various symbols and lines (see Explanation). The primary investigation scope at the Haswell site was to determine the offset of the base of the Nussbaum Alluvium across the Cheraw fault. Between seismic Lines B and E, from southwest to northeast, the overall strike of the Cheraw fault, rotates about ~10° NE. Note that the estimated fault locations (stars) on seismic refraction and reflection lines are very approximate due to line location uncertainty and resolution of the industry seismic data in the near subsurface.



Haswell site. Time-domain Line E crosses the scarp at County Road 19 adjacent to the Haswell site. Both lines show relatively horizontal Upper Cretaceous strata on the footwall side of the fault, and a wide dip panel (~1 km wide) in Upper Cretaceous units on the hanging wall side of the fault which is tilted across a steep (~75°), northwest-dipping normal fault.

An inferred Cheraw fault zone (**Figure 6**) was delineated at the Haswell site by Zellman and Ostenaar (2016) based on: 1) The apparent offset of the basal contact between the bedrock outcrop and the ditch along Colorado State Highway 96, 2) Observed faults and discontinuities exposed in the Niobrara outcrop, and 3) Interpretations of the boring and 2D seismic refraction profiles. From these data, Zellman and Ostenaar (2016) suggested that offset of the basal contact of the early (?) Quaternary Nussbaum Alluvium may be only about 3 m. This zone, with the limited offset of the basal Nussbaum Alluvium contact, was the primary target for this trenching program until Fugro collected an additional unpublished high-resolution seismic survey 2 weeks prior to excavation of the Trench T1 and Trench T2 trenches. This new survey was located adjacent, and oriented parallel to, the excavated Trench T1 and Trench T2 trenches. The new high-resolution survey delineated a deformation zone 20 to 50 m further to the northwest; thus, defining a new primary trenching target.

Figure 6. Detailed map of Haswell site investigation and data locations. Detailed map of the Haswell site shows extent of the SfM data collected by Zellman and Ostenaar (2016) with observed outcrop, trench, boring, and shallow seismic survey locations. Fold structure observed in the trenches are shown adjacent to the trenches and general characteristics of Nussbaum Alluvium outcrops observed in the Hwy 96 ditch exposures are shown as circles and grouped by type. Tilted bedding locations are labeled with site numbers. In-situ basal contact observations of Nussbaum Alluvium are symbolized with yellow dots and labeled with GPS-survey measured elevations. Boreholes are labeled with boring name, and measured elevations of the in-situ Nussbaum Alluvium basal contact.

3.0 METHODOLOGY



3.1 LiDAR-based Mapping of the Cheraw Fault Scarp

We mapped fault scarps at a scale of 1:10,000 from 1 m Light Detection and Ranging (LiDAR) digital elevation model (DEM) hillshade and aspect maps (CGS, 2016). As a secondary basemap, we used 1 m U.S. Department of Agriculture (USDA) National Agriculture Imagery Program (NAIP) color orthoimagery, collected in 2013 (USDA NAIP, 2013) (**Plate 1**). Scarps that have a clear expression in the LiDAR aspect and hillshade maps are symbolized with a solid line to indicate the location of the fault is well constrained. The fault is mapped as a dashed line where inferred and dotted where concealed. The relative sense of motion is indicated with a “U” on the upthrown side, and a “D” on the downthrown side. Based on observations from the Crone et al. (1997) trench, we have mapped the fault near the base of the scarp as an estimate for where the surface trace of the Cheraw fault might be.

The clear expression of the Cheraw fault in the hillshade and aspect maps is a product of the northwest facing scarp which is opposite to the regional landscape that grades the southeast. On the hillshade (**Plate 1, Panel A**), the bright areas correspond to reflections on slopes facing a sunlight azimuth of 315° (northwest). On the slope map (**Plate 1, Panel B**), the northwest facing slopes are highlighted as a shade of magenta but may range to red and blue locally where the scarp change to northerly or westerly orientations. The colors of the scarp contrast with the generally yellow-green to blue-green shades that dominate much of the image and reflect the overall south to southeast slope of the present drainage system and older Quaternary alluvial surfaces in the area. Corresponding areas on the hillshade (**Plate 1, Panel A**), are displayed as uniform areas of grey tone. Sharp color breaks crossing the aspect map (**Plate 1, Panel B**), often green against blue, or blue-green to yellow, most often correspond to changes in valley side slope along drainages, such as Adobe Creek, or to riser slopes between surfaces.

3.2 Trenching Investigations at the Haswell Site

Two trenches totaling 120 linear m were excavated across the Cheraw fault scarp on March 26, 2016 using a track mounted Komatsu PC-200 excavator

equipped with a 1-m-wide bucket. For each trench, topsoil was stockpiled separately from the remaining spoil, and temporary fencing was installed around the open excavations. Trench T1 was 84 m long and had a single bench, allowing safe access to this 1.75 to 2.25 m deep trench. Trench T2 was 36 m long and excavated as a shallow slot trench with no bench. Both walls of Trench T1 and the northwest wall of Trench T2 were manually cleaned by scraping.

The trench locations for this study were chosen based on the previous work by Zellman and Ostenaar (2016), and refined based on additional reconnaissance geophysical profiles (**Figure 6**). As noted previously, the primary goals of the trench investigations were to determine the offset of the basal portion of the early (?) Quaternary Nussbaum Alluvium across the Cheraw fault and to obtain samples for stratigraphic age dating of the Nussbaum Alluvium. In the initial excavation of Trench T1, thickness of Nussbaum Alluvium and depth to Niobrara Formation appeared consistent with expectations based on the prior investigations. However, as the excavation of Trench T1 extended to the northwest, prominent relief on the Niobrara surface indicated a more complex picture of deformation than expected. Accordingly, Trench T1 was extended further to the northwest than originally planned, and Trench T2 was placed to fill the gap between the upper end of Trench T1 and outcrop exposures of the apparently undeformed basal contact of Nussbaum Alluvium, to the southeast (**Figure 6**).

After cleaning, and prior to photography, 20 random control points were established on each wall for the AgiSoft orthophoto rectification process. Each wall was then photographed during flat-light conditions from multiple angles by U.S. Geological Survey and Colorado Geological Survey geologists. The photos were mosaicked and processed with AgiSoft following methods established by Reitman et al (2015) to produce an orthophoto base for each wall (Trench T1 southeast and northwest; Trench T2 northwest). Each of the three walls was logged in detail at a scale of 1:15 on acetate sheets overlying the AgiSoft orthophotos. The log sheets were later scanned and digitized to produce trench logs (**Plate 2**).

The strike and dip of fractures and bedding were measured either with Brunton pocket transits calibrated to a declination of 7°19'E or with GeoID v1.8

iPhone software. The “right hand rule” applied to all attitude measurements. The GeoID software was tested and compared against Brunton and found to consistently match Brunton measured attitudes to within $\pm 2.5^\circ$.

A total of 3 soil profiles (**Appendix A**) were logged and 4 samples for luminescence analyses (**Appendix B**) were collected in Trench T1. Their locations are labeled and shown in **Plate 2**.

The trench was backfilled on April 3, 2016. The site ground disturbance was mitigated by harrowing and reseeding based on recommendations and requirements from the Colorado State Land Board.

After the closure of the trench, we returned to the site and conducted additional surveys of stratigraphic contacts, measured unit thicknesses, and docu-

mented geologic structures and features in nearby ditch exposures (**Figure 6**). The ditch is located to the north of the trenches, and is oriented sub-parallel to State Highway 96 (**Figure 6**). It is about 600 m long, 7 m wide, and its sidewalls are 1 to 3 m high. Exposed in the eroding ditch sidewalls is a similar stratigraphic section, from Niobrara bedrock through the Nussbaum Alluvium, to that exposed in Trenches T1 and T2. At select sites, the ditch walls were scraped and brushed to produce clean exposures for documentation and photographs. Stratigraphic contacts recognized in the trenches were surveyed and attitudes calculated using the spreadsheet from Hasbenarger (2012). One additional sample for luminescence analyses was collected from the ditch exposures.

4.0 LIDAR-BASED MAPPING RESULTS



The new LiDAR-based mapping extends the total length of the topographic scarp that characterizes the Cheraw fault, including the northeast extension, to about 80 km. The new mapping also provides limited confirmation for a secondary, subparallel scarp about 5 km northwest of Haswell, which extends about 20 km northeast along the northeast extension. The southeastern portion of this subparallel scarp was shown as an inferred fault by Kirkham and Rogers (1981), but is not shown on other maps. Data in Zellman and Ostenaar (2016) show that both the main and secondary scarps are associated with fault and fold structures in the underlying Cretaceous and older bedrock units imaged by oil and gas seismic reflection lines which cross the scarps.

4.1 Cheraw Fault Main Scarp

Plate 1 shows hillshade (**Panel A**) and aspect (**Panel B**) images derived from the CGS (2016) LiDAR data. On both images, an obvious northwest-facing scarp can be followed nearly continuously across the entire length of the LiDAR images. For discussion purposes, we divide the fault into three sections: southeast, central, and northeast extension. The southeast and central sections of the fault correspond to the original fault extent shown by Sharps (1976) and Crone et al. (1997).

The southeast section of the scarp, beginning on the left side of **Plate 1**, consists of an almost continuous, and relatively straight scarp for about 8 to 9 km from its southeast end. The scarp is smaller, but visible on the LiDAR images across most of the areas of young alluvium adjacent to Horse Creek, and continues with only minor breaks to about 5 km northeast of Horse Creek, near the Crowley – Otero County line. From this location for about 10 km to the northeast, to the area just northeast of the Crone et al. (1997) trench shown in **Plate 1, Panel D**, the overall strike of the scarp shifts a few degrees to the northeast. Individual mapped scarps in this section of the fault are slightly irregular, and consistently end with a right-stepping geometry and a step-over distance of about 100 m. Many of the stepovers have significant overlap with the adjacent scarp section. The length of the individual scarp sections systematically decreases from about 3 km long at the southeast end, to a few hundred meters just north of the Crone et

al. (1997) trench site. East of the Crone et al. (1997) trench site, the trace of the scarp steps to the right about 1 km, through a series of stepovers.

The transition to the central section of the fault is marked by the stepover which begins at the area outlined as **Plate 1, Panel D**. Beyond this stepover to the northeast, the scarp continues as a relatively uniform and linear trace for about 4 km across an area of smooth topography and slope, on Rocky Flats Alluvium. The strike of the fault makes a small bend, but is still straight and continuous to the northeast as the fault trace drops in elevation over the next 4 to 5 km down the eroded valley side slope into Adobe Creek. Northeast from Adobe Creek, for about 15 km to the sharp change in strike about 6 km southwest of Haswell, the fault makes a gradual shift to a more northerly strike, and exhibits more local irregularity and complexity than what is observed southwest of Adobe Creek. In this area, most of the individual scarp sections are several kilometers in length. The longest single scarp section extends for about 8 km northeast from Adobe Creek, and terminates with a small right step and strike change. Most of scarp section is flanked by a series of smaller, shorter scarps offset up to 1 km southeast of the main scarp section. These flanking scarps end near the midpoint of the next scarp section to the northeast. The northeast half of the central section of the fault is characterized by a series of left-stepping scarps, individually about 1 to 2 km in length. The largest of these left steps, has a stepover width of almost 1 km, accomplished across three scarp sections. The central section of the fault ends with a very sharp, about 30° change in strike to the northeast. The original Cheraw fault, as mapped by Sharps (1976) and Crone et al. (1997) ended about 2 km southwest of this sharp bend (see notations and linework below **Panel C on Plate 1**).

The northeast section of the fault extends about 30 km from the sharp bend in the fault, approximately 5 km southwest of Haswell, to the northeast limit of the CGS (2016) LiDAR coverage. This section of the fault is characterized by a relatively straight alignment, which bends slightly northward and becomes slightly more irregular along the northeast portion. From the origin of the northeast section, near the bend, to Haswell, several subparallel and overlapping scarp

sections are mapped in the eroded landscape below the large Nussbaum surface that begins at Haswell. These scarps continue as a single larger, but broad scarp on the Nussbaum surface northeast of Haswell along Highway 96 for about 8 to 9 km. In this area, Highway 96 bends to the north around the margins of an area of eroded and more complex topography (shown as a closed depression or likely collapse area near Salt Lake on **Figure 4**). The fault trace is indistinct for about 6 km across this feature, until the fault trace crosses Highway 96. Northeast from Highway 96, the scarp is once again present at the surface for another 10 km northeast, but more irregular and curving. Geologic and geomorphic mapping (Figures 3 and 4) show this area to be underlain by Nussbaum Alluvium and covered with a substantial mantle of younger eolian deposits. Thus, some of the irregularity and subtle expression of the scarp trace is likely due to eolian deposits banked up on the prior fault scarp. There is no obvious continuation of the scarp off the northeast edge of the LiDAR extent, but the apparent scarp end is clearly masked by young eolian deposits. Available aerial photography in this area has less resolution than the LiDAR data, and shows many eolian features, but has not identified any lineaments or features that support continuation of the scarp.

Along most of the length of the Cheraw fault, vertical offset associated with the scarp appears to be in the range of 3 to 7 m. The largest scarps are only present in a few areas where older alluvium, mapped as Rocky Flats and Nussbaum Alluvium (see Figures 3 and 4) is preserved. This includes a small remnant of Rocky Flats Alluvium adjacent to the Crone et al. (1997) trench site, with previous estimated vertical offset of about 8 m (Crone et al., 1997) to 12 m (Kirkham and Rogers, 1981). Based on the CGS (2016) LiDAR data, it appears that younger erosion on the hanging wall side of the fault likely removed the Rocky Flats Alluvium adjacent to the fault at this site. If so, offset of the Rocky Flats Alluvium at the Crone et al. (1997) trench site is likely less than 8 m. Scarps heights on the large areas of Rocky Flats Alluvium northeast and southeast of Arlington (Figure 4) generally range from 5 to 7 m. The scarp is smaller, but still visible, where it crosses Holocene and Late Pleistocene alluvium adjacent to active drainages such as Horse Creek and Adobe Creek. In these areas, the scarp is generally less than 1 to 3 m high, locally modified or breached by younger erosion, but still clearly visible across the young alluvium associated with these drainages. Near Haswell, at the southwest end of the longer section of the scarp cutting Nussbaum Alluvium, vertical offset is about 9 m (discussed below in **Section 5**). Northeast from Haswell, the scarp primarily offsets surfaces formed on Nussbaum Alluvium, although these are often mantled with extensive eolian cover. Scarp heights are more difficult to measure in this area due to uncertainties in

surface correlations across the scarp. However, along much of the northeast extension, scarp heights appear to be larger, consistent with expected offset of the Nussbaum surfaces, except for an eroded section, about 7 km long, associated with local drainage into the Salt Lake closed depression (**Figure 4**).

As summarized in **Section 2**, Zellman and Ostenaar (2016) showed that the main Cheraw fault scarp is directly associated with older underlying bedrock structures expressed in oil and gas industry seismic reflection surveys that cross the fault. These older structures, which the younger normal faulting appears to reactivate or exploit, are generally near vertical in dip, with steep local dips to both the northwest and southeast. The young surface offset of the Cheraw fault is down to the northwest, and Zellman and Ostenaar (2016) infer an overall fault dip of 75° to the northwest based on interpretations from the seismic reflection data. The overall trace of the fault scarp across topography and along strike is generally consistent with a steep fault dip to the northwest. In most areas, as the scarp cuts across topography from higher areas to lower areas, the trace of the scarp is generally linear, or migrates slightly to the northwest, consistent with a steep dip in that direction. On a large scale, the central section of the fault scarp, from the Crone et al. (1997) trench site to near Haswell (**Figures 3 and 4; Plate 1**), is somewhat concave to the northwest, also suggestive of dip in that direction. One notable exception, within this central section of the fault, is seen where a continuous mapped scarp descends from the higher terrain flanking both sides of Adobe Creek (**Plate 1, Panel C**), and bows downstream, possibly suggestive of the topographic throw on a steeply southeast dipping fault plane. It should be noted as well, that the average strike of the fault scarp changes significantly on either side of Adobe Creek, and the scarp geometry here may simply be a reflection of that strike change and the complexities of the older structure which younger fault movement is associated with. The apparent downstream bow of the fault scarp may also be enhanced by our mapping convention, which places the line delineating the fault, near the base of the slope break. Thus, as the fault transitions from an area with a higher, broader scarp slope to an area with a lower, narrower scarp slope, the line depicting the fault trace will show a bend or bow to reflect the change in slope width on the scarp.

4.2 Cheraw Fault Secondary Scarp

The CGS (2016) LiDAR coverage (**Plate 1**) includes the southeastern 2 to 3 km of the short, queried, secondary fault shown by Kirkham and Rogers (1981). Both the hillshade (**Panel A**) and slope (**Panel B**) maps show a clear, northwest-facing scarp, about 0.5 to 1 m high, on the gently southeast-sloping Nussbaum

surface at this location. This scarp can be extended further northeast along distinct tonal lineaments and slope breaks visible on the NAIP color airphoto images used as the base map for **Plate 1**. On **Panel C**, the southeastern portion of the scarp visible on the LiDAR-derived images is shown as a solid line trace. The continuation of the scarp to the northeast, based on the lower-resolution aerial photography is shown with dashed trace. The total length of the secondary scarp as currently mapped is about 20 km and is generally subparallel to the main scarp. Near Haswell, the secondary scarp is about 5 km northwest of the main scarp, and at the northeast mapped limit of the secondary scarp it is about 8 km northwest of the Cheraw fault main scarp.

Similar the main scarp of the Cheraw fault, the secondary scarp appears to be a down-to-the-northwest normal fault, with small displacement. **Figure 3** shows the locations of bedrock structures interpreted by Zellman and Ostenaar (2016) on the industry seismic reflection lines that cross the Cheraw fault. These older structures have much larger vertical offsets, and structural styles that suggest primarily reverse or oblique motions. The younger normal faulting is occurring along reactivated, older compressional structures in the underlying Cretaceous and older bedrock units.

5.0 RESULTS OF THE HASWELL TRENCHING INVESTIGATION



Results from the Haswell site support four broad conclusions: 1) The topographic scarp that characterizes the Cheraw fault, including the northeast extension, is associated with a fault and fold structure in the Niobrara Formation bedrock, 2) Overlying early (?) Quaternary Nussbaum Alluvium at the Haswell site is significantly deformed, in a complex fault zone across the site, with vertical offset of the basal contact is greater than 5 to 6 m, and most likely about 9 m, 3) Nussbaum Alluvium exposed at the site is significantly younger than previous interpretations suggested, based on four luminescence ages which suggest deposition ranged from <126 to >>160 ka; and 4) Stratigraphic relations from the trenches indicate that deformation of the Nussbaum Alluvium at the site is younger than about 126 to 160 ka. The study trenches do not provide evidence for the number of, or specific timing of, events related to this deformation.

5.1 Haswell Site Stratigraphy

Stratigraphy exposed in the trenches and ditch exposure consisted of three major groups of units: 1) Cretaceous Niobrara Formation bedrock, 2) early (?) Quaternary Nussbaum Alluvium, and 3) Late Pleistocene or Holocene slope colluvium and channel-fill deposits. Trench logs including detailed descriptions of the units as exposed in the trenches are provided on **Plate 2**.

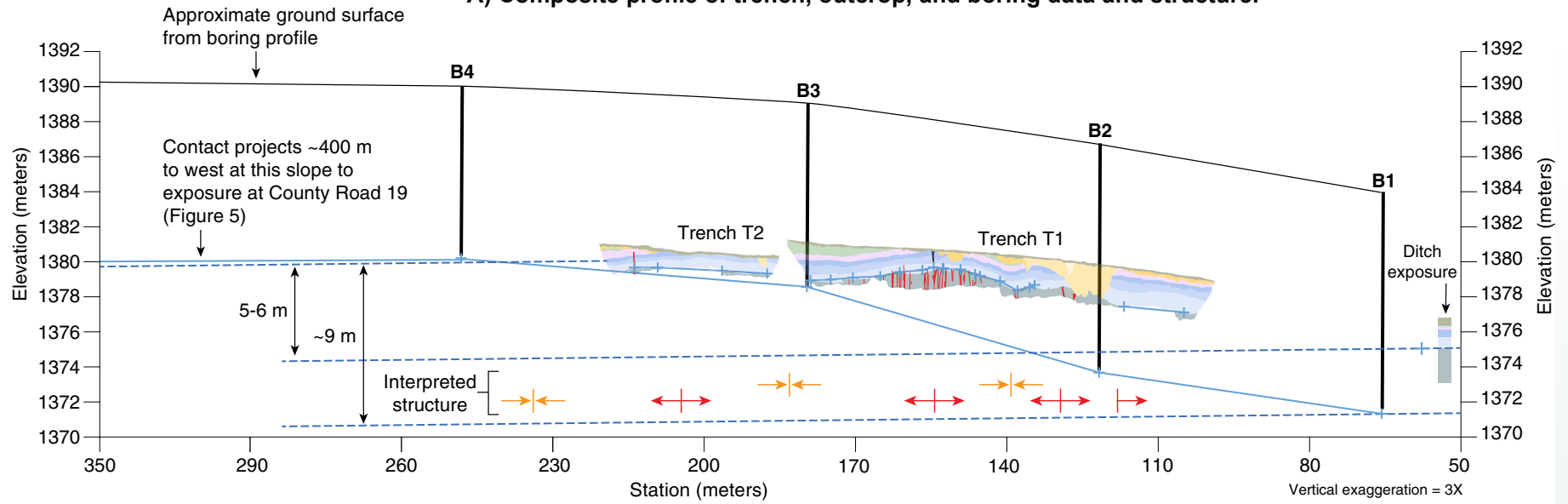
Based on mapping and descriptions from Sharps (1976), bedrock exposed in the trenches is assigned to the Smoky Hill Shale Member of the Niobrara Formation. As exposed and mapped in the trenches (**Plate 2**, unit 10), it consists of highly to completely weathered, slightly fissile, chalky shale. In Trench T1, several weathered, ochre-colored clay beds, between 2 to 20 cm thick, were prominent markers defining the dip and folded structure within the Niobrara Formation. Regionally, Niobrara Formation units on the northwest margin of the Las Animas Arch have gentle regional dip to the northwest as a result of Laramide-age growth of the Las Animas Arch.

A sequence of fluvial deposits and loess, with multiple buried soils, that make up the Nussbaum Alluvium (Scott, 1970; Sharps, 1976) overlie a relatively low-relief erosional surface cut into the Niobrara Formation. Nussbaum Alluvium as exposed in Trenches T1 and T2 consists of a basal section of fining upward

fluvial channel and floodplain deposits (unit 20) capped with well-developed argillic soils (units 25 and 26). In the trenches, this basal section ranges in thickness from 0.8 to 1.75 m. In the ditch exposure about 50 m northwest of Trench T1 (**Figure 6**), this unit, where measured, was about 1.05 m thick (**Figure 7**). The floodplain deposits and soils are unconformably capped by a thin loess unit (unit 30) that is generally about 0.3 m thick in both the trenches and in the ditch exposure to the northwest. A second sequence of fluvial sands (unit 40), only partly exposed in Trenches T1 and T2 and more fully exposed in the ditch outcrop, overlies and erodes the top of the loess. The lower portion of this upper fluvial unit locally has extensive carbonate cementation concentrated in sand beds and sub-vertical pipes between beds. The 40 cm exposure of this unit in the trenches is only a limited thickness of the upper fluvial sands. Extensive, but discontinuous exposures of this unit in the ditch about 50 m northwest of Trench T1 consist of interbedded silt and fine sand overbank deposits, which may have an aggregate thickness of up to about 6 meters. A detailed measurement of the full thickness of unit 40 exposed in the ditch exposure, was not completed due to the discontinuous exposures and complex deformation of this unit in the ditch exposures. Stratigraphic contacts and soil horizon boundaries in all the Nussbaum deposits reflect deposition and soil formation on a fluvial landscape having a gentle slope to the southeast. Regional slope of the basal Nussbaum contact measured over distances of 1 to 40 km northwest from the trench site averages about 0.003 (0.1°) to the southeast.

The youngest units exposed in the trenches consist of hillslope colluvium and channel fills related to erosion and deposition on the generally west-facing topographic slope where the trenches were sited (**Figure 6**). Topographic slope that most influences erosion and deposition of these units is primarily across Trenches T1 and T2. Unit 60 includes mostly loose, slightly carbonate-cemented sands in broad channel-fills up to about 0.5 m thick. Unit 50 channels are filled with similar sands, but locally cross-cut unit 60, are more irregular, and thicker (up to ~3 m). A thin surficial colluvium (unit 70), typically about 0.3 m thick, with a weakly developed soil, cross-cuts all units and extends the length of both trenches.

A) Composite profile of trench, outcrop, and boring data and structure.



B) Profile of Nussbaum Alluvium thickness (20 series units).

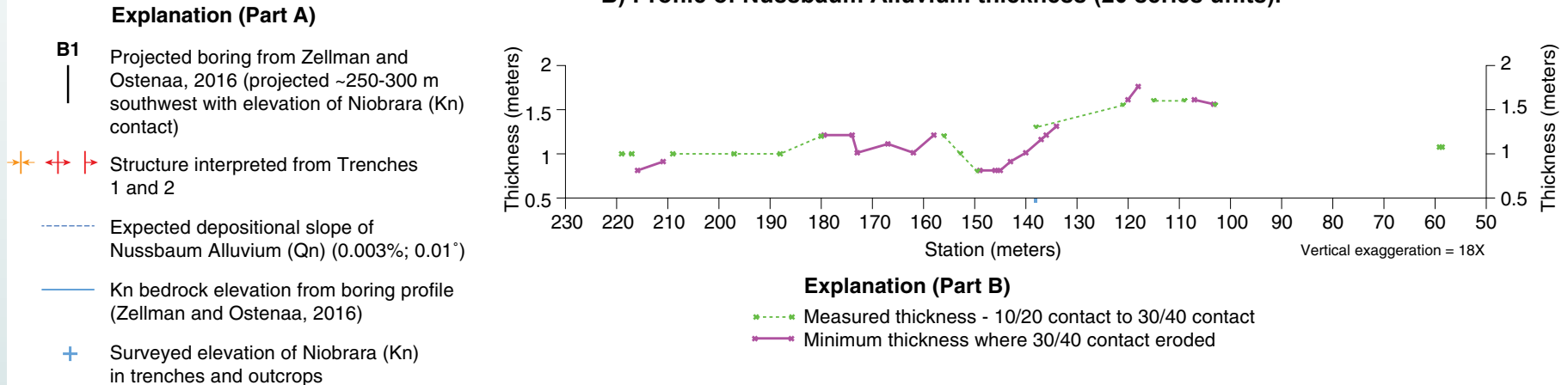


Figure 7. Composite profile with trench and boring data (panel A), and lower Nussbaum Alluvium bed thickness (panel B). Panel A shows the boring profile and outcrop data projected to a profile through Trenches 1 and 2 (See Figure 6 for relative locations and orientations). Elevations of the basal Nussbaum Alluvium contact, as observed on the foot wall from outcrops ~400 m to the southeast, Borings 3 and 4, and southeast portions of the trenches, are consistent with expected pre-faulting depositional slope. The estimated vertical offset of the Nussbaum Alluvium basal contact is about 5 to 6 m between the trenches and ditch, versus about 9 m when considering the boring profile. Note that the offset estimated along the profile alignment at the trenches and ditch exposure does not include the additional deformation at Site 01 and upslope along the ditch, crossed by the boring profile. Panel B shows the measured and minimum thickness of Nussbaum Alluvium beds measured in the trenches and CO Hwy 96 ditch exposure. Variation in bed thickness is interpreted to be attributed to erosion, as no clear increases in thickness are associated with the synformal structures mapped in the trenches. Note that horizontal stationing and scale in panels A and B are aligned to facilitate direct comparison.

5.1.1 Soil Profile Descriptions and Age

Three soil profiles were described in Trench T1 by Paul Reinflesch (USDA NRCS, Denver, Colorado) (**Appendix A**) at approximately stations 176, 153, and 141 (**Plate 2**). These stations were chosen as representative locations where the sequence of soil development exposed in the trench units could be described in single profiles and used to compare the soil development in different structural settings among the folded units. The field sheets for the detailed descriptions are included in **Appendix A**, and **Table 1** shows correlation for geologic units, soil horizon designations, and layer numbers for each of the soil profiles.

The upper portions of each profile reflect soils associated with the present hillslope surface across the trench. Significant soil development represented by the Btk horizons mapped in the trenches as units 25 and 26 (**Plate 2**) provide an indication of the minimum length of times of relative landscape stability represented by each of the soils. Periods of relative landscape stability with significant soil formation followed deposition of the basal Nussbaum Alluvium, but prior to deposition of the lower Nussbaum loess (unit 30), are represented by buried soils mapped as units 25 and 26. Additional Btk soil development in unit 30 was truncated by erosion prior to deposition of the upper Nussbaum Alluvium (unit 40).

The development of prominent and thick Btk horizons within units 25, 26, and 30 is each likely associated with periods of relative landscape stability lasting at least tens of thousands of years.

5.1.2 Luminescence Dating Analysis

Five samples were collected for stratigraphic age analysis and processed at the U.S. Geological Survey Luminescence Dating Laboratory in Denver, Colorado. Four samples were collected from the Nussbaum Alluvium: two from unit 40, one from unit 30, and one from unit 20 near the Nussbaum Alluvium's unconformable basal contact with Niobrara bedrock. The fifth sample was collected from near the base of unit 60, a large channel-fill deposit apparently related to relatively young local erosion and deposition on the hillslope where the trenches are sited. These sample locations were chosen because they have the potential to provide insight into the age and total length of time represented by deposition of stratigraphic section exposed in Trenches T1 and T2, and the ditch exposure. All samples were collected on the northeast wall of Trench T1, except for the sample from unit 30, which was collected from the ditch exposure. Field sample numbers, trench station/location, approximate depth below current ground surface, and the corresponding trench stratigraphic unit are listed below in **Table 2**. All samples were collected from locations within the stratigraphic section which were uncemented, and where the preservation of fine laminations and stratification indicated an absence of disturbance by bioturbation or other post-depositional effects. All samples were processed using infrared stimulated luminescence (IRSL) techniques because of the abundance of feldspar in the sample material. Sample T1E-OSL-3 was processed using both IRSL and optically stimulated luminescence (OSL) because it contained both quartz and feldspar. Sample ages, reported in ka, are shown in **Table 2** and in stratigraphic context on **Plate 2** and **Figure 9**. The U.S. Geological Survey Luminescence Dating Laboratory's Analysis Report is included as **Appendix B**.

5.1.3 Age of Nussbaum Alluvium at the Haswell Site

The luminescence dating results (**Table 2**) indicate a likely depositional age range for the unit 40 portion of the Nussbaum Alluvium ranges from 120 ka to about 160 ka. The two samples from unit 40, T1E-OSL-2 and T1E-OSL-4, were both near the erosional base of this massive to finely stratified unit, and appear to indicate a time span for active deposition at the base of this unit of about 30 to 35 kyr. Both samples were collected from exposures in Trench T1, near the base of unit 40. In the ditch exposures northwest of Trench T1, unit 40 appears to be several meters thick, and the upper portions of this section are potentially

Geologic Unit Groups	SP 1 T1 - Station 176			SP 2 T1 - Station 153			SP 3 T1 - Station 141		
	Trench Unit #	Horizon	Layer #	Trench Unit #	Horizon	Layer #	Trench Unit #	Horizon	Layer #
Surface Soils and Hillslope Colluvium	70	A1	1u	70	A	1	70	A	1
		A2	2u					Btw	2
				50	Btk	2	50	Btk	3
								BCk	4
Nussbaum Alluvium and Soils	40	Bw	3u	26	2Btk1	3	40	2Ck/Bkkm	5
		Bk1	4u						
		Bk2	5u						
	30	Bkkm	6u				30	2Btkb1	6
		2Bkkm	7u						
		2Btkb1	8u						
	26	3Btkb2	1l				26	3Btkb2	7
		3Btkb3	2l						
		3Btkb4	3l						
	25	3Btkb5	4l				25	2Btk2	4
2Btk3				5					
20	4CBt	5l	20	3CBt	6				
	5Bkkm	6l							
Niobrara Formation	10	6R	7l						

Table 1. Trench units and soil profile (SP) horizon correlations.

Geologic Unit Group	Trench Unit #	Type of Deposit	Luminescence Sample and Results		Interpreted Age for Stratigraphic Units	
			Sample Number/ Location	Lab Age	Estimated Age Range	Basis
Surface Soils and Hillslope Colluvium	70	Slope Colluvium			< 5 ka	Surface soils
	60	Alluvium	T1E-OSL-3 T1E - NE Sta. ~121.9	10.7±1.1 ¹ 8.4±1.0 ²	~8 to ~12 ka	Sample age
	50	Alluvium			>8 to 12? ka	Stratigraphic position below unit 60
Nussbaum Alluvium and Soils	40	Alluvium	T1E-OSL-2 T1E - NE Sta. ~179.3 T1E-OSL-4 T1E - NE Sta. ~140	126 ±11 ¹ 159 ±11 ¹	~120 to 160 ka	Range of ages in stratigraphic order
	30	Loess	OSL-5 Ditch Exposure	153 ±8.5 ¹	~150 to 160 ka	Sample ages uncertainty; stratigraphic order
	26	Buried B-horizon			~160 to 200 ka	Time for soil formation
	25	Buried B-horizon				
	20	Alluvium	T1E-OSL-1 T1E - NE Sta. ~105.5	> 160 ¹	>200 ka	Additional time for duration of deposition and strath formation

¹Feldspar post IR-IRSL age, ²Quartz OSL age. See **Appendix B** for luminescence analyses data.

Table 2. Haswell site luminescence dating and interpretations.

younger, but were not dated. Luminescence sample OSL-5, was collected in the ditch exposure from the thin loess (unit 30), which unconformably underlies unit 40. The age result from this sample, 153 ± 8.5 ka, is slightly younger, but with overlapping error ranges, than the older of the two ages on samples near the base of unit 40. This result suggests that the ranges for these two ages may approximate the last deposition, surface exposure, and soil formation within the loess (unit 30) prior to erosion associated with deposition of unit 40.

Beneath unit 30, two well developed soil horizons, mapped as units 25 and 26, are formed in alluvium that caps the basal crossed bedded and channeled alluvium of unit 20. This soil development likely represents at least several tens of thousands of years of relative landscape stability. One luminescence sample, T1E-OSL-1, from unit 20, was saturated at >160 ka. Based on the soil development in horizons overlying this sample, we infer that the minimum age for the lowermost Nussbaum Alluvium exposed in the trenches is likely at least 200 ka (**Table 2**). Erosion on the basal strath cut on Niobrara bedrock must be at least this old, and could be potentially much older.

5.2 Haswell Site Structure and Deformation

5.2.1 Trenches T1 and T2

The most prominent structural features exposed in the trenches are undulations and the overall drop in elevation, to the northwest, of the Niobrara/Nussbaum contact and overlying Nussbaum Alluvium (**Plate 2**). Both the Niobrara Formation and Nussbaum Alluvium appear to be deformed and folded in a similar fashion, across three small-amplitude folds, with a net down-to-the-northwest displacement. Concentrated on the crests of the folds, are numerous fractures in the Niobrara Formation, some of which extend into the overlying Nussbaum Alluvium. The zone of deformation includes the full length of Trenches T1 and T2, as shown by the abnormally steep dips for basal Nussbaum Alluvium present at the northwest end of Trench T1, and the southeast end of Trench T2.

The folding of the Nussbaum Alluvium is represented by broad anticlinal crests at station ~205 in Trench T2 and station ~155 in Trench T1, and a shorter wavelength crest at station ~130. Synclinal troughs are located about 5 to 10 m southeast of Trench T2, in the gap between Trenches T1 and T2 (station ~185), and at station ~140. The northwest end of Trench T1 beyond station ~130 lies on the northwest dipping limb of an anticline, with an additional monoclinical flexure slightly increasing the northwest dip of the underlying Niobrara beds at station ~120. Thus, bedding dips at both ends of the trench exposures appear to require additional structure beyond the trench extent to restore the Nussbaum Alluvium to an original depositional orientation.

As shown on **Plate 2**, dip of bedding in the Niobrara Formation generally deviates by 1° to 2° from the orientation of the erosional contact at the base of the Nussbaum Alluvium. This deviation is shown best by the orientation of marker beds mapped in the lower half of Trench T1, between stations ~145 to 100. Over the length of Trench T1, from northwest to southeast, the erosional contact at the base of the Nussbaum Alluvium cuts down into successively lower strata in the Niobrara Formation. Regionally, Nussbaum Alluvium was deposited on an erosional surface sloping gently to the southeast (~0.003% or 0.1°) across the northwest-tilted Cretaceous rocks exposed across the northwest flank of the Las Animas Arch. Based on the regional structural setting of the site on the northwest flank of the Las Animas Arch (**Section 2 and Figure 1**), and data from nearby industry seismic reflection profiles (Zellman and Ostenaar, 2016), a 1° to 2° northwest dip likely represents the subregional dip of the Niobrara Formation absent local deformation effects of the Cheraw fault. In Trench T1, the dip of

Niobrara Formation bedding ranges from 5° northwest to 1° to 2° southeast. Stratification, bedding, and soils within the Nussbaum Alluvium all appear to be uniformly folded, in a parallel manner, with this depositional surface, and with the underlying Niobrara Formation that previously dipped gently to the northwest. Thus, the growth of small folds, younger than the Nussbaum Alluvium, locally reversed the regional dip direction of the Niobrara Formation bedrock by 3° to 4° and steepened it by to 2° to 3°. There is no clear indication that the much younger channel fill and slope colluvial units related to deposition and erosion on the modern hillslope, are involved in this folding.

Primarily in Trench T1, where there is better exposure, the crestal areas of the small anticlines contain extensive small fractures in the Niobrara Formation, mostly oriented subparallel to the strike of the Cheraw fault. These fractures have little or no vertical offset, and often cannot be extended across the trench to the opposite trench wall. Several of these fractures were observed to be slightly open or filled with loose, uncemented sand from the overlying Nussbaum Alluvium, and some extended through strongly cemented basal layers of the Nussbaum Alluvium and up into the less cemented sandy gravels of the basal alluvium. One of the fractures, at station ~215 in Trench T2, was observed to extend through the entire basal alluvium and into the overlying Nussbaum loess. All the remaining fractures terminate either at the Niobrara/Nussbaum contact, or within the sandy gravel basal alluvium of the lower Nussbaum Alluvium (unit 20).

The only other fracture-like feature observed away from the Niobrara Formation and lowermost sandy gravel of the Nussbaum Alluvium (unit 20) is a wedge-shaped fissure filled with loose, sandy colluvium (unit 71) similar to the surface soil and colluvium (unit 70). This fissure, located on the upper east wall of Trench T1 near station 160, extends down from the base of the surface soil and colluvium (unit 70) and tapers downward into the Btk soil horizons (units 25 and 26) of the Nussbaum Alluvium. It is not traceable into the underlying gravelly alluvium (unit 20) and does not align with prominent sand-filled fractures in the underlying Niobrara Formation. Three interpretations seem plausible for this fissure, 1) frost wedge, 2) desiccation feature, or 3) ground fissure related to recent folding. The form, and lack of connection to underlying fractures could support an origin as a frost wedge or desiccation. Although soils in this feature were not described in detail, soil development across the fissure did not appear strong enough to support a pre-Holocene, Late Pleistocene age for a climate-regime consistent with formation of frost wedges or desiccation features of this scale. Both types of features were common in the large exposures across the Anton escarpment mapped by Noe (2010). No datable material was found within

this feature, and the infill did not appear suitable for luminescence dating analyses. The form, fill, and relatively weak soil development across the fissure could be consistent with an alternative origin as a ground fissure associated with young folding, but absent physical connection to underlying fractures, the fissure origin mechanism is currently unresolved.

5.2.2 Ditch Exposure

Northwest of the trench and boring profile near the base of the Cheraw fault's topographic scarp is a long ditch exposure adjacent to CO Highway 96 (**Figure 6**). With insight gained from the clear exposures of the Nussbaum Alluvium in the trenches, all units found in the trenches were recognized and mapped in the ditch, with the exception of the youngest Holocene channel-fill deposits. Along the southwest end of the ditch extent shown on **Figures 6 and 8**, the basal contact of Nussbaum Alluvium with underlying Niobrara Formation is intermittently exposed on both sides of the ditch. The Niobrara Formation (unit 10) is overlain by gravelly alluvium (unit 20), Btk soil horizons (units 25 and 26), Nussbaum loess (unit 30), and upper Nussbaum sandy alluvium (unit 40). The same stratigraphic sequence is present with comparable stratigraphic thicknesses in a profile aligned through the trench exposures (**Figure 7**). The stratigraphic section portrayed on **Figure 7**, and annotated on **Figure 9**, is near the point where the northwest projection of the fault trench intersects the ditch (**Figures 6 and 8**). The overall bedding orientations of the Niobrara Formation and overlying Nussbaum Alluvium in the southwestern part of the Haswell ditch exposure are generally consistent with orientation of these units in the closest part of Trench T1, about 50 m to the southeast. Most beds have a gentle dip to the northwest, with a small discordance of dip between the Niobrara Formation marker bed compared to dips of Nussbaum Alluvium contacts, similar to that observed in Trench T1. A full comparison and analyses of these data are discussed in more detail in **Section 5.2.4** below.

Exposed in the sidewall outcrops of the ditch, to the northeast of the measured stratigraphic section, is broad zone of deformation expressed by steeply tilted and vertical beds of cemented "hardpan" and silty and sandy intervalled beds of Nussbaum Alluvium (unit 40) (Locations on **Figure 6** and photos on **Figures 8 through 12**). The deformation is expressed over a about 130-m-long zone that is mostly best exposed along the southern wall of the ditch (**Figures 10, 11 and 12**). The zone is bounded to the northeast and southwest by relatively horizontal, or gently dipping Nussbaum Alluvium (**Figures 9 and 11**). Sites 01 through 06 shown in **Figures 6 and 11** designate discrete observations of tilted



Figure 8. Site 01 and stratigraphic site in ditch along CO Hwy 96. View to the northwest across the ditch adjacent to CO Hwy 96 showing tilted and deformed beds of Nussbaum Alluvium (unit 40) at site 01 (see **Figure 6** for location). Steeply tilted and cemented beds in Nussbaum Alluvium are in front of observer, marked with white dashed lines. The stratigraphic section (ditch exposure) compiled on the profiles of **Figure 7**, is to the far left of this view. A detailed view of the exposure is shown in **Figure 9**. The un-labeled black arrows mark outcrop of the Nussbaum “basal hardpan” of unit 40.

bedding in Nussbaum Alluvium unit 40. Between these sites, the ditch wall exposures are mostly obscured. After scraping, cleaning, and close examination of the tilted and deformed bedding, it is clear that these exposures are in-situ rather than resulting from slumping and failure of the excavation walls. The exposures of tilted bedding are observably in-place in the ditch walls and unconformably overlain by slope colluvium. The deformation zone intersects the ditch at a highly oblique angle, which results in the apparently wide zone of deforma-

tion on the southern ditch wall. The actual width of the zone may be no more than 20 m to 40 m wide. The only observation of faults and fractures was at site 01 (Location on **Figure 6** and photos on **Figures 8 and 10**). No structural orientations were measured, but these features appear to project from the ditch northeast to the boring and seismic profile between borings 1 and 3 (**Figure 6**). The zone has no clear geomorphic expression at the ground surface other than its general correspondence to the broad Cheraw fault scarp shown in **Figures 5 and 6**.

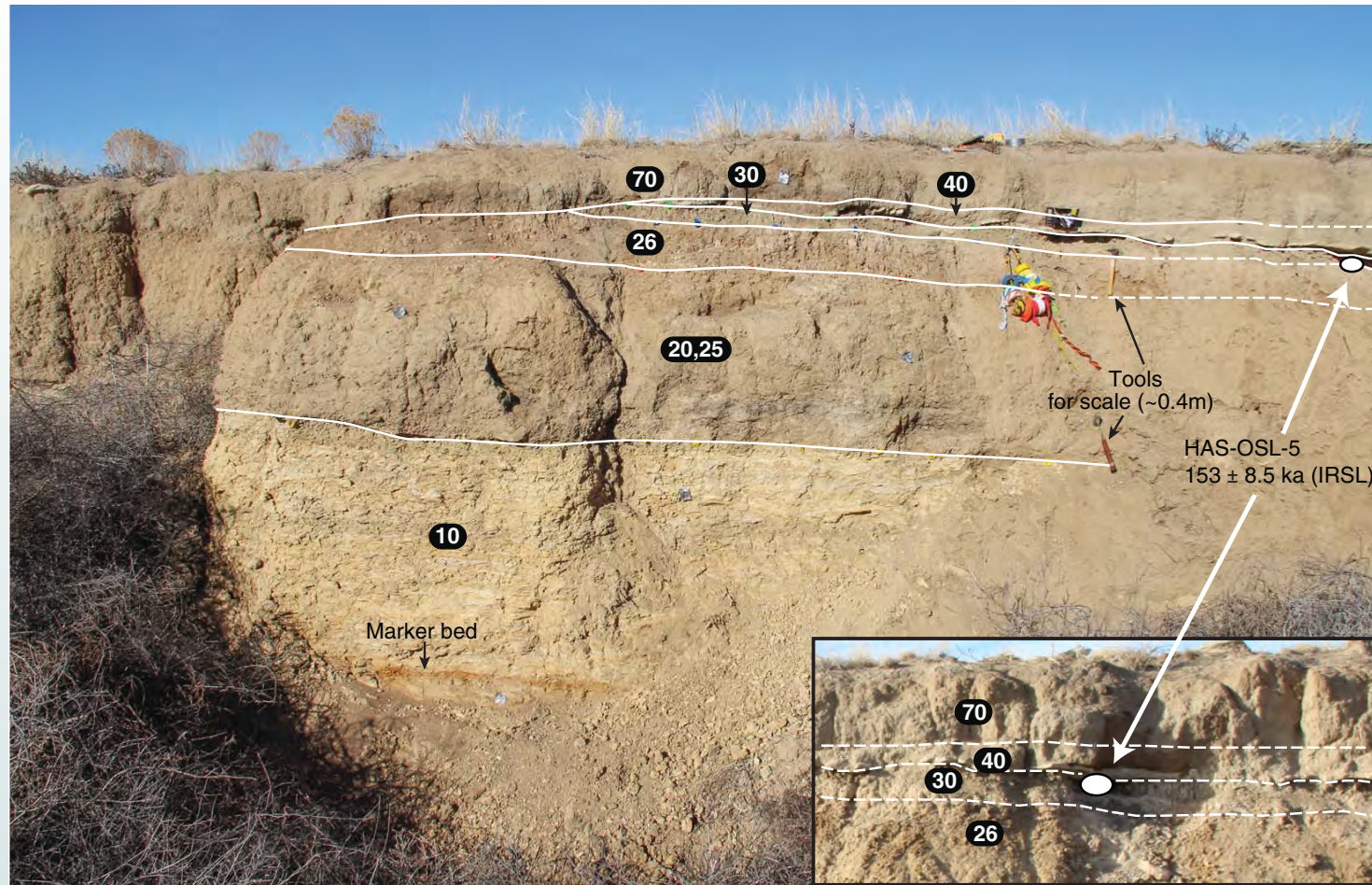


Figure 9. Stratigraphic section of Nussbaum Alluvium exposed in ditch adjacent to CO Hwy 96. Stratigraphy exposed in the northwest wall of the ditch located just southwest of site 01 (See **Figures 5, 6 and 8** for location). Major units are marked with white lines and labeled with numbers which correspond to Nussbaum Alluvium stratigraphy mapped in detail in Trenches T1 and T2. Dip of Marker Bed in the underlying Niobrara Formation (unit 10) is consistent with the southwestern most measured dip of a similar bed in Trench 1 about 50 m southeast, suggesting no significant change in structure between these measurement locations. See **Plate 2** for detailed unit descriptions. Inset photo in lower right shows additional stratigraphic detail near location for luminescence sample OSL-5.

Additional exposures in the ditch to the northeast of site 06 (**Figures 6 and 11**), show gently dipping, fluvial sands, similar to Nussbaum Alluvium unit 40 as mapped in the Trenches T1 and T2. Although we did not measure a detailed stratigraphic section, the extent of these units in the ditch exposure appears to suggest that the original undeformed thickness of unit 40 may have been up to about 6 m.

5.2.3 Relationship of Folding to Basal Nussbaum Alluvium Thickness

The trench logs (**Plate 2**) show a considerable variation in thickness for the basal Nussbaum Alluvium and related soils (units 20, 25, 26) along the length of the trench. The thickest exposure of basal Nussbaum Alluvium lies in the lower portion of Trench T1, station ~115, where it is about 1.75 m thick (**Figure 7**). In comparison, thickness of the same units at the upper end of Trench T1, near



Figure 10. Closeup view of deformed Nussbaum Alluvium beds at site 01 in ditch. Tilted beds, marked with dashed white lines, in Nussbaum Alluvium (unit 40) exposed in ditch along CO Hwy 96 at site 01. Carbonate-cemented pipes and plates (marked with dashed yellow lines) are also prominent features within unit 40 in the ditch exposures. See **Figures 6 and 8** for location. View is to northwest.

station 170, and throughout Trench T2, stations 185 to 220, mostly lie in the range of 1 to 1.2 m. The full section of the basal alluvium unit is not exposed along the entire length of the two trenches because of erosional truncation of the fold crests on the side-hill slope where the trenches are located. **Figure 7** compiles measurements of the basal alluvium sequence along the length of the trenches for comparison to the locations of the mapped fold crests and troughs. Thickness of the basal alluvium sequence is not significantly changed across the fold axes at stations ~215 and ~185. The basal alluvium section thickens abruptly near station ~160, on the southeast limb of the broad (>20 m wide) anticlinal crest at station ~165, then thins on northwest limb of the same anticline. Northwest of

station 145, thickness of the basal alluvium appears to increase uniformly from a minimum of 0.8 to the observed maximum of 1.75 m at station ~120. The increase in thickness of the basal alluvium sequence does not change across the relatively short wavelength, syncline/anticline pair with axis at stations ~140 and ~130, respectively. Northwest of station ~150, the thickest portion of the basal alluvium section, lies on an apparently uniformly tilted, dip panel of Niobrara Formation with a 5° northwest dip. Additional exposures, in the ditch, about 50 m further northwest, (**Figures 6, 8 and 9**) indicate that the basal alluvium section there is about 1.05 m thick.

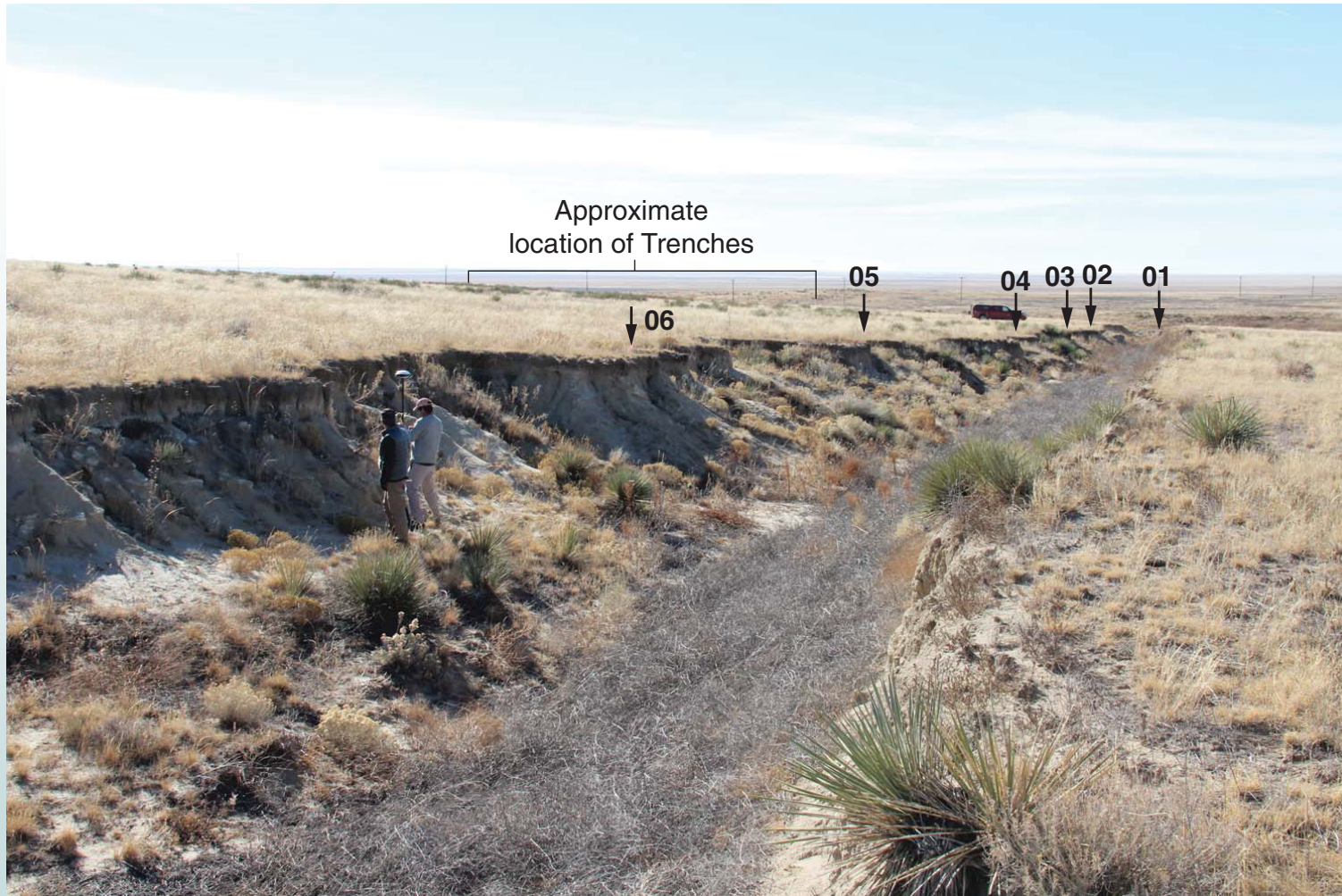


Figure 11. Overview of ditch exposure sites 01 to 06. View is to the southwest, downslope along the ditch. Numbered locations show sites where in-situ tilted and deformed Nussbaum Alluvium is observed in outcrop exposures. Site locations are shown in map view on **Figure 6**. A zone of deformed beds between sites 01 and 06 appears to intersect the ditch at an oblique angle, which exaggerates the apparent width of the zone. Gently dipping, and apparently undeformed Nussbaum Alluvium can be seen to left (northeast) of geologists in foreground. The approximate location of Trenches 1 and 2 are shown along the skyline.

Significant growth of the folds during the period of deposition of the basal alluvium section might be expected to result in a systematic or obvious relation between fold axis locations and the thickness changes in the basal alluvium section. The comparison of thickness for the basal Nussbaum Alluvium (units 20, 25, and 26) to the locations of fold axes defined by bedding in the underlying Niobrara, the geometry of the Niobrara/Nussbaum erosional contact, and the geometries of subcontacts and stratification within the Nussbaum Alluvium does

not demonstrate any such relation. Rather, the maximum difference in section thickness, <0.9 m, appears to be more consistent with the magnitude of local relief likely associated with the combined effects of bedrock erosion at the base of the alluvium (units 10/20 contact), floodplain or depositional relief at the top of the fluvial section, and erosion represented at the top of the section (units 26/30 contact). In this case, all or most of the deformation of the Nussbaum Alluvium would appear to post-date the age of the basal alluvium exposed in the trench.

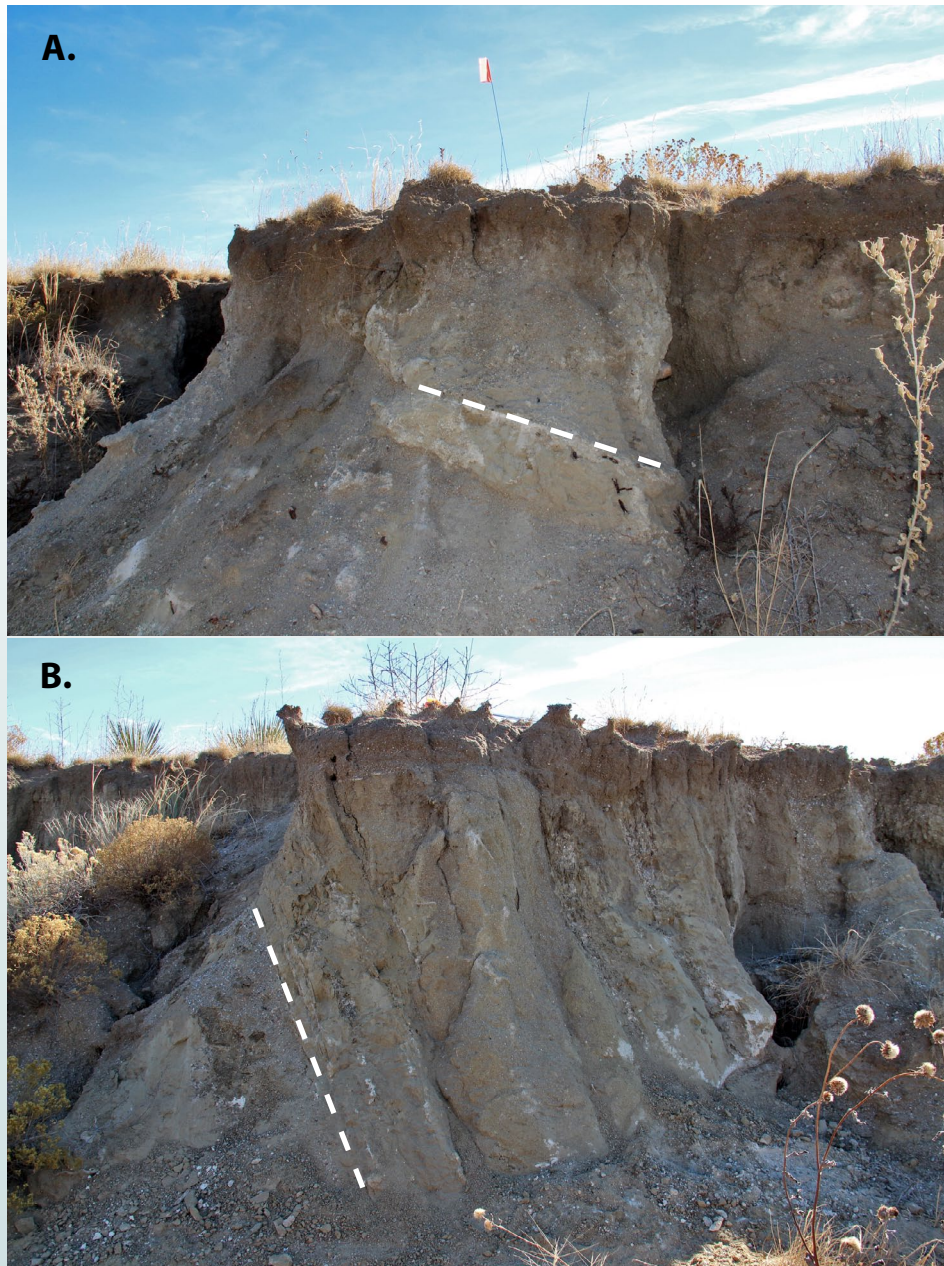


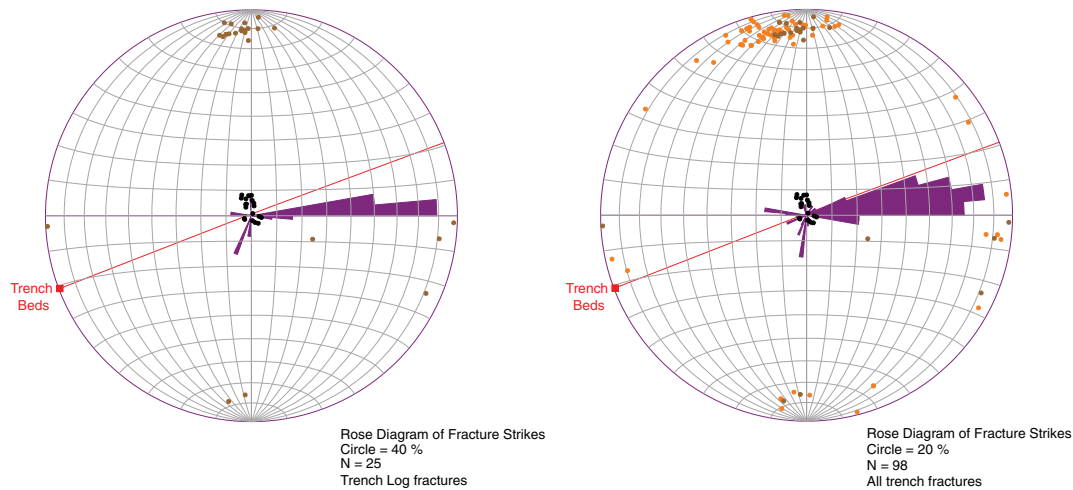
Figure 12. Photos of deformed Nussbaum Alluvium at site 03 (Photo A) and site 05 (Photo B) in ditch. Site locations are shown on **Figures 6 and 11**. Photos A and B show in-situ, tilted, Nussbaum Alluvium. Dashed lines highlight tilted bedding planes, as examples. View is to southeast in each image.

5.2.4 Deformation and Fracture Analyses

To assess the characteristics of deformation of Niobrara Formation and overlying units exposed in the trenches and nearby exposures, and their relationship to the Cheraw fault, we used Stereonet3D (Cardozo and Allmendinger, 2013) to plot and analyze measured strike and dip of fractures and bedding planes mapped in the trench and nearby exposures. The measured data are depicted as poles on the lower hemisphere of an equal-area stereographic plot in a set of figures based on differing subsets of the measured data (**Figure 13 A-D and Figure 14**). On **Figure 13A** poles showing measured Niobrara bedding planes (n=19) form an elongated cluster near the center of the sphere, reflecting the range of gentle but variable dip observed in the trenches (**Plate 2**). Poles to fractures labeled on the Trench T1 logs (n=25) (**Plate 2**) lie mostly around the margins of the sphere with a significant cluster near the north axis. A cylindrical best fit to the bedding plane poles using Stereonet3D gives a fold axis with a trend of 249.2° and plunge 0.6° . In comparison, the Rose Diagram of fracture strike shows a dominant trend of about 80° to 90° that is rotated clockwise about 10° to 20° from the horizontal projection of the fold axis determined from bedding (**Figure 13A**). When the fracture population is increased to include a larger sample of fractures and joints measured throughout the trench, but not specifically located on the trench log (n=73; **Figure 13B**), the Rose Diagram scatter increases somewhat with a dominant set of values near $80^\circ \pm 10^\circ$, slightly reducing the apparent clockwise rotation from the fold axis seen in the smaller data subset.

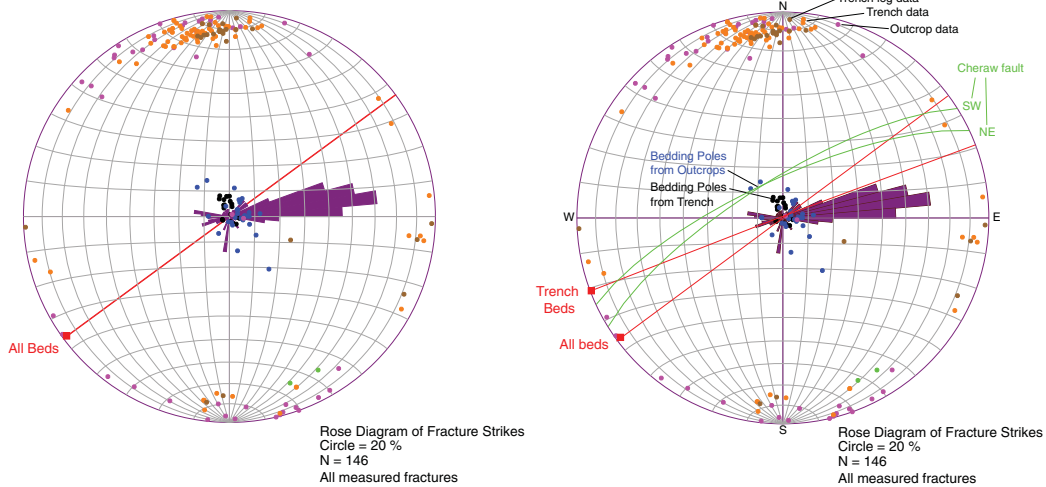
The orientation data measured in Trenches T1 and T2 can also be compared to a set of bedding and fracture data previously collected by Zellman and Osteana (2016) from the outcrop area located within 100 to 200 m south and west of the trenches (**Figure 6**). The dominant strike of fractures included on the Rose Diagram in **Figure 13C** is little changed with the addition of additional fracture orientations measured from outcrops (total N=146). Bedding poles measured from outcrops have larger scatter but generally plot over the range of those measured in Trench T1. **Figure 13D** shows the cylindrical best fit to the complete set of trench and outcrop bedding plane poles (N=47) using Stereonet3D. The fit defines a fold axis with a trend of 233.7° and plunge of 2.2° , an orientation suggesting dominant fracture strike is rotated about 25° clockwise from the horizontal projection of the fold axis.

Exposures in the ditch (**Figures 6 and 8**) provide another set of comparisons. Bedding orientations for the Niobrara marker bed, and basal contacts of Nussbaum Alluvium units 20 and 40 were determined from the orientations of planes



A. Haswell trench fracture log (annotated fractures from Plate 2 only)

B. Haswell trench fracture log (all measured Haswell trench fractures)



C. Combined Haswell trench and outcrop data

D. Haswell site stereonet summary (trench and outcrop data)

- | <u>Fault and Fracture Poles</u> | <u>Explanation</u> |
|---------------------------------|------------------------|
| ● Cheraw fault | ● <u>Bedding Poles</u> |
| ● Trench log data | ● Trench data |
| ● Trench data (all) | ● Outcrop data |
| ● Outcrop data | |
- Fracture strike
 ■ Fold axis pole and horizontal projection

Note: Stereo plots show lower hemisphere equal area projection.

defined by the combinations of three-point solutions surveyed from individual mapped beds or contacts. Calculation of three point solutions was done based on Hasbargen (2012) and the full results are tabulated in **Appendix C**. Based on available exposures along the ditch, individual survey points were generally spaced about 5 to 10 m apart along each contact. The number of surveyed points and potential three-point combinations for each bed are shown in **Table 3**.

Bed or Contact	Number of Surveyed Elevation Points	No. of Potential Three-Point Combinations (Strike and Dip)
Niobrara marker bed	4	4
Nussbaum Alluvium contact (Base of unit 20)	7	35
Nussbaum Alluvium contact (Base of unit 40)	13	286

Table 3. Three point combinations from Haswell ditch exposure.

Figure 13. Lower hemisphere, stereonet plots of Niobrara Formation bedding poles and fracture orientations from trench and outcrop exposures. Figures 13A and 13B show poles and Rose Diagram of strikes for subset of fractures measured and shown on trench log (13A) and larger subset measured, but not depicted on the trench log (13B). The red line on Figures 13A and 13B shows the horizontal projection of fold axis defined by Niobrara Formation bedding measured in the trenches. Note that fracture orientations are rotated about 10-20 east from the fold axis strike. Figure 13C shows a larger subset of bedding and fracture data, combing data from the trenches and outcrops across the Haswell site. See Figure 6 for locations of trenches and outcrop measurements. Divergence of mean fold axis orientation and fracture orientations increases as the spatial distribution of the bedding plane measurements increases. Figure 13D summarizes and compiles all the data sets. The green symbols show lower hemisphere projections of nearby sections of the Cheraw fault, northeast and southwest of the site, based on strike of the fault scarp and dip from industry seismic lines (Zellman and Ostenaar, 2016).

Figure 14 shows poles to bedding planes and contacts derived from separate strike-and-dip solutions computed from the three-point combinations of surveyed elevation data tabulated in **Table 3**. A total of 325 bedding poles are plotted on **Figure 14** from the Niobrara Formation marker bed (N=4), Nussbaum Alluvium base of unit 20 (N=35), and Nussbaum Alluvium base of unit 40 (N=286). These poles generally show similar orientations to the bedding poles measured from Trenches T1 and T2 and natural outcrops to the southeast (**Figures 6 and 8**), but the ditch exposures include a few measurements with somewhat steeper dip. The fold axis pole from a great circle fit to the Nussbaum Alluvium bedding poles (N=321) and the horizontal projection of that fold axis shown on **Figure 14** are very similar in orientation to fold axes derived from bedding measurements of trench and nearby outcrop data shown on **Figure 13**.

Figures 13D and 14 also includes two poles and planes representing the average orientation of adjacent sections of the Cheraw fault determined from the strike of the fault scarp nearest the Haswell trench site (**Figure 5**). Both fault sections are assigned a dip of 75° NW determined from depth-migrated seismic profiles to 2 to 3 km depth near the site (Zellman and Ostenaar, 2016). Northeast of the Haswell trench site, average strike of the fault based on the mapped scarp is about 245°, while southwest of the Haswell trench site, average strike is 238°. A much larger change in strike, to an average of about 225°, near the end of the original fault extent mapped by Sharps (1976), occurs about 6 km southwest of Haswell (**Figures 3 and 4**).

The orientations for the fault scarps nearest the Haswell site (238° to 245°) lie within the range of fold axis strikes based on bedding orientations in Trench T1 and from the larger data set including nearby outcrops (223° to 249°) and exposures in the ditch. The strike of the fault scarp just southwest of the Haswell site is rotated in similar manner to the fold axis determined from the combined outcrop and trench bedding orientation data (238° vs 234°). Thus, both sets of data appear consistent with their relative spatial positions. When data southwest of the trench are added to the analysis, the results reflect more strongly the influence of the difference in fault strike northeast and southwest of the Haswell site. The similarity of bedding orientations and fold axes between ditch exposures and Trench T1 suggests that the full zone of deformation extends beyond Trench T1, and includes the southwestern portion of the ditch shown on **Figure 6**.

The measured fractures in trenches and outcrops are dominantly steeper than the seismic-profile measured dip (75°) of the Cheraw fault (**Figure 13D**). The preponderance of fracture poles in the opposite hemisphere relative to the

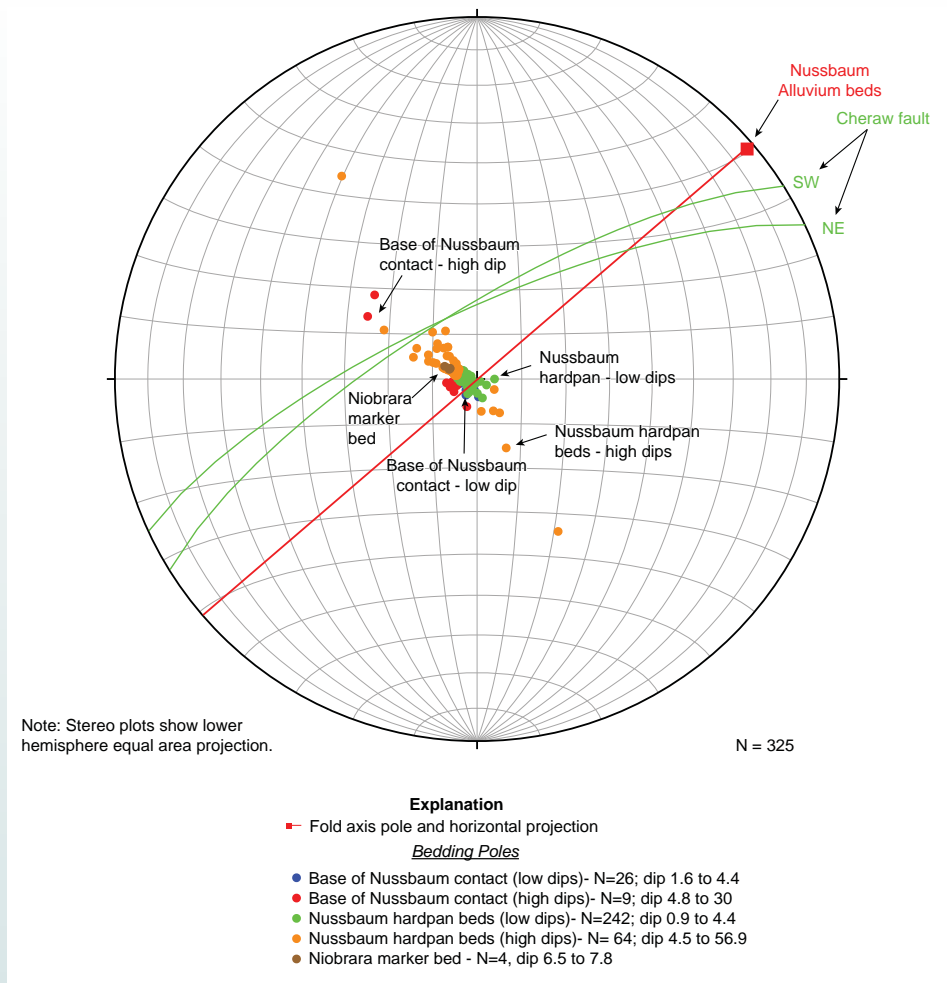


Figure 14. Lower hemisphere, stereonet plot of Nussbaum Alluvium and Niobrara Formation bedding poles from ditch exposures along CO Hwy 96. Red line on figure shows the horizontal projection of a fold axis derived from bedding poles of deformed Nussbaum Alluvium beds exposed in the ditch adjacent to CO Hwy 96. Comparison to **Figure 13D** shows the similarity of this deformation to fold axis orientations derived from Niobrara Formation bedding across the Haswell site.

Cheraw fault appears to indicate most of these fractures are antithetic to the main Cheraw fault structure, and in association with the folding, probably related to incomplete near-surface propagation of slip along the trace and hanging wall of the fault. The apparent trend of the deformation zone found in the ditch exposure, based on projection of the deformed beds from the ditch to the boring and

seismic profile (**Figure 6**) approaches the dominant ENE-WSW strike of fractures mapped in the trenches and outcrops (**Figures 13C and 14**).

5.2.5 Deformation of Nussbaum Alluvium

The general pattern of elevation changes in the soils and erosional stratigraphic contacts within and at the base of the Nussbaum Alluvium seen within the trenches (**Plate 2 and Figure 7**) indicates that there is significant deformation of the Nussbaum Alluvium and that the deformation zone extends beyond the extent of the current trenches. The end points of the trenches do not contain clear sections of Nussbaum Alluvium with a dip orientation that appears to reflect the expected depositional attitude (i.e., approximately 0.1° dip to the southeast; **Figure 7**). Within the area spanned by the trenches, the maximum amplitude of folding, measured between adjacent pairs of anticline and syncline axis ranges up to about 1.5 m. Similarly, within the area exposed by the trenches, the maximum elevation difference derived from projections of contacts across the full length of the trench ranges from about 2.3 m to 3 m. The smaller values being associated with projections using erosional contacts bounding the lower Nussbaum loess (unit 30) and larger values associated with projections based on the basal Nussbaum Alluvium/Niobrara Formation (units 10/20) contact.

Placing the trenches in the slightly larger context of outcrop exposures and boring data from the site area (**Figures 6, 7, and 15**) suggests that total offset of the basal Nussbaum Alluvium associated with the Cheraw fault at this site is likely at least 5 to 6 m, and most likely about 9 m (**Figure 7**). Offset of 5 to 6 m is accumulated if the monocline limb exposure in Trench T1 (see **Plate 2**; stations 125 to 100) continues to the ditch exposure about 50 m northwest. Measured dips of Nussbaum Alluvium and Niobrara Formation in the ditch exposure are very similar to those in the nearby portion of Trench T1, about 50 to 80 m southeast. Projection of Nussbaum Alluvium contacts from Trench T1 to the ditch exposure suggests a relatively uniform monocline-limb dip between these two exposures (**Figure 7**). However, at this location, the zone of deformation extending to site 01 in the ditch exposure would project to the southwest, beyond the ditch, suggesting that additional offset is present.

Larger offset values rely on the insight gained from the trenching that the natural relief on the basal bedrock strath surface below the Nussbaum Alluvium is likely relatively small, perhaps less than 0.5 m. Combined with the larger scale observation that the regional depositional slope of the Nussbaum Alluvium would have been to the southeast, at a relatively modest slope, about 0.003 (0.1°), implies to a first order that the maximum elevation differences for the basal con-

tact observed between trenches, outcrops, and boring data across the site may be indicative of the total displacement across the Cheraw fault at the site. The profile on **Figure 7**, with these data, accounts for the expected depositional slope of the Nussbaum Alluvium, and links available trench, outcrop, and boring elevations of the base of the Nussbaum Alluvium. This interpretation indicates a minimum of 5 to 6 m displacement through the area of the trenches and southwestern ditch exposure, and up to 9 m across the area of the prior boring transect (**Figure 7**). The zone of deformation intermittently exposed in the ditch outcrops (**Figures 6, 10, 12** and Section 5.2.2) includes both down-to-the-northwest faulting, and folding. Trenches T1 and T2; Borings 2, 3, and 4, and the southwestern ditch exposures all appear to lie on the same folded and tilted block with about 5 to 6 m of vertical displacement. Boring 1 and the ditch exposures northwest of the deformed zone (**Figures 6 and 7**) record an additional 3 to 4 m of additional vertical displacement.

Zellman and Ostenaar (2016) estimated that offset of the base of the Nussbaum Alluvium could be no more than about 3 m, but this estimate lacked high-resolution survey data for key outcrops northwest of Trench T1 in the ditch area (**Figure 6**), and used conservative projections through the borehole data which did not account for the depositional slope of the Nussbaum Alluvium strath surface. With the exposures of that surface provided by the trenching for this study, the amount of original relief on the basal strath surface appears to be relatively small. That observation implies that the primary cause of significant elevation differences observed across the site area is likely tectonic and related to post-depositional deformation associated with the Cheraw fault.

5.2.6 Timing of Deformation

The luminescence ages (**Sections 5.1.2 and 5.1.3**) and characteristics of deformation within the Nussbaum Alluvium (**Sections 5.2.1 and 5.2.3**) provide limits on the timing of Quaternary deformation observed at the Haswell site. Four luminescence ages, and soil development within the Nussbaum Alluvium exposed at the site indicate that deposition of these units spanned a time period from <126 ka to likely >200 ka (**Table 2 and Section 5.1.3**). The overall pattern of folding within the Nussbaum Alluvium suggests growth of the folds primarily post-dates deposition. Measured variations in thickness of the basal alluvium (units 20, 25, and 26; age ~ 160 to >200 ka) do not correlate with fold axis (**Figure 7**). Folding of the overlying loess (unit 30; ~ 150 to 160 ka), appears similar to the basal alluvium and top of bedrock, but exposure is truncated by hillside erosion in critical areas, as is the upper alluvium (unit 40; ~ 120 to 160 ka). Numerous

discontinuous fractures, mostly concentrated near anticlinal fold axes, generally die out upwards in the lower basal alluvium, but a few extend upwards into the soils formed in basal alluvium (units 25 and 26) and one into the overlying loess (unit 30). Sand infilling within these fractures appears to be sourced from the upper alluvium (unit 40), thus formation and infill of these fractures are younger than unit 30 (~150 to 160 ka) and younger than the basal portion of the upper alluvium (<126 ka to 160 ka). In the ditch exposure (**Section 5.2.2**), extensive deformation of unit 40 demonstrates significant younger activity; however, thickness variations in unit 40 that might relate to fold growth or faulting are not available from those exposures.

The hillslope alluvium and colluvium (units 50, 60, and 70) that are younger than the Nussbaum Alluvium have no clear relationship to the deformation exposed at the site (**Section 5.2.1**). Because the trenches and ditch exposure are located along a side hill slope, mostly at high angles to the overall fault trend, hillside erosion has removed any potential younger deposits related to individual deformation events.

5.2.7 Interpretation of the Cheraw Fault Structure at the Haswell Site

The initial interpretation of the location of the Cheraw fault at the Haswell site presented in Zellman and Ostenaar (2016) interpreted the main trace of the Cheraw fault as extending from the outcrop of Niobrara bedrock to the interval between borings 2 and 3 (**Figure 6**). This interpretation was based on the orientations of faults exposed in and near the bedrock outcrop, results from the shallow seismic surveys, top of Niobrara bedrock contours developed from boreholes and mapping, and continuity of the geomorphic scarp expressed on 10 m NED and other imagery. The paleoseismic trenches of this study were positioned to intersect the faulted base of the Nussbaum Alluvium along this interpreted alignment (**Figure 6**). Rather than exposing planar faulting and vertical offsets, similar to the findings of Crone et al. (1997), these trenches exposed folding and fractures within a broad zone of deformation. Reassessment of the Haswell site data and new observations of a deformation zone in the ditch to the north of the trenches provide a basis for re-interpreting the location and structure of the Cheraw fault at this site.

The following key observations provide the basis for a revised interpretation of the Cheraw fault at the Haswell site:

- 1) The topographic scarp associated with the Cheraw fault (**Figures 4 and 5**) changes in width and about 10° in strike directly to the southwest and northeast of the site,
- 2) A relatively flat basal contact of Nussbaum Alluvium, defined from multiple outcrop observations and boring 4, delineates this relatively planar contact on the Cheraw fault footwall (**Figures 5, 6, and 15**) and a southeastern limit of the fault zone extent,
- 3) The folding and characteristics of the basal Nussbaum Alluvium contact in the trenches suggest that a significant portion of the elevation differences of that contact defined in the boring profile are likely related to folding and tilting rather than erosion, or direct fault offsets,
- 4) Faults observed in the Niobrara bedrock outcrop at the Haswell site strike to the north-northeast and northeast towards Trenches T1 and T2, but do not intersect the trenches,
- 5) Stereonet analysis of fractures and folding define overall trends for features which are east-northeast and west-southwest (**Figure 13**), and
- 6) A broad zone of tilted and faulted Nussbaum Alluvium, with a comparable trend as shown in the stereonet plots (**Figure 13**), is exposed in the ditch to the north of Trenches T1 and T2 (**Figures 6, 10, 11, and 12**).

In aggregate, these observations suggest that an overall 10° strike change of the Cheraw fault scarps nearest the Haswell site is accomplished within a left-stepping, complex fault zone located between the boring transect and the Niobrara outcrops at the southwest edge of the site (**Figures 5 and 15**). Trenches T1 and T2, located on the erosional edge of the Nussbaum Alluvium surface to expose offset along the base of that unit, exposed deformation associated with the ramp between the left-stepping fault segments. The fault section to the southwest dies-out before intersecting Trenches T1 and T2. The deformation zone exposed in the ditch, if it extends northeast through the boring profile, is too far to the north to have been encountered in the trenches sited along the base of the Nussbaum Alluvium. Fault offset estimated from the boring profile appear to cross the entire zone (**Figure 5**), but fault offset estimated solely from the trenches, and projections to the ditch exposure (**Figure 7**) do not extend across the full set of fault traces.

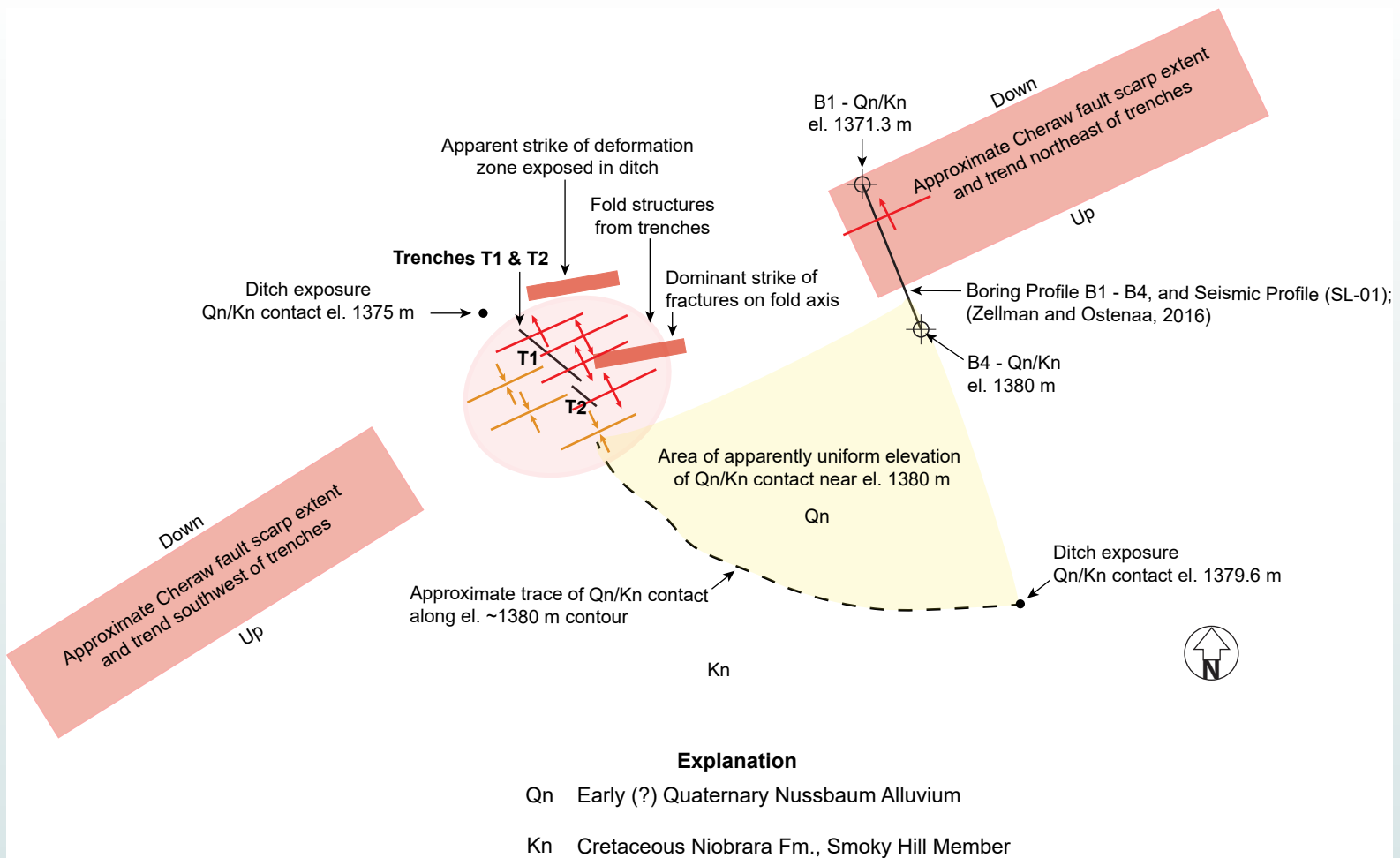


Figure 15. Schematic summary of compiled tectonic and outcrop data from the Haswell site. Haswell trenches T1 and T2 were located on a hillslope along the basal contact of the Nussbaum Alluvium (Figures 5 and 6). This location masked a small, <math><10^\circ</math> change in strike for fault scarp sections (red shaded boxes) southwest and northeast of the trenches. Folds and fractures measured in nearby outcrops and in the trenches apparently reflect fault step-overs, and distributed deformation associated with this strike change.

6.0 IMPLICATIONS FOR SEISMIC HAZARD CHARACTERIZATION



The new mapping of the Cheraw fault scarp demonstrates that the total length of Quaternary faulting (~80 km) is substantially longer than known from prior studies (Sharps, 1976; Kirkham and Rogers, 1981; Crone et al., 1997; Zellman and Ostenaar, 2016). Compared to maximum fault lengths of 45 and 60 km used in prior seismic hazard models such as CEUS-SSCn (2012) and Petersen et al. (2014), the increased length of Quaternary surface rupture will require new consideration of potential earthquake magnitudes and rupture model scenarios. Although slip rate data for the fault are still spatially limited, the new mapping does not suggest large variations in late Quaternary total slip along the 80 km fault length.

Table 4, modified from Zellman and Ostenaar (2016), shows updated ages, vertical offsets, and slip rates for the Cheraw fault derived from the new data at the Haswell site. The new ages derived from luminescence dating of the Nussbaum Alluvium are roughly an order of magnitude younger than the prior ages derived from regional data (compare **Section 2.0** and ages from **Table 2**). Taken

with the combined boring and trenching data from the Haswell site which indicates that offset of the base of the Nussbaum Alluvium is most likely about 9 m implies that minimum long-term vertical slip rates since about 125 to 160 ka at the Haswell site are greater than 0.055 to 0.071 mm/yr. To the southwest, along the fault, scarp heights measured on the CGS LiDAR (2016) data imply somewhat smaller offsets on surfaces over Rocky Flats Alluvium near Arlington (maximum ~ 7 m). No ages are available on deposits mapped as Rocky Flats Alluvium in this area, but these surfaces are inset well below abandoned surfaces mapped as Nussbaum Alluvium (40 to 45 m vs 80 to 90 m above local base level; **Figure 4**). Thus, Rocky Flats Alluvium and surfaces near the Cheraw fault must be significantly younger than nearby Nussbaum Alluvium, and are possibly as young as about 60 to 80 ka based on the new ages from the Haswell site for Nussbaum Alluvium and their relative elevations above current base level. Assuming an age for Rocky Flats Alluvium near the Cheraw fault of about 70 ka, and a maximum offset of 7 m from scarp profiles near Arlington, indicates a Cheraw fault vertical slip rate for the latest Pleistocene of about 0.1 mm/yr.

The new slip rate estimates based on the local ages of Rocky Flats and Nussbaum Alluviums are much higher than prior estimates for these units because of the new, younger age constraints from the Haswell site. Despite remaining uncertainty regarding the possible local age of the Rocky Flats Alluvium, slip rates from the younger Quaternary units trenched by Crone et al. (1996) are about two to four times higher than the new rates derived from the older Quaternary alluviums (**Table 4**). This progression may imply 1) an increasing slip rate on the Cheraw fault through the late Quaternary, 2) alternating temporal variability through time, or 3) reflect the initiation of extensional faulting on the Cheraw fault during the mid- to late Quaternary. In any case, the average slip rate and activity since about 100 ka, must be markedly different than the period from about 100 ka to >200 ka. Most or all of the 9 m vertical offset observed at the Haswell site appears to be younger than about 126 ka, with little or no deformation evident during the time of deposition for Nussbaum Alluvium in the vicinity of the Cheraw fault.

Datum	Age (ka)	Source/Type of Data/Vertical Offset (m)/Slip Rates (mm/yr)										
		Sh76, Cr97		KR81	Cr97			ZO16		This Study		
		Stratigraphic		Geomorphic			Trench		NF	FF	Geomorphic and Stratigraphic	
		6	8	12	6	8	3.2	4.1	30	98	7	9
Early Cenozoic	15000	0.0004	0.0005						0.0020	0.0065		
	5000	0.0012	0.0016						0.0060	0.0196		
Nussbaum Alluvium	160											0.056
	126											0.071
Rocky Flats Alluvium	2000			0.006								
	1200				0.005	0.007						
	400			0.030								
	70 (?)										0.10 (?)	
Late Pleistocene	25						0.13	0.16				
	20						0.16	0.21				

Notes: Sources – SH76 (Sharps, 1976); KR81 (Kirkham and Rogers, 1981); Cr97 (Crone et al., 1997); ZO16 (Zellman and Ostenaar, 2016). Type of Data– Stratigraphic, Geomorphic, and Trench data are structure contours, surface profiles, and exposures. NF (near fault) and FF (far field) are based on seismic reflection profiles described in Section 4.1 of ZO16. Age values used for datums are from sources, e.g., KR81, and Cr97; or values based on new age dates from this study. Cenozoic datum uses an estimated age range for the onset of extensional tectonism (ZO16).

Table 4. Cheraw fault stratigraphic datums, estimated vertical offsets, and slip rates (updated from Zellman and Ostenaar, 2016).

The larger vertical stratigraphic offsets ($\gg 30$ m; **Table 4**) in early Cenozoic and older bedrock units, observed by Zellman and Ostenaar (2016), must have contributions from the compressional deformation during the Laramide orogeny. Currently, there are no known locations along the Cheraw fault where deposits with ages younger than early Cenozoic and older than the Nussbaum Alluvium are preserved. Likewise, excepting the Haswell site, there are no sites where the maximum offset of the base of either Rocky Flats or Nussbaum Alluvium has been well documented. Thus, further detailed partitioning of offset amount resulting from late Cenozoic extension and early Cenozoic compression is not presently feasible.

Crone et al. (1997) suggested that the most recent three events on the Cheraw fault occurred since 20 to 25 ka, with interseismic periods ranging from 4 to 12 kyr. Total offset associated with these events was 3.2 to 4.1 m. They further suggested a much longer interseismic period prior to these events, with no additional events since >100 ka. (1997) Thus, Crone et al. interpreted the additional offset of Rocky Flats Alluvium present at their site as older than about 100 ka. Partly to account for this additional offset, CEUS-SSCn (2012) proposed a weighted characterization of the Cheraw fault which reflected extended

periods of quiescence, with slip rates more than an order of magnitude lower than suggested by the most recent events.

The results from new LiDAR mapping and from the Haswell site are not consistent with the Crone et al. (1997) suggestion of a long period of quiescence from about 25 to >100 ka, and only 3 to 4 m of offset since >100 ka. The Haswell site results indicate that about 9 m of slip has likely occurred since about 125 to 160 ka and new mapping on the CGS (2016) LiDAR indicates only slightly smaller offsets of the Rocky Flats surfaces must be much younger than that. Because the Rocky Flats surfaces are inset 40 to 50 m below the Nussbaum surfaces, the 5 to 7 m scarp heights present on these surfaces must also post date the local stabilization and abandonment of both the Nussbaum and Rocky Flats surfaces. These findings imply that slip rate variability at the Crone et al. (1997) site over different time intervals of the past 100 kyr is likely no more than about a factor of 2 to 4 (Compare values in **Table 4**). Further, the recognition that the Cheraw fault scarp extends much further to the northeast than previously known, allows the possibility for alternate models of rupture behavior on the southern and central portions of the fault versus the northeastern portion where the Haswell site is located.

7.0 SUMMARY OF RESULTS



The new mapping for this study shows that the total length of the fault scarp associated with the Cheraw fault is at least 80 km, with the northeast extent defined by the limit of presently available LiDAR data. Preliminary evaluation of new CGS LiDAR data suggests similar amounts of late Quaternary offset along the entire length of the scarp. Both the main Cheraw fault scarp, and a subparallel secondary fault northwest of the northeast extension, are coincident with older, compressional and/or oblique-slip structures observed in industry seismic data reviewed by Zellman and Ostenaar (2016).

The trenches excavated during this study indicate that the strath surface on which Nussbaum Alluvium was deposited is complexly folded and warped with a net down-to-the-northwest sense of displacement (**Figures 7 and 15**). These trenches did not expose a simple, or clear, fault offset to account for the elevation differences observed in the base of the Nussbaum Alluvium by Zellman and Ostenaar (2016). While the amplitude of individual folds exposed in the trenches is no more than 3 m, the combined trench and outcrop data shown in profile view on **Figure 7** indicates minimum net down-to-the-northwest displacement of at least 5 to 6 m. This estimate also accounts for the expected southwest depositional slope of Nussbaum Alluvium. When combined with the prior boring data on a profile located less than 300 m northeast of the trenches, the total displacement of the base of the Nussbaum Alluvium is likely about 9 m (**Figure 7**), consistent with estimates from preliminary surface profiles from the LiDAR.

The details of the age and event history for deformation of the Nussbaum Alluvium seen in the trenches is uncertain. Stratigraphic contacts, internal stratification, and soils within the Nussbaum Alluvium sequence exposed in Trenches T1 and T2 all appear to be folded in a similar manner to the basal contact on the underlying Niobrara Formation. This same fold structure is also expressed by changes in bedding attitudes in Niobrara Formation. A small discordance in the dip of the erosional contact at the base of the Nussbaum Alluvium with bedding in the Niobrara Formation indicates the existence of a small pre-Nussbaum dip to the northwest for the Niobrara Formation, consis-

tent with the Laramide-age uplift of the Las Animas Arch (Tickoff and Maxson, 2001). Although thickness of the Nussbaum Alluvium varies across the length of the trenches, these variations do not appear to correlate with fold axes in the Niobrara Formation as would be expected if some fold growth occurred during deposition of the Nussbaum Alluvium. Rather, it appears that all deformation post-dates deposition of the Nussbaum deposits exposed in Trenches T1 and T2. Post-Nussbaum Alluvium deposits exposed in the trenches are apparently Late Pleistocene or Holocene in age (see **Table 2**), and thus, are significantly younger. These deposits are apparently related to erosion of the hillside upslope, and across the trench locations, and show no indications of folding.

The absence of a discrete fault break significantly displacing the Niobrara – Nussbaum contact in Trenches T1 and T2, along with the results of the fold and fracture analysis, appear to be consistent with a small change in strike of Cheraw fault scarp just southwest and northeast of Haswell (**Figures 5, and 13B**). Northeast of the Haswell site, the average strike of the fault scarp extending for several kilometers is about 245° (**Figures 3 and 4**). Southwest from the Haswell site, the fault strikes about 238° for about 6 km, then makes a sharp bend to an average strike of about 225°, at the end of the fault originally mapped by Sharps (1976). As shown by the geomorphic mapping (**Figure 3**), there are many local strike changes along the Cheraw fault, particularly the concave-northwest section near Arlington.

Measured fracture and fold axis orientations in the trenches and nearby outcrops lie outside the range of fault scarp strike for 1 to 3 km along strike in either direction from the Haswell site (**Figures 13D, 14, and 15**). Surface folding and associated fracturing observed in the trenches can be considered to be the result of a combination of a small local clockwise strike change, accompanied by folding and tilting of a relay ramp between left-stepping fault segments (**Figure 15**). The fault section extending northeast likely includes the zone of deformation observed in the ditch along CO Highway 96 (**Figure 6**). The fault section extending southwest, shown by the fault southwest of the site, apparently dies out just southwest of Trenches T1 and T2 (**Figure 5 and 6**).

Deformation within the step-over zone may partly reflect incomplete rupture propagation to the surface of a buried normal fault, and fault-propagation folding (Jackson et al., 2006) above the shallow buried tip of the Cheraw fault within this step-over zone.

Based on our studies, we conclude that:

- 1) The Cheraw fault scarp is closely associated with an underlying bedrock fault and fold structure.
- 2) The total length of Quaternary faulting associated with the Cheraw fault is at least 80 km and appears to be relatively uniform in vertical offset.
- 3) The surface expression of the Cheraw fault at the Haswell site is complex, as a local 10° change in fault strike is partly accommodated through a left-step of the main fault trace. Trenches T1 and T2 expose deformation associated with the fault relay ramp between two left-stepping fault traces.
- 4) Nussbaum Alluvium at the Haswell site is deformed and its basal contact is vertically offset at least 5 to 6 m in the trenches, and total offset is likely about 9 m when combined with boring data.
- 5) Internal stratigraphy within the Nussbaum Alluvium, exposed in the trench walls, is deformed in the same manner as its basal contact with bedrock, suggesting that all deformation postdates the youngest Nussbaum strata at the site.
- 6) Deposition of the Nussbaum Alluvium, and erosion of the basal strath surface which underlies that alluvium, is much younger than previously inferred from regional correlations. New luminescence ages from the Haswell site indicate deposition of units within the Nussbaum Alluvium spanned an age range from <126 ka to >160 ka.
- 7) Deformed stratigraphy and age constraints from luminescence dating suggests that post-Nussbaum Alluvium slip on the Cheraw fault occurred after <126 to 160 ka, yielding a minimum vertical slip rate of ~0.06 to 0.07 mm/yr at the Haswell site since that time.
- 8) Inset relations of Rocky Flats Alluvium near the Cheraw fault, indicate that it must be significantly younger than the Nussbaum Alluvium at Haswell. Scarps on the Rocky Flats Alluvium appear to range from 5 to 7 m in height, suggesting a similar or slightly higher late Quaternary slip rate than the rate derived from the Nussbaum Alluvium at Haswell.

8.0 ACKNOWLEDGEMENTS




Initial funding for this research was provided by Colorado Geological Survey under a contract to Fugro Consultants, Inc., and subcontract to Ostenaar Geologic LLC. That contract supported the trench excavation field studies, development of preliminary report with trench logs and figures. Completion of the initial trench studies and subsequent analyses has been a truly collaborative effort, and many individuals and organizations contributed to the outcome of this investigation. These efforts were supported by participation from the Colorado Geological Survey (CGS), the U.S. Geological Survey (USGS), Ostenaar Geologic LLC, and Fugro Consultants, Inc. (FCL). The authors would like to specifically thank Karen Berry, Matt Morgan and F. Scot Fitzgerald (CGS); Rich Briggs, Chris DuRoss, Nadine Reitman, Steve Personius, Will Levandowski and Shannon Mahan (USGS); and Paul Reinflesch U.S. Department of Agriculture Natural Resource Conservation Service (USDA NRCS) for supporting this project, and assistance in the field. Support for the luminescence dating at the site was provided by Shannon Mahan and the U.S. Geological Survey Luminescence Dating Laboratory. The Colorado State Land Board provided permission for site access and Mr. Delton Ikenberg provided site mitigation after trenching. Jason Holmberg of FCL prepared the trench logs and figures included in this report. And finally, Jamey Turner and Janet Sowers of FCL provided very useful editorial reviews of the early versions of this report.

The authors would also like to thank those who attended the trench review for thoughtful comments and insight: Matt Morgan, Kevin McCoy, Kassandra Lindsey of (CGS); Bob Kirkham of Geological Solutions; Kendra Johnson and Ed Nissen of Colorado School of Mines (CSM); Steve Personius, Nadine Reitman, Chris DuRoss, and Rich Briggs (USGS); Randy Cumbest of Lettis Consultants International (LCI); Dan O'Connell (FCL); and Laura Craven, Jeff Goats, and Ana Vargo (USDA NRCS).

The Cheraw fault LiDAR data was collected in 2016 as a joint project of the Colorado Geological Survey, Colorado Water Conservation Board, and Colorado Office of Information Technology.

The final version of this report was greatly improved by review and comments from Matt Morgan of CGS and Vince Matthews (retired CGS). Final graphical presentation was completed by Larry Scott of CGS.

9.0 REFERENCES

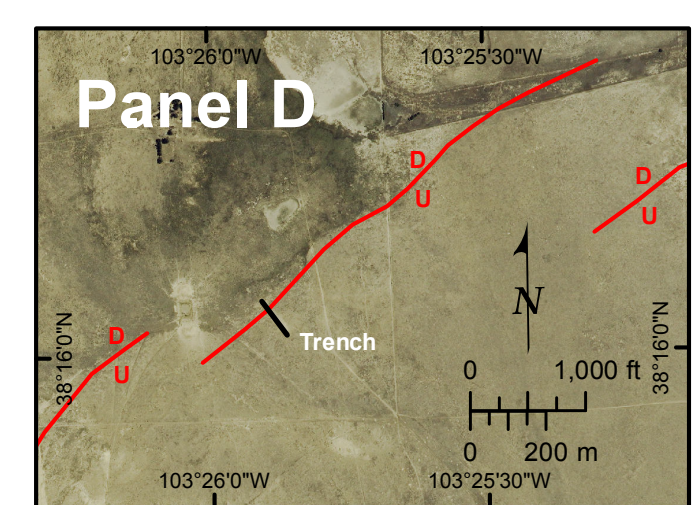
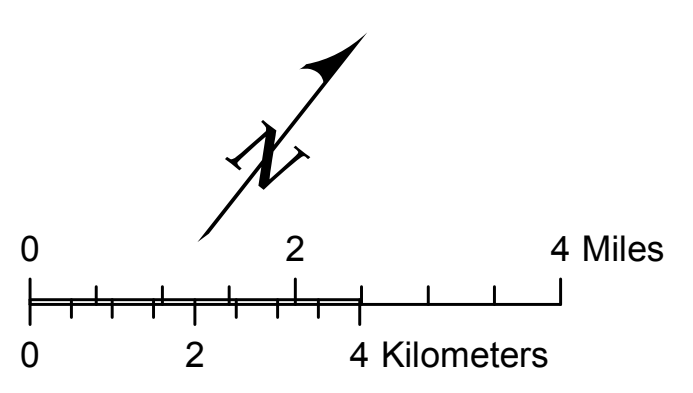
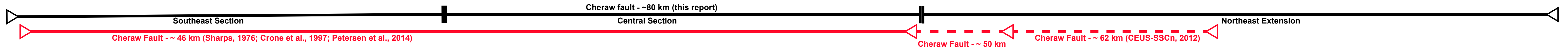
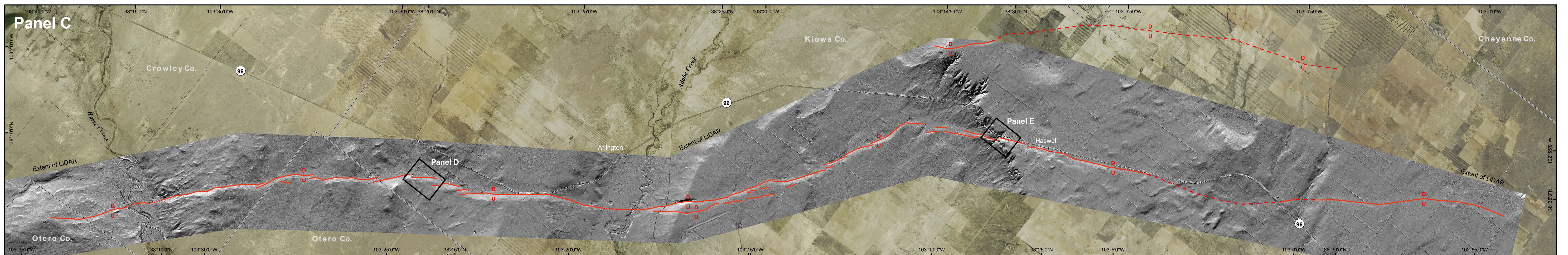
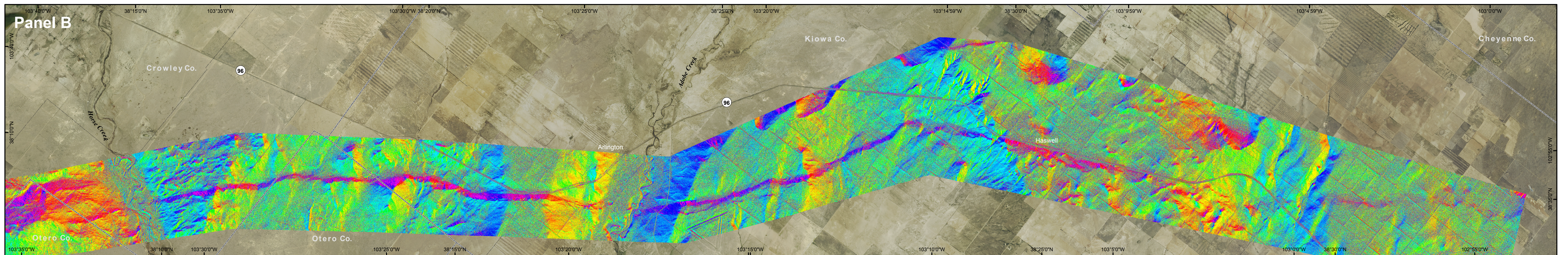
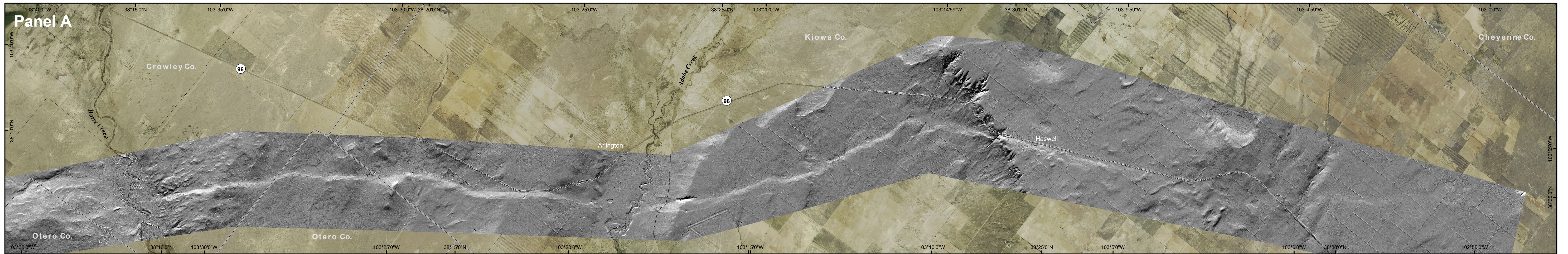
- 
- Birkeland, P.W., Miller, D.C., Patterson, P.E., Price, A.B., Shroba, R.R., 1999, Soil-geomorphic relationships near Rocky Flats, Boulder and Golden, Colorado area, with a stop at the Pre-Fountain Formation paleosol of Wahlstrom (1948). Geological Society of America Field Trip No. 18.
- Cardozo, N. and Allmendinger, R.W. 2013, Spherical projections with OSXStereonet, Computers and Geosciences 51, 193–205.
- Carlson, Marvin P., 2007, Precambrian accretionary history and Phanerozoic structures – A unified explanation for the tectonic architecture of the Nebraska region, USA, Geological Society of America Memoirs; 200; 321–326.
- CEUS–SSCn, 2012, Central and Eastern United States seismic source characterization for nuclear facilities: Palo Alto, California, EPRI, U.S. DOE, and U.S. NRC, [variously paged]. (Also available at <http://www.ceus-ssc.com/Report/Downloads.html>).
- Colorado Geological Survey, (CGS) 2016, Cheraw fault LiDAR data, a joint project of the Colorado Geological Survey, Colorado Water Conservation Board (CWCB), and Colorado Office of Information Technology (COIT).
- Colorado Oil and Gas Information System (COGIS), 2015, Oil and gas well database: <http://cogcc.state.co.us/>. Website accessed last accessed October 18, 2018.
- Crone A.J., Machette, M.N., Bradley, L.-A., and Mahan, S.A., 1997, Late Quaternary surface faulting on the Cheraw fault, southeastern Colorado: U.S. Geological Survey Miscellaneous Geological Investigations I-2591, 7p. Pamphlet, 1 oversize pl.
- Crone, A.J., and Machette, M.N., 1995, Holocene movement on the Cheraw fault, SE Colorado – Another hazardous late Quaternary fault in the stable continental interior: Eos, Transactions of the American Geophysical Union, v.76, no. 46, November 7, 1995 supplement, p. F362.
- Crone and Wheeler, 2000, Data for Quaternary faults, liquefaction features and possible tectonic features in the Central and Eastern United States, East of the Rocky Mountain front, U.S. Geological Survey Open-File Report 00-260.
- Curtis, B.F., 1988, Sedimentary rocks in the Denver basin, in Baars, D.L., and 15 others, eds., Basins of the Rocky Mountain region – Decade of North American geology: Boulder, Colorado, Geological Society of America, The Geology of North America, v. D-2, p. 109–221.
- Duhnforth, M., Anderson, R., Ward, D., Blum, A., 2012, Unsteady late Pleistocene incision of streams bounding the Colorado Front Range from measurements of meteoric and in situ ^{10}Be , Journal of Geophysical Research, v117.
- Foster, M., Duhnforth, M., Anderson, R., 2013, Young strath terraces on western High Plains record climate-paced variations in sediment supply from Colorado Front Range, Abstract, Geological Society of America Annual Meeting, Denver, CO.
- Foster, M., Anderson, R., Mahan, S., 2014, Use of ^{10}Be to deduce variations in sediment supply from the Front Range to the High Plains, with implications for generation of fill and strath terraces, Abstracts with Programs, Geological Society of America Annual Meeting
- Herrmann, Robert, B., 2009, Moment Tensor Solution. Accessed in April 2014 from website: http://www.eas.slu.edu/eqc/eqc_mt/MECH.NA/20090817002212/index.html.
- Hasbargen, L., 2012, A test of the three point vector method to determine strike and dip utilizing digital aerial imagery and topography, in Whitmeyer, S.J., Bailey, J.E., De Paor, D.G., and Ornduff, T., eds., Google Earth and Virtual Visualizations in Geoscience Education and Research: Geological Society of America Special Paper 492, p. 199–208, doi:10.1130/2012.2492(14). Spreadsheet downloaded from Geol. Soc. Amer. Data Repository <https://www.geosociety.org/datarepository/2012/>; last accessed 3/3/2017.
- Jackson, C.A.L., Gawthorpe, R.L., and I.R. Sharp, 2006, Style and sequence of deformation during extensional fault-propagation folding: examples from the Hammam Faraun and El-Qaa fault blocks, Suez Rift, Egypt: Jour. Struct. Geol., v. 28, 519–535.
- Johnson, K.S., and Neal, J.T., 2003, Evaporite Karst and Engineering / Environmental Problems in the United States, Oklahoma Geological Survey, Circular 109.

- Johnson, K., Nissen, E., Saripalli, S., Arrowsmith, J.R., McGarey, P., Scharer, K., Williams, P., and Blisniuk, K., 2014, Rapid mapping of ultrafine fault zone topography with structure from motion: *Geosphere*, v. 10, no. 5, p. 969–986, doi: 10.11130/GES01017.1
- Kirkham R.M., and Rogers, W.P., 1981, Earthquake potential in Colorado – A preliminary evaluation: *Colorado Geological Survey Bulletin* 43, 171 p., 3 pls.
- Kluth, CF., and Coney, P.J., 1981, Plate tectonics of the Ancestral Rocky Mountains, *Geology*, v.9, no.1, p10–15.
- Merewether, E. A., 1987, Oil and gas plays of the Las Animas Arch, southeastern Colorado: U.S Geological Survey Open-File Report 87-450D, 22p.
- Meriam, D.F., 1963, The Geologic History of Kansas, State Geological Survey of Kansas Bulletin 162.
- NCEDC, 2014, Northern California Earthquake Data Center. UC Berkeley Seismological Laboratory. Dataset. doi:10.7932/NCEDC.
- Noe, D., 2010, Anton Escarpment Paleoseismologic Investigation, Washington County, Colorado: U.S. Geological Survey (USGS) National Earthquake Hazard Reduction Program (NEHRP) External Grant Award Number 07HQGR0090.
- Petersen, M.D., et al., 2014, 2014 update to the National Seismic Hazard Map (NSHM), U.S. Geological Survey: last accessed February 26, 2016 from the USGS website: <http://earthquake.usgs.gov/hazards/2014prelim/>.
- Rascoe, B., Jr., 1978, Late Paleozoic structural evolution--the Las Animas arch; *in* Energy Resources of the Denver Basin: Rocky Mountain Association of Geologists, 1978 Symposium, p. 113–127.
- Reitmain, N., Bennett, S., Gold, R., Briggs, R., DuRoss, C., 2015, High resolution trench photomosaics with structure from motion: workflow and accuracy assessment, *Bulletin of the Seismological Society of America*, V. 105,
- Riihimaki, C.A., Anderson, R.S., Safran, E.B., Dethier, D.P., Finkel, R.C., and Bierman, P.R., 2006, Longevity and progressive abandonment of the Rocky Flats surface, Front Range, Colorado: *Geomorphology*, v. 78, pp. 265–278.
- Schildgen T., Dethier, D.P., Bierman, P., Caffee, M., 2002, 26Al and 10Be Dating of Late Pleistocene and Holocene Fill Terraces: A Record of Fluvial Deposition and Incision, *Colorado Front Range, Earth Surface Processes and Landforms*, 27, 773–787.
- Scott, Glenn R., 1963, Nussbaum Alluvium of Pleistocene (?) age at Pueblo, Colorado; Article 72, U.S. Geological Survey Professional Paper, C49-C52.
- Scott, Glenn R., 1965, Nonglacial Quaternary of the Southern and Middle Rocky Mountains, *in* Wright, H.E., and Frey, D.G., ed., *The Quaternary of the United States*: Princeton Univ. Press, p. 243–254.
- Scott, Glenn R., 1970, Quaternary faulting and potential earthquakes in east-central Colorado, Geological Survey Professional Paper 700-C.
- Scott, Glenn R., 1975, Cenozoic surfaces and deposits in the southern Rocky Mountains, *in* Cenozoic history of the Southern Rocky Mountains: Geological Society of America Memoir 144, p. 227–248.
- Scott, Glenn R., 1982, Paleovalley and geologic map of northeastern Colorado: U.S. Geological Survey Miscellaneous Geologic Investigations Map I-1378, scale 1:250,000
- Sharps, J.A., 1976, Geologic map of the Lamar quadrangle, Colorado and Kansas: U.S. Geological Survey Miscellaneous Geologic Investigations Map I-944, scale 1:250,000.
- Sims, P.K., Bankey, V., Finn, C.A., 2001, Preliminary Precambrian basement map of Colorado – A geologic interpretation of an aeromagnetic anomaly map, USGS Open-File Report 01-0364.
- Tickoff, B., and Mason, J., 2001, Lithospheric buckling of the Laramide foreland during Late Cretaceous and Paleogene, western United States, *Rocky Mountain Geology*, v.36, n1, p13–35.
- U.S. Geological Survey (USGS), 2016, Quaternary fault and fold database for the United States, Accessed January 5, 2016, from USGS website: <http://earthquake.usgs.gov/hazards/qfaults/>.
- Walker, Graham Thomas, 1985, High Plains Depressions in Eastern Colorado: Distribution, Classification, and Genesis, Unpublished Ph.D. Dissertation, University of Denver.
- White, Jonathan L., 2012, Colorado Map of Potential Evaporite Dissolution and Evaporite Karst Subsidence Hazards: Map Discussion, Colorado Geological Survey.

- Whitmeyer, S. and Karlstrom K., 2007, Tectonic model for the Proterozoic growth of North America, *Geosphere*, v.3, n.4, p.220–259.
- Ye, H., Royden, L., Burchfiel, C., and Schuepbach, M., 1996, Late Paleozoic Deformation of Interior North America: The Greater Ancestral Rocky Mountains, *AAPG Bulletin* v80, n9, p1397–1432
- Zellman, M. and Ostenaar, D., 2014, Preliminary results from new investigations of the Cheraw fault, SE Colorado (abstract and presentation), Geological Society of American Rocky Mountain and Cordilleran Section Meeting, Bozeman, MT, May 2014.
- Zellman, M., and Ostenaar, D., 2016, Geophysical and Paleoseismic Investigation of the Cheraw Fault, Southeastern Colorado, U.S. Geological Survey, National Earthquake Hazard Reduction Program, Final Technical Report, U.S. Geological Survey, Award Number G15AP0002, 53p.

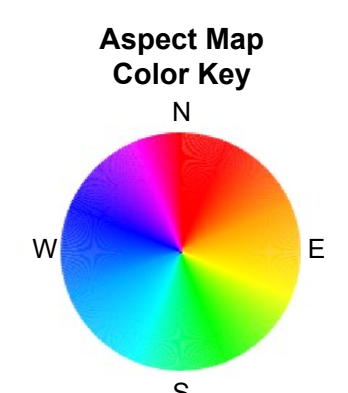
Paleoseismic Investigation of the Cheraw Fault at Haswell, Colorado

By Dean A. Ostenaar and Mark S. Zellman
2018



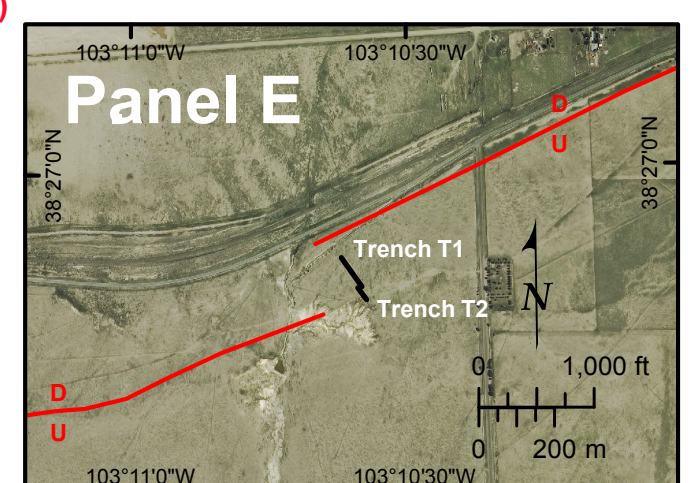
Explanation

— — — — — Fault; solid where certain, dashed where inferred, dotted where concealed.
U on upthrown side and D on downthrown side.



Notes:

- Hillshade map in Panels A and C, and Aspect map in Panel B derived from 2015 CGS LiDAR.
- Hillshade map produced with sunlight azimuth of 315° and altitude of 45°.
- Airphoto basemap in all panels from USDA NAIP, 2013.
- Color on Aspect map (Panel B) corresponds to slope direction azimuth indicated by color on Aspect Map Color Key.



Appendix A

Soil Profile Field Logs

Series	User Pedon ID	Date & Time	By
Taxonomic unit	Location: UTM (NAD83) e n	Location: N 38.4473 W 103.1765	MU symbol
Air temp. (F)	Soil temp. @ 50 cm (F)	Weather: PC Windy	Photos (File location)
Land use:	Topo Quad	Production (#/ac):	Ecosite:
Current vegetation	Landscape	Landform	Position on landform
Parent material: (Type of Deposit & Rock type)	Aspect: Cardinal Direction: Elevation (m/feet): Slope (%) Slope Shape, Complexity		
Drainage: X SX W MWD SPD	Water table depth (ft.)	Depth to Least Permeable Layer (for Ksat)	Flooding: (N) VR R O F
Soil temperature regime	Soil moisture regime		Depth Class: VS SH MD D

SURFACE ROCK FRAGMENTS			
% 5-75 mm	% 2-5 mm Gravel	% Cobbles	% Stones
Gravel			
37 x	3 x	137 x	425 x
Total Surface RF %			% Rock outcrop (Area)
/1402 =			Mean Rock Height:

CONTROL SECTION			
Depth: cm	Particle-size class:	mineralogy	% clay
DIAGNOSTIC HORIZONS		Topography: B/S SDiss MDiss SDiss Ballena	
Depth to paralithic contact: cm	Depth to Lithic contact: cm	Depth to Hardpan: cm	Carbonate Stage: I+ II+ III III+ IV V VI
Soil Sampled? Horizon(s), Sample Numbers	Soil Special Features	Desert Pavement	Varnish
N		None Weak Moderate Strong	None Weak Moderate Strong

Thickness LAYER	Horizon	Depth cm	COLOR		USDA texture	% ROCK FRAGMENTS (vol.)					PARTICLE-SIZE ESTIMATES %		
			Dry	Moist		Stones	Cobbles	Gravel (5-75 mm)	Gravel (2-5 mm)	Total RFs	Sand	Silt	Clay
1 ()	A1	0-4	10YR4/3		L	0	0	0.1	5	5	50	36	14
2 ()	A2	4-13	10YR4/3	10YR3/3	L	0	0	0.01	3	3	45	40	15
3 ()	Bw	13-32	10YR4/3	10YR3/3	SL	0	0	0.1	5	5	74	15	11
4 ()	Bk1	32-51	10YR5/3	10YR4/3	LS	0	0	0.1	2	2	79	14	7
5 ()	Bk2	51-66	10YR6/3	10YR5/3	LS	0	0	<1	5	5	82	14	4
6 ()	Bkkm	66-69	2.5Y7/2	2.5Y5/2	CEM.	0	0	N/O	N/O	-	80	-	-
7 ()	2Bkkm	69-76	2.5Y8/2	2.5Y4/3	SIL	0	0	0	0	0	15	69	16
8 ()	2Btkbl	76-97	2.5Y6/3	2.5Y4/4	SIC	0	0	0	0	0	15	47	38

LAYER	Structure	CONSISTENCE		Cementation	CHEMICAL PROPERTIES					P&V Feat; Conc.	Roots (#/area)	Pores (#/area)	Boundary
		Dry/Moist	Wet		% CaCO3	Efferv.	pH	SAR	Salinity (ds/m)				
1	2TK PL → 2MSBK	SH NFR	SG IPO			NE	.				Y		CW
2	2MSBK	SH IFR	SS ISP			NE	.				Y		CW
3	1MSBK	SH IFR	SS IPO			NE	.				Y		GW
4	1FSBK → SG	SH NFR	SO IPO	-		NE	.				Y		GW
5	MA → SA	SH NFR	SO IPO	W		NE	.			5	Y		AW
6	MA	VH IEF	- I -	M		ST	.			6	N		AW
7	2VKPL Geogenic	HA IFR	SS ISP	M		VE	.			7	N		AW
8	3MPR	VH IFR	SS IMP	-		VS	.			8	Y		

Concentrations: Kind, quantity, size, (contrast), color, shape, location, hardness, boundary (ie. CAM, 15%, 1, p, 10yr/1, t, MAC, so, c) Ped & Voids: Kind, percent, distinctness, color and location (ie. CAF, 35%, d, 10yr/1, UR)

II
II
III
III

- | | | | |
|----|-----------------------|----|------------------------------|
| #1 | | #2 | |
| #3 | | #4 | CAM 2% C+V |
| #5 | CAM C+V 8% | #6 | FDC (MAT) CEM |
| #7 | FDC (MAT) CAM C+V 80% | #8 | FDC (MAT), CAF 35% VE (Pods) |

Additional Notes:

Calculations:

PSC Thickness: _____

PSC RFs/PSC Thick=

PSC Clay/PSC Thick =

		Horizon Thickness (cm)					
Horizon RFs							
Horizon Clay							

Crusts		Diagrams, Photo Numbers, etc		
B i o l o g i c a l	Types IBC = Incipient Fungal/Algal Crust FBC = Fungal Crust UBC = Unblackend Algal Crust BCC = Blackened Algal Crust LBC = Lichen Crust BBC = Bryophyte Crust		Profile Diagram	
	P h y s i c a l			VC = Vesicular Crust RC = Rain Drop Impact Crust DC = Depositional Crust
	C h e m i c a l			HCC = Halite Crust GCC = Gypsum Crust MCC = Mirabilite Crust

Series: User Pedon ID: **001** Date & Time: **3/30/16** By: **PRR**

Taxonomic unit: MU symbol:

Location: **UTM (NAD83) e n Across pit from** Location: **N 38.4473 W 103.1765** Pedon PC? NASIS? Analysis?

Air temp. (F): Soil temp. @ 50 cm (F): Weather: **Upper desc** Photos (File location): Pedon Type: **Ma Mi MMU MS**

Land use: Topo Quad: Production (#/ac):

Current vegetation: Ecosite:

Landscape: Landform: Position on landform:

Parent material: (Type of Deposit & Rock type):

Aspect: Cardinal Direction: Elevation (m/feet): **4532** Slope (%): Slope: Shape, Complexity $\updownarrow \leftrightarrow$

Drainage: **X SX W MWD SPD** Water table depth (ft.): Depth to Least Permeable Layer (for Ksat): Flooding: **N VR R O F** Depth Class: **VS SH MD D**

Soil temperature regime: **MESIC - THERMIC - HYPERTHERMIC** Soil moisture regime: **ARIDIC USTIC**

SURFACE ROCK FRAGMENTS

% 5-75 mm	% 2-5 mm Gravel	% Cobbles	% Stones	% Boulders	Total Surface RF %	% Rock outcrop (Area)
37 x	3 x	137 x	425 x	800 x	/1402 =	Mean Rock Height:

CONTROL SECTION

Depth: cm Particle-size class: mineralogy % clay % RF (vol.) % > VFS (wt.)

DIAGNOSTIC HORIZONS

Epipedon Subsurface Topography: **B/S SDiss MDiss SDiss Ballena**

Depth to paralithic contact: cm Depth to Lithic contact: cm Depth to Hardpan: cm Carbonate Stage: **I+ II+ III+ IV V VI**

Soil Sampled? Horizon(s), Sample Numbers Soil Special Desert Pavement Varnish Soil Crusts: Please See Physical Chemical Biological

Y N Features None Weak Moderate Strong None Weak Moderate Strong (circle one) Back

LAYER	Thickness	Horizon	Depth cm	COLOR		USDA texture	% ROCK FRAGMENTS (vol.)					PARTICLE-SIZE ESTIMATES (%)		
				Dry	Moist		Stones	Cobbles	Gravel (5-75 mm)	Gravel (2-5 mm)	Total RFs	Sand	Silt	Clay
1 (II)	3Btkb2	97-109	7.5YR 6/4	7.5YR 5/4	CL	0	0	3	5	8	25	46	29	
2 (II)	3Btkb3	109-128	7.5YR 5/4	7.5YR 4/6	CL	0	0	2	5	7	30	35	35	
3 (II)	3Btkb4	128-146	10YR 5/6	10YR 4/6	SLL	0	0	1	3	4	55	19	26	
4 (II)	3Btkb5	146-161	10YR 4/4	10YR 4/4	SLL	0	0	0.01	1	1	50	27	23	
5 (MA)	4CBE	161-185	10YR 5/4	10YR 4/6	OR LS	0	0	10	15	25	75	17	8	
6 (IV)	5Btkm	185-198	10YR 8/3	10YR 6/4	GR SL	0	0	10	5	15	60	24	16	
7 ()	6R	198-242												
8 ()														

LAYER	Structure	CONSISTENCE		Cementation	CHEMICAL PROPERTIES					P&V Feat; Conc.	Roots (#/area)	Pores (#/area)	Boundary
		Dry/Moist	Wet		% CaCO ₃	Efferv.	pH	SAR	Salinity (dS/m)				
1	2VTR PL	HA IFR	MS IMP			NE	.				Yalga		AS
2	2M PR → 2MSBK	HA IFR	MS IMP			NE	.				N		GW
3	1VC PR → 1MSBK	HA IFR	MS ISP			NE	.				N		GW
4	1VC PR → 1MSBK	HA IFR	MS ISP			ST	.				N		GW
5	MA → SG	SH IVFR	SO IPO			SL	.				N		CS
6	MA	VH IFI	SS IPO	W to ST		ST	.				N		CS
7	MA	- I -	- I -	ST		VE	.				N		
8		I	I				.						

Lower Trench Wall
Thickness of 2Btkb varies from 25-35cm

Concentrations: Kind, quantity, size (contrast), color, shape, location, hardness, boundary (ie. CAM, 15%, 1, p, 10yr/8/1, i, MAC, so, c) Ped & Voids: Kind, percent, distinctness, color and location (ie. CAF, 35%, d, 10yr/8/1, BR)

- | | | | |
|----|---------------------------------------|----|-----------------------|
| #1 | CLF 40 BF, TF | #2 | CAF 30 VF, CLF 65 PF |
| #3 | CAF 40 BF, TF; CAM 15 Threads, masses | #4 | BRE 25 BG CAM 12% MAT |
| #5 | CAM 6% MAT, BRE 30 BG 1 CLF SP | #6 | |
| #7 | BRE 15 BG | #8 | |

Additional Notes:

Blank area for additional notes.

Calculations:

PSC Thickness: _____

PSC RFs/PSC Thick=

PSC Clay/PSC Thick =

		Horizon Thickness (cm)					
	Horizon RFs						
	Horizon Clay						

Crusts		Diagrams, Photo Numbers, etc	Profile Diagram
B i o l o g i c a l	Types IBC = Incipient Fungal/Algal Crust FBC = Fungal Crust UBC = Unblackend Algal Crust BCC = Blackened Algal Crust LBC = Lichen Crust BBC = Bryophyte Crust		
P h y s i c a l	VC = Vesicular Crust RC = Rain Drop Impact Crust DC = Depositional Crust		
C h e m i c a l	HCC = Halite Crust GCC = Gypsum Crust MCC = Mirabilite Crust		

Series	User Pedon ID	Date & Time:	By:
Taxonomic unit	Location: UTM (NAD83) e n		MU symbol
Location: UTM (NAD83) e n	Location: N 38.4474 W 103.1768		Pedon PC? NASIS? Analysis?
Air temp. (F)	Soil temp. @ 50 cm (F):	Weather: MC	Photos (File location)
Land use:	Topo Quad	Pedon Type: Ma Mi MMU MS	
Current vegetation	Ecosite:		Production (#/ac):

Landscape	Landform	Position on landform
Plains	Hill slope	BS/SS
Parent material: (Type of Deposit & Rock type)		
Alluvium, sandwash		
Aspect:	Cardinal Direction:	Elevation (m/feet):
°		4530
Slope (%)	Slope Shape, Complexity	
	↕ L ↔ L	
Drainage: X SX W MWD SPD	Water table depth (ft.)	Depth to Least Permeable Layer (for Ksat)
		Flooding: N VR R O F
Soil temperature regime		Soil moisture regime
MESIC - THERMIC - HYPERThERMIC		ARIDIC USTIC

SURFACE ROCK FRAGMENTS						
% 5-75 mm	% 2-5 mm Gravel	% Cobbles	% Stones	% Boulders	Total Surface RF %	% Rock outcrop (Area)
37 x	3 x	137 x	425 x	800 x	/1402 =	Mean Rock Height:

CONTROL SECTION					
Depth: cm	Particle-size class:	mineralogy	% clay	% RF (vol.)	% > VFS (wt.)

DIAGNOSTIC HORIZONS					
Epipedon	Subsurface			Topography:	
				B/S SDiss MDiss SDiss Ballena	
Depth to paralithic contact: cm	Depth to Lithic contact: cm	Depth to Hardpan: cm		Carbonate Stage: I II+ III III+ IV V VI	
Soil Sampled? Horizon(s), Sample Numbers	Soil Special Features	Desert Pavement	Varnish		Soil Crusts: Please See (circle one) Back
Y N		None Weak Moderate Strong	None Weak Moderate Strong		Physical Chemical Biological

Thickness LAYER	Horizon	Depth cm	COLOR			% ROCK FRAGMENTS (vol.)					PARTICLE-SIZE ESTIMATES (%)		
			Dry	Moist	USDA texture	Stones	Cobbles	Gravel (5-75 mm)	Gravel (2-5 mm)	Total RFs	Sand	Silt	Clay
1 ()	A	0-5	10YR 4/3	10YR 3/2	L	∅	∅	1	3	4	50	33	17
2 (Transj) I	B+k	5-16	10YR 4/3	10YR 3/3	SL			0.1	3	3	60	21	19
3 (II)	2 Bk1	16-28	7.5YR 4/4	7.5YR 4/4	CL			0.1	1	1	40	25	35
4 (II)	2 Bk2	28-57	10YR 4/4	10YR 4/4	CL			1	2	3	40	28	32
5 (II)	2 Bk3	57-76	10YR 5/4	10YR 4/4	SCL	↓	↓	2	1	3	55	17	28
6 ()	3	76+	Equivalent of			40Bk in descr. Cheraw PD1							
7 ()													
8 ()													

LAYER	Structure	CONSISTENCE			Cementation	CHEMICAL PROPERTIES					P&V Feat; Conc.	Roots (#/area)	Pores (#/area)	Boundary
		Dry/Moist	Wet			% CaCO ₃	Efferv.	pH	SAR	Salinity (dS/m)				
1	2VK PL → 1M SBK	SH	FR	SS	SP	N/A		NE	.			Y		CW
2	1M SBK	SH	INFR	SS	PO			ST	.					AW
3	3 R → 2 M SBK	HA	FI	MS	IMP			VS	.					GW
4	3 M PR → 2 M SBK	VH	FI	MS	IMP			SL	.					GW
5	1 VC PR → 2 M SBK	VH	FI	SS	IMP	↓		SL	.			↓		CS
6									.					
7									.					
8									.					

Concentrations: Kind, quantity, size, (contrast), color, shape, location, hardness, boundary (i.e. CAM, 15%, 1. p, 10yr8/1, i, MAC, so, c) Ped & Voids: Kind, percent, distinctness, color and location (CAF, 35%, d, 10yr8/1, BR)

- #1
- #3 CLF 90% PF, CAF 25 MAT
- #5 CAM Med 7%, BRF-BG 60%; CLF 20 VF
- #7
- #2 CAM M+C 8% BRF-BG 15
- #4 CAM M 15%, CLF 60 VF
- #6
- #8

Additional Notes:

Calculations:
PSC Thickness: _____

		Horizon Thickness (cm)					
PSC RFs/PSC Thick=							
	Horizon RFs						
PSC Clay/PSC Thick =	Horizon Clay						

Crusts		Diagrams, Photo Numbers, etc		
B i o l o g i c a l	<p>Types</p> <p>IBC = Incipient Fungal/Algal Crust</p> <p>FBC = Fungal Crust</p> <p>UBC = Unblackend Algal Crust</p> <p>BCC = Blackened Algal Crust</p> <p>LBC = Lichen Crust</p> <p>BBC = Bryophyte Crust</p>	<table border="1"> <thead> <tr> <th>Profile Diagram</th> </tr> </thead> <tbody> <tr> <td style="height: 200px;"></td> </tr> </tbody> </table>	Profile Diagram	
Profile Diagram				
P h y s i c a l	<p>VC = Vesicular Crust</p> <p>RC = Rain Drop Impact Crust</p> <p>DC = Depositional Crust</p>			
C h e m i c a l	<p>HCC = Halite Crust</p> <p>GCC = Gypsum Crust</p> <p>MCC = Mirabilite Crust</p>			

Series	User Pedon ID	Date & Time:	By:
	Choraw 003	13:06 3/31/16	PRR
Taxonomic unit			MU symbol
Location: UTM (NAD83) e n			Location: N 38, 4475 W 103, 1768
Air temp. (F)	Soil temp. @ 50 cm (F):	Weather:	Photos (File location)
		MC, Windy	
Land use:	Topo Quad	Production (#/ac):	
Current vegetation			Ecosite:

Landscape	Landform	Position on landform		
Diagnosis	Hillslope	BS/SS		
Parent material: (Type of Deposit & Rock type)				
Aspect:	Cardinal Direction:	Elevation (m/feet):	Slope (%)	Slope: Shape, Complexity
		4535		↑ L ↔ L
Drainage:	Water table depth (ft.)	Depth to Least Permeable Layer (for Ksat)	Flooding:	Depth Class:
X SX W MWD SPD			N VR R O F	VS SH MD (D)
Soil temperature regime		Soil moisture regime		
MESIC THERMIC - HYPERTHERMIC		ARIDIC USTIC		

SURFACE ROCK FRAGMENTS						
% 5-75 mm	% 2-5 mm Gravel	% Cobbles	% Stones	% Boulders	Total Surface RF %	% Rock outcrop (Area)
Gravel						
37 x	3 x	137 x	425 x	800 x	/1402 =	Mean Rock Height:

CONTROL SECTION						
Depth: cm	Particle-size class:	mineralogy	% clay	% RF (vol.)	% > VFS (wt.)	
DIAGNOSTIC HORIZONS						
Epipedon	Subsurface			Topography: B/S SDiss MDiss SDiss Ballena		
Depth to paralithic contact: cm	Depth to Lithic contact: cm		Depth to Hardpan: cm		Carbonate Stage: I I+ II II+ III III+ IV V VI	
Soil Sampled? Horizon(s), Sample Numbers	Soil Special	Desert Pavement		Varnish		Soil Crusts: Please See
Y N	Features	None Weak Moderate Strong	None Weak Moderate Strong	None Weak Moderate Strong	(circle one)	Back Physical Chemical Biological

Thickness LAYER	Horizon	Depth cm	COLOR			% ROCK FRAGMENTS (vol.)					PARTICLE-SIZE ESTIMATES (%)		
			Dry	Moist	USDA texture	Stones	Cobbles	Gravel (5-75 mm)	Gravel (2-5 mm)	Total RFs	Sand	Silt	Clay
1 ()	A	0-9	10YR 4/3	10YR 3/3	L	Ø	Ø	0.1	3	3	45	39	16
2 ()	B ₂ W	9-24	7.5YR 4/4	7.5YR 3/4	SL	Ø	Ø	0.1	3	3	55		17
3 (II)	B ₂ K	24-42	10YR 6/3	10YR 4/3	SL	Ø	Ø	0.1	4	4	63	19	18
4 (II)	B ₂ C	42-55	2.5Y 6/3	2.5Y 5/3	LCOS	Ø	Ø	0.1	7	7	80	14	6
5 (III)	2B ₂ K/B ₂ Km	55-62	2.5Y 7/2	2.5Y 5/3	L	Ø	Ø	Ø	2	2	35	46	19
6 (II)	2B ₂ Kb1	62-96	2.5Y 6/3	2.5Y 5/3	S ₁ C	Ø	Ø	Ø	Ø	Ø	15	47	38
7 ()	3B ₂ Kb2	96+	Equivalent of 3B ₂ Kb2 in Choraw - Ø Ø 1, has Fe staining sim.										
8 ()			to horizon above										

LAYER	Structure	CONSISTENCE		Cementation	CHEMICAL PROPERTIES					P&V Feat; Conc.	Roots (#/area)	Pores (#/area)	Boundary
		Dry/Moist	Wet		% CaCO ₃	Efferv.	pH	SAR	Salinity (dS/m)				
1	2VK PL 2M S ₂ BK	SH NFR	SS IPO			NE	.				4		CW
2	2M S ₂ BK	SH IFR	I			NE	.				4		GW
3	2M S ₂ BK	SH NFR	SS/SP			VE	.				4		CW
4	1M S ₂ BK → SG	SH NFR	SD IPO			ST	.				4		AW
5	MA/MA	SD NFR	MS/PS	B ₂ Km MA		SL	.				4		AW
6	3M PR → 3M S ₂ BK	VH IFR	MS/PS	-		NE	.				Few shh Ped fac's		CW
7		I	I	-		.	.				N		
8		I	I	-		.	.						

Concentrations: Kind, quantity, size, (contrast), color, shape, location, hardness, boundary (ie. CAM, 15%, 1, p, 10YR/1, t, MAC, so, c) Ped & Voids: Kind, percent, distinctness, color and location (ie. CAF, 35%, d, 10YR/1, BR)

II 2CK
 SO on note on back
 2CK; CAM F+M 8% MAT
 #1
 #3
 #5
 #7

#1
 #3 CAM F+M 25% MAT; BRF → BG 30
 #5 B₂Km is equiv. to B₂Km of Choraw - Ø Ø 1
 #7 2CK: Fe conc 10%, 5YR 4/6 MAT Post-Pedogenic

#2 BRF - BG 35%
 #4 CAM C+VC 15% MAT
 #6 CAM MAC 10%; CAF 15 PF CLF 70 PF
 #8 Fe conc. 8 5YR 4/6 MAT, Post-pedogenic

Additional Notes:

2C is sandy lense that is sandwiched between BKKm which is discontinuous/broken in this exposure and 2BKKbl. It is variable in texture from sand to FS to silt
 2C: CAN MTC Mod - strong cemented 5%

Calculations:

PSC Thickness: _____

PSC RFs/PSC Thick=

PSC Clay/PSC Thick =

		Horizon Thickness (cm)					
	Horizon RFs						
	Horizon Clay						

Crusts		Diagrams, Photo Numbers, etc		
B i o l o g i c a l	Types IBC = Incipient Fungal/Algal Crust FBC = Fungal Crust UBC = Unblackened Algal Crust BCC = Blackened Algal Crust LBC = Lichen Crust BBC = Bryophyte Crust	<table border="1"> <thead> <tr> <th>Profile Diagram</th> </tr> </thead> <tbody> <tr> <td style="height: 200px;"></td> </tr> </tbody> </table>	Profile Diagram	
Profile Diagram				
P h y s i c a l	VC = Vesicular Crust RC = Rain Drop Impact Crust DC = Depositional Crust			
C h e m i c a l	HCC = Halite Crust GCC = Gypsum Crust MCC = Mirabilite Crust			

Appendix B

Luminescence Dating - Sample Analysis Report Summary

TABLE 1: Data and ages from Quartz OSL and Feldspar post IR-IRSL

Sample information	% Water content ^a	K (%) ^b	U (ppm) ^b	Th (ppm) ^b	Total Dose (Gy/ka) ^c	Equivalent Dose (Gy)	n ^d	Scatter ^e	Age (ka) ^f
Haswell T1E OSL-1	3 (46)	2.39 ± 0.04	5.30 ± 0.24	7.51 ± 0.29	5.98 ± 0.13	>955	10 (10)	-	>160
Haswell T1E OSL-2	1 (22)	3.73 ± 0.05	2.08 ± 0.25	11.0 ± 0.20	6.70 ± 0.11	845 ± 72	5 (5)	0%	126 ± 11
Haswell T1E OSL-3	1 (25)	3.52 ± 0.04	2.70 ± 0.23	8.35 ± 0.29	6.31 ± 0.13 4.73 ± 0.10	67.8 ± 6.8 38.5 ± 4.6	6 (20) 2 (20)	54% 66%	10.7 ± 1.1 8.14 ± 1.0
Haswell T1E OSL-4	5 (52)	2.52 ± 0.04	4.27 ± 0.33	18.2 ± 0.92	6.96 ± 0.24	1,108 ± 62	10 (10)	0%	159 ± 11
Haswell T1E OSL-5	3 (23)	1.85 ± 0.10	4.40 ± 0.37	18.2 ± 0.73	6.92 ± 0.22	1,057 ± 51	10 (10)	0%	153 ± 8.5

^aField moisture, with figures in parentheses indicating the complete sample saturation %. Ages calculated using 25% of the saturated moisture (i.e. 3 (46) = 46 * 0.25 = 12).

^bAnalyses obtained using high-resolution gamma spectrometry (high purity Ge detector).

^cIncludes cosmic doses and attenuation with depth calculated using the methods of Prescott and Hutton (1994). Cosmic doses were around 0.27-0.22 Gy/ka.

^dNumber of replicated equivalent dose (De) estimates used to calculate the equivalent dose. Figures in parentheses indicate total number of measurements included in calculating the represented equivalent dose and age using the central age model (CAM) on single aliquot regeneration and the minimum age model (MAM) for HAS-3.

^eDefined as "over-dispersion" of the D_e values. Obtained by the "R" radial plot program. Values >30% are considered to be poorly bleached or mixed sediments.

^fDose rate and age for fine-grained 180-90 microns K-feldspar, post IR230C; fade of 3.5%/decade. Exponential + linear fit used on equivalent dose, errors to one sigma.

Appendix C

Three-Point Strike and Dip Solutions from Surveyed Points Along Haswell Ditch Exposure

This worksheet calculates the strike and dip, given 3 points on a plane.

Last modified: Dec. 4, 2011 by LEH

GSA Archive data site

[Hasbargen, L., 2012. A test of the three point vector method to determine strike and dip utilizing digital aerial imagery and topography, in Whitmeyer, S.J., Bailey, J.E., De Paor, D.G., and Ornduff, T., eds., Google Earth and Virtual Visualizations in Geoscience Education and Research: Geological Society of America Special Paper 492, p. 253-262, doi:10.1130/2012.2492\(18\). Spreadsheet downloaded from Geol. Soc. Amer. Data Repository](#)

The calculation finds the pole to the plane by computing the cross product of two vectors constructed between 3 pts on a plane.

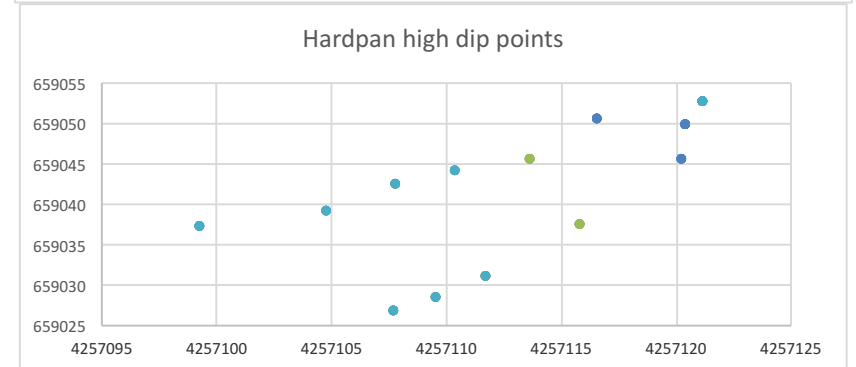
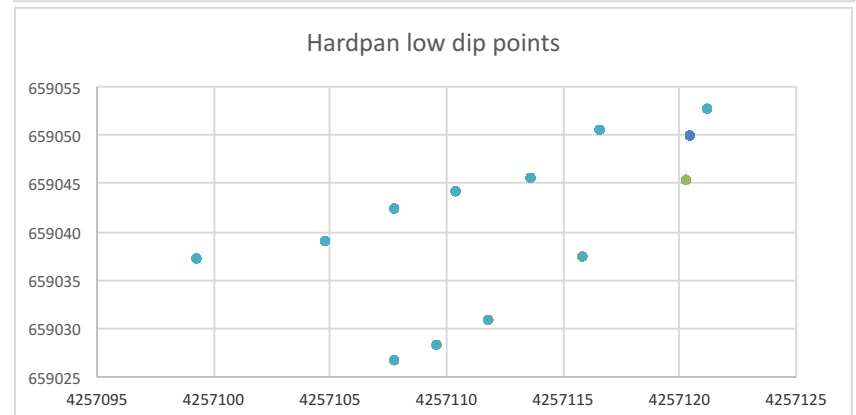
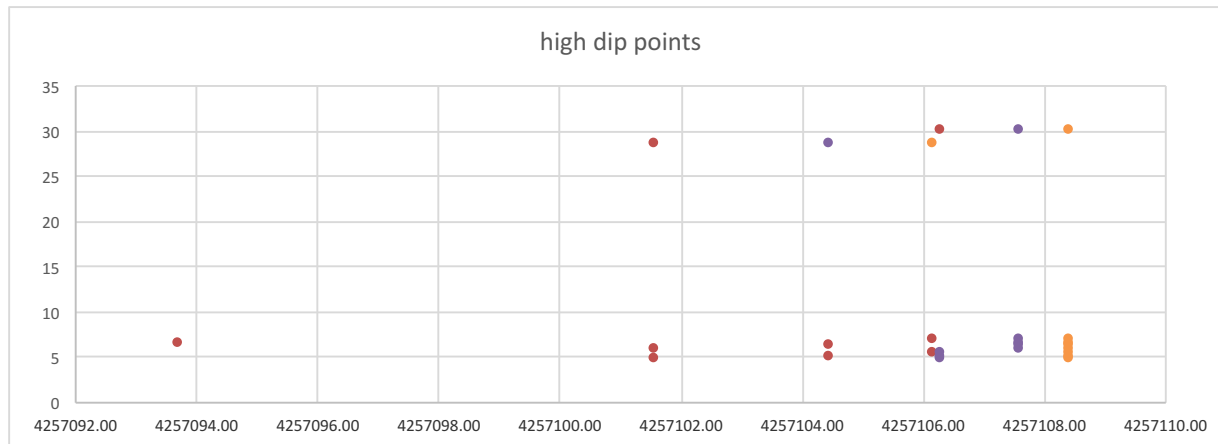
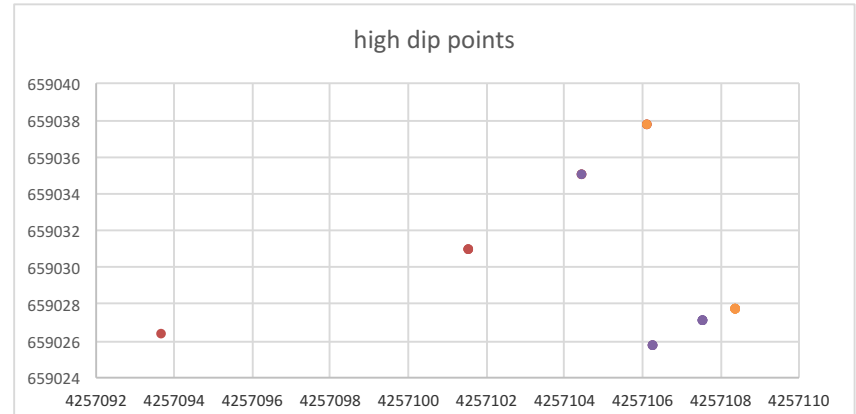
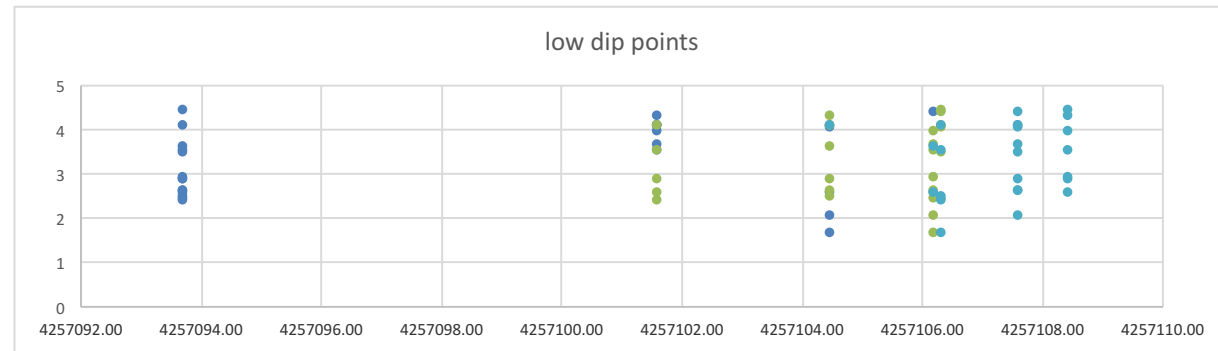
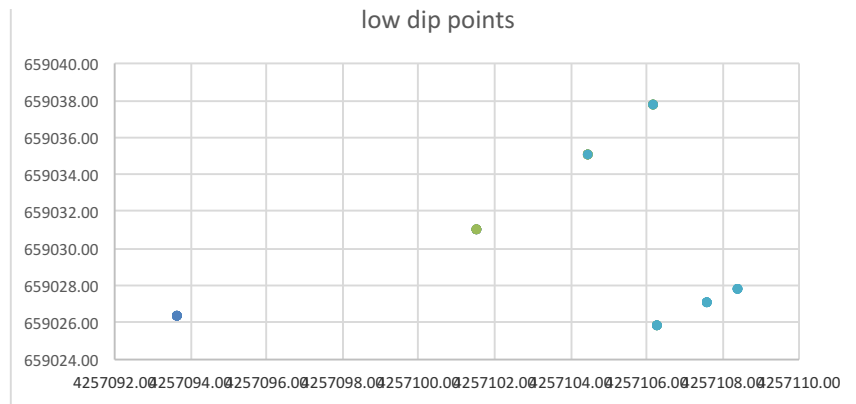
$$\begin{aligned}
 U_1 i &= ((y_1 - y_2) * (z_3 - z_2) - (y_3 - y_2) * (z_1 - z_2)) i \\
 -U_2 j &= -((x_1 - x_2) * (z_3 - z_2) - (x_3 - x_2) * (z_1 - z_2)) j \\
 U_3 k &= ((x_1 - x_2) * (y_3 - y_2) - (x_3 - x_2) * (y_1 - y_2)) k \\
 S &= ((U_2 * 1 - 0 * U_3), -(U_1 * 1 - 0 * U_3), (U_1 * 0 - 0 * U_2)) = (U_2, -U_1, 0) = (E, N, 0)
 \end{aligned}$$

Output values of strike and dip.

Strike is consistent with right hand rule

Strike vector has been corrected for pole orientation

ID	Point 1			Point 2			Point 3			Calculated Values						Strike vector	
	Easting, m	Northing, m	Elevation, m	Easting, m	Northing, m	Elevation, m	Easting, m	Northing, m	Elevation, m	U ₁ i	-U ₂ j	U ₃ k	easting	northing	Strike, degrees	Dip, degrees	** = High Dip
Example Row	591506	3719215	89	591530	3719201	102	591534	3719187	96	-278.8	-209.2	284.5	209.2	-278.8	143.1	50.8	
Niobrara Bedding Points																	
NUSS MARK	4257104.21	659034.54	1374.63	4257105.1	659033.81	1374.48	4257102.25	659029.77	1374.64	0.7	-0.3	5.7	0.3	0.7	21.5	7.8	
NUSS MARK	4257105.1	659033.81	1374.48	4257102.25	659029.77	1374.64	4257106.35	659025.86	1374.04	-3.0	1.1	-27.7	1.1	3.0	19.1	6.6	
NUSS MARK	4257102.25	659029.77	1374.64	4257106.35	659025.86	1374.04	4257104.21	659034.54	1374.63	-2.9	1.1	-27.2	1.1	2.9	21.4	6.5	
NUSS MARK	4257106.35	659025.86	1374.04	4257102.25	659029.77	1374.64	4257104.21	659034.54	1374.63	2.9	-1.1	27.2	1.1	2.9	21.4	6.5	
Nussbaum Base Contact Points																	
NUSS BASE	4257104.48	659034.96	1375.13	4257106.19	659037.69	1375.06	4257106.32	659025.74	1375.16	0.6	0.2	20.8	-0.2	0.6	342.3	1.6	
NUSS BASE	4257104.48	659034.96	1375.13	4257106.19	659037.69	1375.06	4257107.61	659027.01	1375.05	0.8	0.1	22.1	-0.1	0.8	353.9	2.0	
NUSS BASE	4257093.71	659026.33	1375.68	4257101.59	659030.91	1375.40	4257106.32	659025.74	1375.16	2.5	-0.6	62.4	0.6	2.5	12.5	2.4	
NUSS BASE	4257093.71	659026.33	1375.68	4257106.19	659037.69	1375.06	4257106.32	659025.74	1375.16	6.3	1.3	150.6	-1.3	6.3	348.0	2.4	
NUSS BASE	4257093.71	659026.33	1375.68	4257104.48	659034.96	1375.13	4257106.32	659025.74	1375.16	4.8	1.3	115.2	-1.3	4.8	344.5	2.5	
NUSS BASE	4257104.48	659034.96	1375.13	4257106.19	659037.69	1375.06	4257108.44	659027.72	1374.94	1.0	0.0	23.2	0.0	1.0	2.7	2.5	
NUSS BASE	4257093.71	659026.33	1375.68	4257101.59	659030.91	1375.40	4257106.19	659037.69	1375.06	-0.3	-1.4	-32.4	-1.4	0.3	283.8	2.5	
NUSS BASE	4257093.71	659026.33	1375.68	4257106.19	659037.69	1375.06	4257107.61	659027.01	1375.05	6.7	0.8	149.4	-0.8	6.7	353.6	2.6	
NUSS BASE	4257093.71	659026.33	1375.68	4257104.48	659034.96	1375.13	4257107.61	659027.01	1375.05	5.1	0.9	112.6	-0.9	5.1	350.4	2.6	
NUSS BASE	4257093.71	659026.33	1375.68	4257101.59	659030.91	1375.40	4257107.61	659027.01	1375.05	2.7	-1.1	58.3	1.1	2.7	21.7	2.8	
NUSS BASE	4257093.71	659026.33	1375.68	4257104.48	659034.96	1375.13	4257108.44	659027.72	1374.94	5.6	0.1	112.1	-0.1	5.6	358.7	2.9	
NUSS BASE	4257093.71	659026.33	1375.68	4257106.19	659037.69	1375.06	4257108.44	659027.72	1374.94	7.5	-0.1	150.0	0.1	7.5	0.8	2.9	
NUSS BASE	4257093.71	659026.33	1375.68	4257106.32	659025.74	1375.16	4257107.61	659027.01	1375.05	-0.7	-0.7	-16.8	-0.7	0.7	315.4	3.5	
NUSS BASE	4257093.71	659026.33	1375.68	4257101.59	659030.91	1375.40	4257108.44	659027.72	1374.94	3.0	-1.7	56.5	1.7	3.0	29.6	3.5	
NUSS BASE	4257101.59	659030.91	1375.40	4257106.19	659037.69	1375.06	4257106.32	659025.74	1375.16	3.4	0.5	55.9	-0.5	3.4	351.5	3.5	
NUSS BASE	4257093.71	659026.33	1375.68	4257104.48	659034.96	1375.13	4257106.19	659037.69	1375.06	-0.9	0.2	-14.6	0.2	0.9	11.7	3.6	
NUSS BASE	4257101.59	659030.91	1375.40	4257106.19	659037.69	1375.06	4257107.61	659027.01	1375.05	3.7	0.4	58.8	-0.4	3.7	353.3	3.6	
NUSS BASE	4257101.59	659030.91	1375.40	4257106.19	659037.69	1375.06	4257108.44	659027.72	1374.94	4.2	0.2	61.1	-0.2	4.2	357.1	3.9	
NUSS BASE	4257104.48	659034.96	1375.13	4257106.32	659025.74	1375.16	4257107.61	659027.01	1375.05	-1.0	-0.2	-14.2	-0.2	1.0	346.1	4.0	
NUSS BASE	4257093.71	659026.33	1375.68	4257101.59	659030.91	1375.40	4257104.48	659034.96	1375.13	0.1	-1.3	-18.7	-1.3	-0.1	265.6	4.0	
NUSS BASE	4257101.59	659030.91	1375.40	4257106.32	659025.74	1375.16	4257107.61	659027.01	1375.05	-0.9	-0.2	-12.7	-0.2	0.9	346.4	4.1	
NUSS BASE	4257101.59	659030.91	1375.40	4257104.48	659034.96	1375.13	4257107.61	659027.01	1375.05	2.5	0.6	35.7	-0.6	2.5	346.0	4.1	
NUSS BASE	4257101.59	659030.91	1375.40	4257104.48	659034.96	1375.13	4257106.32	659025.74	1375.16	2.4	0.6	34.1	-0.6	2.4	346.2	4.1	
NUSS BASE	4257101.59	659030.91	1375.40	4257104.48	659034.96	1375.13	4257108.44	659027.72	1374.94	2.7	0.5	37.0	-0.5	2.7	349.2	4.3	
NUSS BASE	4257106.19	659037.69	1375.06	4257106.32	659025.74	1375.16	4257107.61	659027.01	1375.05	-1.2	-0.1	-15.6	-0.1	1.2	353.1	4.4	
NUSS BASE	4257093.71	659026.33	1375.68	4257106.32	659025.74	1375.16	4257108.44	659027.72	1374.94	-1.2	-1.7	-26.2	-1.7	1.2	304.7	4.4	
NUSS BASE	4257101.59	659030.91	1375.40	4257106.32	659025.74	1375.16	4257108.44	659027.72	1374.94	-1.6	-0.5	-20.3	-0.5	1.6	341.7	4.8	**
NUSS BASE	4257104.48	659034.96	1375.13	4257106.32	659025.74	1375.16	4257108.44	659027.72	1374.94	-2.0	-0.5	-23.2	-0.5	2.0	346.6	5.0	**
NUSS BASE	4257106.19	659037.69	1375.06	4257106.32	659025.74	1375.16	4257108.44	659027.72	1374.94	-2.4	-0.2	-25.6	-0.2	2.4	354.3	5.5	**
NUSS BASE	4257101.59	659030.91	1375.40	4257107.61	659027.01	1375.05	4257108.44	659027.72	1374.94	-0.7	-0.4	-7.5	-0.4	0.7	331.2	5.9	**
NUSS BASE	4257104.48	659034.96	1375.13	4257107.61	659027.01	1375.05	4257108.44	659027.72	1374.94	-0.9	-0.3	-8.8	-0.3	0.9	343.4	6.3	**
NUSS BASE	4257093.71	659026.33	1375.68	4257107.61	659027.01	1375.05	4257108.44	659027.72	1374.94	-0.4	-1.0	-9.3	-1.0	0.4	290.3	6.6	**



# each type	shot	N_corr	E_corr	shift elev	desc	
	1	15 #####	659050	1375.56	HARDPAN 20	0.0
	2	16 #####	659045	1375.55	HARDPAN 20	0.0
	3	17 #####	659037	1375.64	HARDPAN 20	
	4	18 #####	659031	1375.9	HARDPAN 20	
	5	19 #####	659028	1376.04	HARDPAN 20	
	6	20 #####	659027	1376.17	HARDPAN 20	
	7	1 #####	659052	1375.61	HARDPAN 20 BASE	
	8	2 #####	659050	1375.78	HARDPAN 20 BASE	
	9	3 #####	659045	1375.79	HARDPAN 20 BASE	
	10	4 #####	659044	1375.99	HARDPAN 20 BASE	
	11	5 #####	659042	1376.08	HARDPAN 20 BASE	
	12	6 #####	659039	1376.27	HARDPAN 20 BASE	
	13	7 #####	659037	1376.61	HARDPAN 20 BASE	
	1	8 #####	659026	1375.68	NUSS BASE	
	2	9 #####	659031	1375.4	NUSS BASE	
	3	10 #####	659035	1375.13	NUSS BASE	
	4	14 #####	659038	1375.06	NUSS BASE	
	5	21 #####	659028	1374.94	NUSS BASE	
	6	22 #####	659027	1375.05	NUSS BASE	
	7	23 #####	659026	1375.16	NUSS BASE	